ANL/NE-12/4

The SAS4A/SASSYS-1 Safety Analysis Code System

Nuclear Engineering Division

ANL/NE-12/4

The SAS4A/SASSYS-1 Safety Analysis Code System

Chapter 7:
Balance of Plant Thermal/Hydraulic Models

L. L. Briggs, J. Y. Ku, and P. A. Pizzica
Nuclear Engineering Division
Argonne National Laboratory

January 31, 2012

TABLE OF CONTENTS

LIST OF FIGURES

LIST OF TABLES

NOMENCLATURE

Symbol	Definition	Units
a	Constant (9.325×10^{-2})	
a_0, a_1, a_2, a_3	Momentum equation coefficients	
A	Flow area	m^2
b	Constant (2.356×10^{-4})	
B	Valve damping coefficient	kg-m/s
c, c_p	Specific heat	J/kg-K
c_b	Bucket coefficient	
c_n	Nozzle velocity coefficient	
c_r	Reaction coefficient	
C	Valve calibration constant	m^2
CF	Calibration factor	
CV	Elevation of heater center	m
C_1, C_2, C_3, C_4	Coefficients in the expression for the Moody friction factor ($C_1 = 0.0055, C_2 = 20{,}000, C_3 = 106, and\ C_4 = 1/3$)	
D_h, D_H	Hydraulic diameter	m
Ê	Total energy	J/kg
f_l	Liquid friction factor	
f_{tp}	Two-phase friction factor	
F	Force	N
F	Heat flux	W/m^2
F	Pressure loss coefficient	
FL	Fouling resistance	m^2-K/W
FR	Friction calibration coefficient	
F_1	Valve driving function	kg-m/s^2
g	Gravitational constant	m/s^2
G	Mass flux	kg/m^2-s
G_2	Orifice coefficient	
h	Specific enthalpy	J/kg
hp	Primary side heat transfer coefficient in the simple heater model	W/m^2-K
h_{tot}, H	Total heat transfer coefficient	W/m^2-K
H	Height	m

H	Work	W
I	Moment of inertia	kg-m^2
j	Lowermost node in a region	
k	Thermal conductivity	W/m-K
k	Valve spring constant	kg/s^2
k_p	Thermal conductivity of the primary side in the simple heater model	W/m-K
K	Loss constant	
L	Element length, or distance	m
L_B/D_B	Effective length-to-diameter ratio per bend	
m, M	Mass	kg
n	Index on the discretized time variable	
n	Number of nodes in a region	
N_B	Number of bends along a flow path	
Nu	Nusselt number	
P, P^*	Pressure	Pa
POD	Pitch-to-diameter ratio	
Pr	Prandtl number	
q	Heat flux	J/s-m^2
Q	Heat source	J/s
Q	Volumetric heat source	W/m^3
Q	Energy transfer rate	W
r	Radius	m
r_5	Two-phase multiplier	
R	Thermal resistance	K/W
R	Loss factor	
Re	Reynolds number	
s	Distance	m
s	Specific entropy	J/kg-K
$sgn(j,l)$	1 if the steady state flow in segment j is entering volume l -1 if the steady state flow in segment j is leaving volume l	
t	Time	s
T	Temperature	K
TP	Elevation of two-phase interface	m

u, v	Fluid velocity	m/s
U_{pseu}	Pseudo-heat conduction coefficient	W/K
v	Specific volume	m^3/kg
V	Volume	m^3
V_a, V_b	Steam velocities relative to the blade and parallel to the blade motion at the blade entrance and exit, respectively	m/s
V_1	Absolute steam velocity at the blade entrance	m/s
V_2	Steam velocity relative to the blade at the blade entrance	m/s
V_3	Steam velocity relative to the blade at the blade exit	m/s
V_4	Absolute steam velocity at the blade exit	m/s
w	Mass flow rate	kg/s
WR	Wall resistance on water side	
$WRNA$	Wall resistance on sodium side	
x	Quality	
y	Valve stem position	m
z	Spatial variable	m
Z	Spatial location, region length, or elevation of pipe center	m
Δz	$z_0 - z_I$, the elevation difference between the outlet and the inlet of a flow element	m
α	Void fraction	
α	Nozzle exit angle	rad
β	Volumetric quality	
γ	Blade exit angle	rad
δ	Thickness	m
ε	Element roughness	m
η	Efficiency	
θ	Angle of inclination with respect to the vertical	
μ	Dynamic viscosity	Pa-s
v	Specific volume	m^3/kg
ρ	Density	kg/m^3
τ	Viscous stress tensor	Pa
τ	Torque	N - m

φ	Valve characteristic	
χ	Quality	
ω	Rotor angular velocity	rad/s

Subscripts

ACC	Accumulated pressure at which value fully opens
b	Bottom
B	Blade
BLD	Blowdown pressure at which valve closes
D	Drain, or DNB
E	Exhaust
f	Liquid
fg	Vapor minus liquid
g	Vapor
G	Generator
hf	Location of hf
hg	Location of hg
i	Node number, region number, inside
I, in	Inlet
j	Segment number
m	Metal tube, or tube wall
$misc$	Miscellaneous
M	Moisture, or mid-wall
nz	Nozzle
Na	Sodium
o	Outside, theoretical
O, out	Outlet
r	Reference
R	Rotation
s	Sodium, shell side, steam drum
S	Surface
sat	Saturation
SC	Subcooled zone
SG	Steam generator
SH	Superheated zone

t	Top, tube side, total
T	Total, turbine
TP	Boiling zone
u	Upper
w	Water
l	Volume number
∞	Ambient
Superscripts	
k, n	Time step index
n	Normalized
u	Unnormalized
$-$	Isentropic quantity

BALANCE OF PLANT THERMAL/HYDRAULIC MODELS

7.1 Introduction

A balance-of-plant thermal/hydraulic model has been developed for use with the SASSYS-1 liquid metal reactor systems analysis code. This model expands the scope of SASSYS-1 so that the code can explicitly model the waterside components of a nuclear power plant. Previously, only the water side of the steam generators could be modelled, with the remainder of the water side represented by boundary conditions on the steam generator. This chapter is organized with a structure that reflects the three major areas of the balance-of-plant thermal/hydraulics module: 1) the network model, 2) the steam generator model, and 3) the component models.

The balance-of-plant network thermal/hydraulics model represents the water side as a network of components, similar to the representation used by SASSYS for the sodium side of the plant. The model will handle subcooled liquid water, superheated steam, and saturated two-phase fluid. With the exception of heated flow paths in heat exchangers, the model assumes adiabatic conditions along flow paths. This assumption simplifies the solution procedure while introducing very little error for a wide range of reactor plant problems.

The balance-of-plant steam generator thermal/hydraulics model is totally new, and completely replaces the previous SASSYS-1 steam generator model. A number of modeling improvements have been implemented in the new steam generator model to achieve better accuracy, capability, and computational performance. First, variable spatial nodalization has been introduced to permit more accurate estimates of heat fluxes. Second, an improved treatment of heat transfer regime transitions is employed to promote numerical stability. Third, donor cell spatial differencing is used with a semi-implicit time-differencing scheme to add further numerical stability and to allow larger time stops. Fourth, the steady-state initialization process has been improved to accommodate a wider variety of heat transfer and flow regimes. Finally, the new steam generator model contains a preliminary method for variable time step selection.

The steam generator model simulates the two most likely configurations for LMR plants with their high core outlet/inlet temperatures. The two configurations are: 1) the once-through system where the superheater is an integral part of the evaporator, and 2) the external recirculation type where the balance-of-plant components are used to connect the separate superheater to the evaporator through the steam drum.

The balance-of-plant components thermal/hydraulics models extend the scope of the network model, to treat nonadiabatic and two-phase conditions along flow paths, and to account for work done across the boundaries of compressible volumes. Simple conservation balances and extensive component data in the form of correlations constitute the basis of models of heaters (deaerators, steam drums, condensers, reheaters, flashed heaters, drain coolers, desuperheating heaters, and desuperheater/drain coolers), turbines, and relief valves. Except for the turbine nozzle, the mass and momentum equations for the component models are the same as the network equations. The component energy equations contain a heat source due to

energy transfer across a flow boundary or to work done through a shaft. To handle two-phase conditions, the equation of state is expressed differently for each phase in terms of the quality and separate intensive properties.

The next three sections describe the network steam generator, and component models.

7.2 Network Thermal/Hydraulic Model

7.2.1 Discretization of the Balance of Plant

SASSYS-1 represents the balance of plant as a network of one-dimensional flow paths which are joined at flow junctions. Junctions are of two types; those in which there is no separation of liquid and vapor (in which case perfect mixing is assumed) and those in which liquid and vapor are strictly separated (in which case instantaneous separation and saturation conditions are assumed). As a result of using this representation, the mass, momentum, and energy equations that describe the system can be reduced to one-dimensional forms. The network of junctions and paths is just a discretization of the balance of plant using a non-uniform spatial mesh; the network is perhaps best described as a nodalization of the plant. The momentum equation is solved along each flow path, and the mass and energy equations are solved at each flow junction. Flow is assumed uniform throughout each flow path. Because the junctions are regions of fixed volume and are used in part to model compressibility effects in the system, they are given the name compressible volumes. Flow paths are known simply as flow segments.

The balance of plant is a collection of several types of components: pipes, valves, check valves, pumps, heaters, inlet and outlet plena, and piping junctions. The steam generator is intentionally omitted form this list, since it is treated as a separate model (Section 7.3). Components which primarily affect mass flow rate and pressure drop in a flow segment are best described through the momentum equation and are modelled as sections of flow segments; these sections are called flow elements. The cross-sectional area is constant throughout a given flow element. Element types include pipes, valves, check valves, and pumps. Flow segments then become strings of one or more flow elements; for example, a flow segment might consist of a length of pipe (element 1), followed by a pump (element 2), followed by a check valve (element 3). The flow would be the same in all three elements, but the geometry could differ from element to element.

Components which join two or more flow segments are best described through the mass and energy equations and are modelled as compressible volumes; these include inlet and outlet plena, piping junctions, and open heaters. Closed heaters must be described through a combination of flow elements and a compressible volume (Section 7.4).

More detailed information about constructing a nodalization of a plant will be presented in Section 7.2.7.

7.2.2 Analytical Equations

The general analytical equations are

$$\text{mass}: \frac{\partial \rho}{\partial t} = -\left(\underline{\nabla} \cdot \rho \underline{u}\right), \tag{7.2-1}$$

$$\text{momentum}: \frac{\partial}{\partial t}\left(\rho \underline{u}\right) = -\left[\underline{\nabla} \cdot \rho \underline{u}\underline{u}\right] - \underline{\nabla} P - \left[\underline{\nabla} \cdot \underline{\tau}\right] + \rho \underline{g}, \tag{7.2-2}$$

$$\text{energy}: \frac{\partial}{\partial t}\left(\rho \hat{E}\right) = -\left(\underline{\nabla} \cdot \rho \overline{E} \underline{u}\right) - \underline{\nabla} \cdot \underline{q} - \left[\nabla \cdot P u\right] - \left(\underline{\nabla} \cdot \left[\underline{\tau} \cdot \underline{u}\right]\right) \tag{7.2-3}$$

These can be simplified by making the following assumptions:

1) One-dimensional flow,
2) Neglect the work done by viscous forces on a compressible volume (this is the $\underline{\nabla} \cdot \left[\underline{\tau} \cdot \underline{u}\right]$ term in Eq. 7.2-3),
3) Neglect kinetic energy and gravitation energy,
4) The viscous term in the momentum equation can be expressed as $\frac{F \rho u |u|}{2}$.

In addition, if the total energy (which is now assumed to equal the internal energy) is expressed in terms of the enthalpy, the mass, momentum, and energy equations take the simpler forms

$$\text{mass}: \frac{\partial \rho}{\partial t} = -\frac{\partial \rho u}{\partial z} \tag{7.2-4}$$

$$\text{momentum}: \frac{\partial \rho u}{\partial t} = -\frac{\partial \rho u^2}{\partial z} - \frac{\partial P}{\partial z} - F \frac{\rho u |u|}{2} + \rho g cos\theta \tag{7.2-5}$$

$$\text{energy}: \frac{\partial \rho h}{\partial t} = -\frac{\partial \rho h u}{\partial z} - \frac{\partial q}{\partial z} + \frac{\partial P}{\partial t} \tag{7.2-6}$$

The system is closed by using an equation of state; for single-phase fluid, this takes the form

$$\frac{\partial \nu}{\partial t} = \left(\frac{\partial \nu}{\partial P}\right)_h \frac{dP}{dt} + \left(\frac{\partial \nu}{\partial h}\right)_P \frac{dh}{dt}, \tag{7.2-7}$$

while for two-phase fluid, the equation of state is

$$\frac{\partial v}{\partial t}=\left(\frac{\partial v}{\partial P}\right)_h \frac{dP}{dt}+\left(\frac{\partial v}{\partial x}\right)_P \frac{dx}{dt}\,. \tag{7.2-8}$$

The coefficient F in the momentum equation needs further explanation. The term $F\rho u|u|/2$ accounts for pressure losses along the flow path due to friction, bends, area changes, and orifices or baffles. The coefficient F is the sum of three factors:

1) the frictional factor, fL/D_h, with L the flow element length, D_h the element hydraulic diameter, and f the friction factor. For turbulent single-phase flow, f is the Moody friction factor

$$f=C_1\left\{1+\left(C_2\frac{\varepsilon}{D_h}+\frac{C_3}{\mathrm{Re}}\right)^{C_4}\right., \tag{7.2-9}$$

where C1 - C4 are constants (see Ref. 7-1), ε is the element roughness, and Re is the Reynolds number,

$$RE=\frac{D_h|w|}{A\mu}\,, \tag{7.2-10}$$

with μ the fluid dynamic viscosity. For laminar single-phase flow, f is calculated from

$$f=64/\mathrm{Re}\,. \tag{7.2-11}$$

2) the term $f(L_B/D_B)N_B$, which accounts for pressure losses due to bends. Here, NB is the number of bends along the flow path, and the term (L_B/D_B) is the effective length-to-diameter ratio per bend. The same value is used for (L_B/D_B) on the water side as is used on the sodium side. The friction factor f is the same one just described in 1).

3) the orifice coefficient, G_2. There is no formalism for independently calculating the initial value of G2; in the SASSYS-1 balance-of-plant coding, this coefficient is usually calculated by the code in the steady-state initialization so as to balance the remaining terms in the momentum equation. During the transient calculation, G_2 will vary as orifices change size (e.g., a valve opening or closing). A detailed explanation of how G_2 is computed for various types of components is presented in Section 7.2.3.2 below.

The factor F is then defined as

$$F=f\left(L/D_h\right)+f\left(L_B/D_B\right)N_B+G_2\,. \tag{7.2-12}$$

In the case of two-phase flow, F is still given by Eq. 7.2-12, but now a two-phase friction correlation must be used rather than the single-phase expression of Eqs. 7.2-9 and 7.2-11. The question of modelling pressure drop in a two-phase flow has been examined at length in the literature. The approach taken in the balance-of-plant model is that set forth by Thom in Ref. 7-2, in which he describes a homogeneous equivalent model which makes use of two-phase multipliers to adjust the homogeneous gravitational, acceleration, and frictional pressure drop terms to accommodate general two-phase flow. The assumption is made in the balance-of-plant model that slip between the phases can be neglected. In this case, Ref. 7-2 shows that the gravitational and acceleration terms keep the same forms as for single-phase flow, with the appropriate mixture densities used. The same is assumed to be true for the orifice term. The frictional term is adjusted by multiplying the single-phase liquid friction factor by an empirically-determined two-phase multiplier. This multiplier adjusts the pressure drop computed for saturated liquid at a specific flow and pressure to give the pressure drop corresponding to two-phase flow at the same pressure and mass flow rate. The multiplier is a function of both quality and pressure.

Reference 7-2 presents a table of the two-phase multiplier appropriate to flow through an unheated pipe. The multiplier is given at discrete values of pressure from 250 to 3000 psi and at qualities between 0 and 1. These values were used to develop an expression to be used in the balance-of-plant model for the two-phase multiplier r_5 as a function of pressure and quality. The expression was derived using the method of least squares; it has the form

$$r_5 = 0.9124 + 0.198 \cdot \overline{P} + x\left(-7.38 + 108.7 \cdot \overline{P} - 4.166 \cdot \overline{P}^2\right), \qquad (7.2\text{-}13)$$

where the pressure P is in psi, $\overline{P}$ = P/250, and x is the quality. This expression is accurate to 11% or better for all qualities and for pressures between 250 and 3000 psi; at most points, it is accurate to better than 5%. The two-phase friction factor f_{tp} is then just

$$f_{tp} = r_5 f_\ell \ . \qquad (7.2\text{-}14)$$

7.2.3 Discretized Equations

The analytical forms of the mass, momentum, and energy equations and the equation of state now need to be discretized over the compressible volumes and flow elements of the balance-of-plant nodalization. The result of the discretization will be a set of fully implicit equations which can be solved simultaneously for the changes in pressure, flow, and enthalpy in a timestep. All other quantities (e.g., densities, heat sources) will be computed explicitly.

The first step is to use the momentum equation to express the change over a timestep in the mass flow rate in each segment as a function of the changes in the segment endpoint pressures. Next, the mass and energy equations and the equation of

state can be combined to express the change in pressure within a compressible volume as a function of the changes in the flows of all segments which are attached to the volume. If these two sets of equations are combined by eliminating the change in flow, the resulting matrix equation can be solved for the change in pressure in each compressible volume. The changes in flow and enthalpy, as well as the changes in all explicit variables, can then be determined.

7.2.3.1 Discretization of the Momentum Equation

The momentum equation is discretized segment by segment. In order to represent momentum transport correctly through a segment made up of more than one flow element, the momentum equation must be integrated along the length of the segment, giving

$$\sum_k \frac{L_k}{A_k}\frac{\partial w}{\partial t} = P_{in} - P_{out} - \sum_k \frac{w^2}{A_k^2}\left[\frac{1}{\rho_{O_k}} - \frac{1}{\rho_{I_k}}\right] - \sum_k F(k)\frac{w|w|}{2\bar{\rho}_k A_k^2} - \bar{\rho} g (z_{out} - z_{in}) \tag{7.2-15}$$

where the summation is over all elements in a segment. The form of Eq. 7.2-15 is valid for all element types except pumps; the convective and viscous terms have a different form for pumps, and Eq. 7.2-15 is modified accordingly when a flow segment contains a pump.

The momentum equation must also be discretized over time. The right-hand side of Eq. 7.2-15 is a function only of flow and time and is the net pressure imbalance across the segment, labelled $\Delta P_{net}(w,t)$. If Eq. 7.2-15 is differenced over a timestep $\Delta t = t^{n+1} - t^n$, with $\Delta P_{net}(w,t)$ chosen at the advanced time t^{n+1} and then linearized, the result is

$$\sum_k \frac{L_k}{A_k}\Delta w = \Delta t\left\{\Delta P_{net}(w,t) + \left[\Delta t\left(\frac{\partial \Delta P_{net}}{\partial t}\right)_w + \Delta w\left(\frac{\partial \Delta P_{net}}{\partial w}\right)_t\right]\right\}. \tag{7.2-16}$$

If ΔP_{net} in Eq. 7.2-16 is replaced with the right-hand side of Eq. 7.2-15 and terms are rearranged, the result is an expression for the change in segment flow, Δw, as a function of ΔP_{in} and ΔP_{out}, the changes in pressure at the segment inlet and outlet, respectively:

$$\Delta w = \left\{a_1 + \left[a_2 + \Delta t \cdot \left(\Delta P_{in} - \Delta P_{out}\right)\right]\right\} / \left(a_0 - a_3\right), \tag{7.2-17}$$

where

$$a_0 = \sum_k \frac{L_k}{A_k}, \tag{7.2-18}$$

$$a_1 = \Delta t[P_{in}(t) - P_{out}(t)] + \sum_k \Delta a_1(k),$$

$$\Delta a_1(k) = -\Delta t\left\{\frac{w^2}{A_k^2}\left[\frac{1}{\rho_{O_k}} - \frac{1}{\rho_{I_k}}\right] - F(k)\frac{w|w|}{2\bar{\rho}_k A_k^2} - \bar{\rho}_k g \Delta z_k\right\}, \quad (7.2\text{-}19)$$

$$a_2 = \sum_k \Delta t \frac{\partial}{\partial t}\left(\Delta a_1(k)\right), \quad (7.2\text{-}20)$$

$$a_3 = \sum_k \frac{\partial}{\partial w}\left(\Delta a_1(k)\right), \quad (7.2\text{-}21)$$

7.2.3.2 Further Details on Element Component Models

The discretized momentum equation, Eq. 7.2-17, models flow along a one-dimensional flow path. The path can contain bends, baffles or orifices, and the cross-sectional area of the path can vary. This flow path model serves as the basis for the models for pipes, valves, and check valves. What distinguishes these three component models is the way in which the coefficient *F* is varied with time. The only contributors to *F* which may vary with time are the friction factor and the size of a flow orifice. The friction factor is treated identically in all component models, and so the differences among component models are determined by the way in which each model calculates the orifice coefficient.

The model of a pipe assumes that the orifice coefficient calculated in the steady state is valid through the transient. Therefore, the pipe model keeps the orifice coefficient constant at all times. The valve models, on the other hand, simulate the opening and closing of the valve by varying the orifice coefficient. The pressure drop across a valve is related to the flow through the valve by the equation

$$\Delta P = \frac{w|w|}{\rho C^2 \phi^2(y)}. \quad (7.2\text{-}22)$$

The functional relationship between the valve characteristic ϕ and the stem position y depends on the valve design and is input by the user through tables. The valve is opened or closed by varying the stem position; the user has the option of adjusting y directly or through the harmonic equation

$$m\frac{d^2y}{dt^2} + B\frac{dy}{dt} + ky = F_1(t), \quad (7.2\text{-}23)$$

so that y is controlled by the driver function $F_1(t)$, which is user-input. Since the pressure drop across the valve is related to the orifice coefficient G_2 by

$$\Delta P = G_2 \frac{w|w|}{2\rho A^2}, \tag{7.2-24}$$

where A is the flow area when the valve is fully open, the orifice coefficient can be expressed in terms of the valve calibration constant and characteristic as

$$G_2 = 2\left(\frac{A}{C\phi}\right)^2. \tag{7.2-25}$$

Thus, the valve aperture changes by recomputing the orifice coefficient each timestep, and the value of the coefficient is controlled by the stem position.

The check valve model works much the same as the standard valve model. However, there are a few differences. A check valve is normally either completely open or completely closed, whereas a standard valve can operate partially closed. A check valve changes between open or closed when a user-specified flow or pressure drop criterion within the valve is met. The valve then changes state by adjusting the orifice coefficient to a user-input value within a span of time that is also user-input. The criteria for opening and closing the valve, as well as the length of time the valve takes to open or close, must be set so as to avoid creating numerical instabilities in the calculation.

Because both valve models simulate valve closure by setting the orifice coefficient to a very large value, the flow through a valve in never actually zero. However, if the orifice coefficient is set sufficiently large, the resulting flow through the valve will be negligible.

Modelling pumps must be approached in a different way from that used in modelling pipes, valves, and check valves, since the convective and viscous terms are no longer simple functions of the mass flow rate. The head/flow relationships represented by these terms are instead described by a set of homologous pump curves. Two types of pump curves are available in the balance-of-plant model, one using polynomial fits and one using more complex functional forms. Both options are identical to the corresponding options used in SASSYS-1 for sodium pumps. See Chapter 5 for details of the pump models.

Superheaters are simply steam-filled pipes in which heat transfer is occurring along the length of the pipe. The balance-of-plant model therefore simulates a superheater as a pipe for which the orifice coefficient and the lengthwise-averaged enthalpy, temperature, and density are computed explicitly by a separate superheater model. The superheater model is similar to the steam generator evaporator model, except that no phase change occurs in a superheater. A detailed description of the superheater model is given in Section 7.3.

7.2.3.3 Discretization of the Mass and Energy Equations and the Equation of State

The derivation that follows assumes perfect mixing within a compressible volume. Volumes in which liquid and vapor are separated are discussed in Section 7.4.

The mass and energy equations and the equation of state are solved at each compressible volume. Because the fluid within each volume is assumed to be perfectly mixed, the enthalpy and pressure are uniform within a volume (neglecting the pressure variations due to gravitational head). Therefore, the energy equation can be discretized in space by integrating Eq. 7.2-6 over each volume l and writing a separate energy equation for each volume,

$$V_\ell \frac{\partial \left(\rho_\ell h_\ell\right)}{\partial t} = - V_\ell \nabla\left(\rho u h\right)_\ell + Q_\ell + V_\ell \frac{\partial P_\ell}{\partial t} , \tag{7.2-26}$$

where Q_l is the net rate at which heat enters volume ℓ. Equation 7.2-26 will be easier to work with if density and velocity are eliminated and the equation is rewritten in terms of flows and masses. This is accomplished by using the simple relationship between mass and density, $\rho V = m$, and recognizing that the enthalpy convection term is just the rate at which enthalpy is convected into the volume, so that

$$V_\ell \nabla\left(\rho u h\right)_\ell = - \sum_j h_j \, w_j \, \mathrm{sgn}\left(j, \ell\right) , \tag{7.2-27}$$

where the sum is over all segments which are attached to volume ℓ. Substituting in Eq. 7.2-26 for the convective term and density gives the desired form of the energy equation,

$$\frac{\partial (m_l h_l)}{\partial t} = \sum_j h_j w_j sgn(j, l) + Q_l + V_l \frac{\partial P_l}{\partial t} \tag{7.2-28}$$

Now, the time derivative of the total enthalpy $m_\ell \, h_\ell$ needs to be expanded so that the time derivatives of the mass and the specific enthalpy can be handled separately. To do this, three operations are performed: 1) the derivative of the total enthalpy in Eq. 7.2-28 is discretized over time, 2) the advanced time terms are linearized, and 3) second-order terms are dropped. The result is

$$\frac{\partial \, m_\ell}{\partial t} h_\ell^n + m_\ell^n \frac{\partial h_\ell}{\partial t} = \sum_j h_\ell^{n+1} \, w_j^{n+1} \, \mathrm{sgn}\left(j, \ell\right) + Q_\ell^n + V_\ell \frac{\partial P_\ell}{\partial t} . \tag{7.2-29}$$

This form of the energy equation is a linear function of the volume mass, enthalpy, and pressure and of the enthalpies and flows from the segments attached to the volume. The heat source Q is assumed to be treated explicitly, and the enthalpy convection term is evaluated at the advanced time.

The next step is to eliminate the mass time derivative from the energy equation. This is done by using the mass conservation equation written for volume ℓ and multiplied by the volume V_ℓ,

$$V_\ell \frac{\partial \rho_\ell}{\partial t} = -V_\ell \frac{\partial}{\partial z}(\rho u)_\ell \,. \tag{7.2-30}$$

The left-hand side of Eq. 7.2-30 is just the time derivative of the mass, and the right-hand side is the mass convection term, which is just the net flow into the volume, so that Eq. 7.2-30 can be rewritten as

$$\frac{\partial m_\ell}{\partial t} = \sum_j w_j \,\mathrm{sgn}(j,\ell) \,. \tag{7.2-31}$$

Equation 7.2-31 is just the expression needed to eliminate the mass time derivative from the energy equation; when it is substituted into Eq. 7.2-29, the result is

$$m_l^n \frac{\partial (h_l)}{\partial t} = -h_l^n \textstyle\sum_j w_j^{n+1} sgn(j,l) + \sum_j h_j^{n+1} w_j^{n+1} sgn(j,l) + Q_l^n + V_l \frac{\partial P_l}{\partial t}. \tag{7.2-32}$$

There is one difficulty with the form of the energy equation shown in Eq. 7.2-32 -- the enthalpies at the interfaces between the compressible volume and the attached flow segments are treated implicitly. For the range of problems for which this model has been developed, treating these enthalpies explicitly introduces only small errors at worst. Treating them implicitly results in a solution procedure which is unnecessarily complicated and cumbersome. Therefore, it is assumed that these enthalpies can be treated explicitly. Applying this assumption to Eq. 7.2-32 and also finite differencing the time derivatives and linearizing the advanced time flows produces an energy equation of the form

$$\begin{aligned} m_\ell^n \frac{\Delta h_\ell}{\Delta t} = &-h_\ell^n \sum_j \left(w_j^n + \Delta w_j\right) \mathrm{sgn}(j,\ell) + \sum_j h_j^n \left(w_j^n + \Delta w_j\right) \mathrm{sgn}(j,\ell) \\ &+ Q_\ell^n + V_\ell \frac{\Delta P_\ell}{\Delta t} \,. \end{aligned} \tag{7.2-33}$$

Equation 7.2-33 expresses the change in volume enthalpy as a function of the change in volume pressure and the changes in flow in the attached segments. If the change in enthalpy can be eliminated, the result will be an equation relating the change in volume pressure to the changes in the segment flows. This can then be combined with the expression derived from the momentum equation which relates the change in flow in a segment to the changes in pressure in the volumes at the segment endpoints, producing a matrix equation which can be solved for the pressure changes in the compressible volumes in the system.

The change in volume enthalpy can be eliminated from Eq. 7.2-33 by using the equation of state, Eqs. 7.2-7 and 7.2-8 above. Consider first the case of a volume containing single-phase fluid. The equation of state is then Eq. 7.2-7. An expression for the change in volume enthalpy can be derived from Eq. 7.2-7 if the time derivative of the specific volume is rewritten as

$$\frac{\partial \nu}{\partial t} = -\nu^2 \left(\frac{\partial \rho}{\partial t} \right) = -\frac{\nu^2}{V} \frac{\partial m}{\partial t} = -\frac{\nu^2}{V} \sum_j \left(w_j + \Delta w_j \right) \mathrm{sgn}\left(j, \ell \right). \tag{7.2-34}$$

Therefore, the equation of state takes the form

$$-\frac{\nu_\ell^2}{V_\ell} \sum_j \left(w_j^n + \Delta w_j \right) \mathrm{sgn}\left(j, \ell \right) = \left(\frac{\partial \nu_\ell}{\partial P} \right)_h^n \frac{\Delta P_\ell}{\Delta t} + \left(\frac{\partial \nu_\ell}{\partial h} \right)_P^n \frac{\Delta h_\ell}{\Delta t}, \tag{7.2-35}$$

where the remaining time derivatives have been finite differenced. Equation 7.2-35 is another expression for the change in volume enthalpy as a function of the change in volume pressure and the changes in the segment flows and so can be substituted into the energy equation, Eq. 7.2-33, to eliminate the change in volume enthalpy, giving

$$\begin{aligned} -\frac{\left(\nu_\ell^n \right)^2}{V_\ell} \sum_j \left(w_j^n + \Delta w_j \right) \mathrm{sgn}\left(j, \ell \right) &= \left(\frac{\partial \nu_\ell}{\partial P} \right)_h^n \frac{\Delta P_\ell}{\Delta t} + \left(\frac{\partial \nu_\ell}{\partial h} \right)_P^n \frac{1}{m_\ell^n} \\ &\cdot \left\{ -h_\ell^n \sum_j \left(w_j^n + \Delta w_j \right) \mathrm{sgn}\left(j, \ell \right) + \sum_j h_j^n \left(w_j^n + \Delta w \right) \mathrm{sgn}\left(j, \ell \right) \right. \\ &\left. + Q_\ell^n + V_\ell \frac{\Delta P_\ell}{\Delta t} \right\} \end{aligned} \tag{7.2-36}$$

If the mass of volume ℓ is expressed in terms of V_ℓ and ρ_ℓ and the equation is then rearranged, the result is an equation for the change in volume pressure as a function of the changes in the segment flows:

$$\begin{aligned} \Delta P_\ell = -\Delta t \left\{ Q_\ell^n + \sum_j w_j^n \left[h_j^n - h_\ell + \nu_\ell^n \left(\frac{\partial h_\ell}{\partial \nu} \right)_P^n \right] \mathrm{sgn}\left(j, \ell \right) \right. \\ \left. + \sum_j \Delta w_j \left[h_j^n - h_\ell^n + \nu_\ell^n \left(\frac{\partial h_\ell}{\partial \nu} \right)_P^n \right] \mathrm{sgn}\left(j, \ell \right) \right\} / \\ \left[V_\ell \left(1 + \frac{1}{\nu_\ell^n} \left(\frac{\partial \nu_\ell}{\partial P} \right)_h^n \left(\frac{\partial h_\ell}{\partial \nu} \right)_P^n \right) \right]. \end{aligned} \tag{7.2-37}$$

If volume l contains two-phase fluid, the equation of state must be expressed by Eq. 7.2-8, and the resulting equations are more complex. In the case of a two-phase fluid, the specific volume is a function of pressure and quality, rather than pressure and enthalpy, and so Eq. 7.2-8 cannot be used directly to derive an expression for the change in enthalpy. Instead, the following approach must be taken.

The saturated liquid specific volume and enthalpy can be written respectively as

$$\nu_l = \nu_f + \left(\nu_g - \nu_f\right) x_\ell = \nu_f + \nu_{fg}\, x_\ell \tag{7.2-38}$$

and

$$h_\ell = h_f + h_{fg}\, x_\ell \ . \tag{7.2-39}$$

Differencing Eq. 7.2-38 with respect to time gives

$$\frac{d\nu_\ell}{dt} = \frac{d\nu_f(\ell)}{dt} + x_\ell \frac{d\nu_{fg}(\ell)}{dt} + \nu_{fg}(\ell)\frac{dx_\ell}{dt} \ . \tag{7.2-40}$$

Since the saturated liquid and vapor specific volumes are functions only of pressure, Eq. 7.2-40 can be rewritten in terms of the time derivative of pressure,

$$\frac{d\nu_\ell}{dt} = \frac{dP_\ell}{dt}\frac{d\nu_f(\ell)}{dP} + x_\ell \frac{dP_\ell}{dt}\frac{d\nu_{fg}(\ell)}{dP} + \nu_{fg}(\ell)\frac{dx_\ell}{dt} \ . \tag{7.2-41}$$

Similarly, Eq. 7.2-39 can be expressed as

$$\frac{dh_\ell}{dt} = \frac{dP_\ell}{dt}\frac{dh_f(\ell)}{dP} + x_\ell \frac{dP_\ell}{dt}\frac{dh_{fg}(\ell)}{dP} + h_{fg}(\ell)\frac{dx_\ell}{dt} \ . \tag{7.2-42}$$

The time derivative of quality can be eliminated between Eqs. 7.2-41 and 7.2-42 to give

$$\begin{aligned}\frac{d\nu_\ell}{dt} = -\frac{\nu_\ell^2}{V_l}\sum_j w_j^{n+1}\,\mathrm{sgn}(j,\ell) = \frac{dP_\ell}{dt}\Bigg[&\frac{d\nu_f(\ell)}{dP} + x_\ell\frac{d\nu_{fg}(\ell)}{dP} \\ &-\left(\frac{dh_f(\ell)}{dP} + x_\ell\frac{dh_{fg}(\ell)}{dP}\right)\frac{\nu_{fg}(\ell)}{h_{fg}(\ell)}\Bigg] + \frac{dh_\ell}{dt}\frac{\nu_{fg}(\ell)}{h_{fg}(\ell)} \ .\end{aligned} \tag{7.2-43}$$

Equation 7.2-43 can be used in place of Eq. 7.2-8 to give an expression for the change in volume enthalpy in a two-phase volume. This expression can then be used in the same manner that Eq. 7.2-35 was used above, producing an equation for the change in volume pressure as a function of the changes in the flows in the attached segments:

$$\begin{aligned}\Delta P_\ell = -\Delta t\Bigg\{ & Q_\ell^n + \sum_j w_j^n \left[h_j^n - h_\ell^n + \nu_\ell^n \frac{h_{fg}(\ell)}{\nu_{fg}(\ell)} \right] \mathrm{sgn}(j,\ell) \\ & + \sum_j \Delta w_j \left[h_j^n - h_\ell^n + \nu_\ell^n \frac{h_{fg}(\ell)}{\nu_{fg}(\ell)} \right] \mathrm{sgn}(j,\ell) \Bigg\} / \\ & \Bigg\{ V_\ell \left(1 + \frac{1}{\nu_\ell^n} \left[\left(\frac{d\nu_f(\ell)}{dP} \right)^n + x_\ell \left(\frac{d\nu_{fg}}{dP} \right)^n \right] \frac{h_{fg}(\ell)}{\nu_{fg}(\ell)} \right. \\ & \left. - \left[\left(\frac{dh_f(\ell)}{dP} \right)^n + x_\ell \left(\frac{dh_{fg}}{dP} \right)^n \right] \right) \Bigg\}. \end{aligned} \tag{7.2-44}$$

Equation 7.2-44 for two-phase volumes is equivalent to Eq. 7.2-37 for single-phase volumes.

If the terms

$$\begin{aligned} \mathrm{DHDN} &= \left(\frac{\partial h_\ell}{\partial \nu} \right)_P^n \quad \text{for } \ell \text{ a single-phase volume,} \\ &= \frac{\mathrm{h_{fg}}(\ell)}{\nu_{fg}(\ell)} \quad \text{for } \ell \text{ a two-phase volume} \end{aligned} \tag{7.2-45}$$

and

$$\begin{aligned} \mathrm{DHDN} &= V_\ell \left[1 + \frac{1}{\nu_\ell^n} \left(\frac{\partial \nu_\ell}{\partial P} \right)_h^n \left(\frac{\partial h_\ell}{\partial \nu} \right)_P^n \right] \quad \text{for } \ell \text{ a single-phase volume,} \\ &= V_\ell \left\{ 1 + \frac{1}{\nu_\ell^n} \left[\left(\frac{d\nu_f(\ell)}{\partial P} \right)^n + x_\ell \left(\frac{d\nu_{fg}(\ell)}{dP} \right)^n \right] \frac{\mathrm{h_{fg}}(\ell)}{V_{fg}(\ell)} \right. \\ &\quad \left. - \left[\left(\frac{dh_f(\ell)}{\partial P} \right)^n + x_\ell \left(\frac{dh_{fg}}{dP} \right)^n \right] \right\} \quad \text{for } \ell \text{ a two-phase volume} \end{aligned} \tag{7.2-46}$$

are defined and substituted into Eqs. 7.2-37 and 7.2-44, a single expression for the combined mass and energy equation can be written as

$$\Delta P_\ell = -\Delta t \left\{ Q_\ell^n + \sum_j w_j^n \left[h_j^n - h_\ell^n + \nu_\ell^n \left(DHDN(\ell) \right) \right] \mathrm{sgn}(j,\ell) + \sum_j \Delta w_j \left[h_j^n - h_\ell^n + \nu_\ell^n \left(DHDN(\ell) \right) \right] \mathrm{sgn}(j,\ell) \right\} / DENOM(\ell) . \quad (7.2\text{-}47)$$

7.2.3.4 Further Details Concerning Energy Transfer

Two aspects of energy transfer still have not been discussed in detail. One of these is the calculation of the heat source Q in a heater volume, and the other is the calculation of the enthalpy distribution along an unheated flow segment. These two topics will now be taken up.

7.2.3.4.1 A Simple Heater Model

Because of the wide variety of types of heaters which can be part of a power plant water side, the balance-of-plant model includes nine different heater representations. Eight of these are detailed models of specific types of heaters; these are the focus of most of Section 7.4, and the reader is referred to Section 7.4 for information on them. The ninth model is a very simple, basic one which is retained as an option for the user who wishes to include a heater component in a plant layout but does not want the level of detail involved in using one of the other heater models. This simple model will now be described.

The heat source Q is computed from Newton's law of cooling in the simple heater model. The fluid on the primary side of a heater is modelled as a compressible volume and is in thermal contact with a fluid on the heater secondary side. The heater is assumed to have subcooled liquid as the primary side fluid. The secondary side is assumed to be at a uniform temperature T_s, where T_s is time-dependent and is input by the user in the form of a table of temperature versus time. Neither the secondary side nor the tube separating the two sides is modelled in detail; rather, they are lumped together as a single thermal resistance which is constant throughout the transient. On the primary side, the heat transfer coefficient is computed from the Dittus-Boelter equation in the steady state and is updated during the transient from the Dittus-Boelter correlation (see Appendix 7.2).

The initialization of the heater model in the steady state begins by finding the steady-state heat source from the net rate of enthalpy convection into the heater volume,

$$Q(0) = \sum_j h_j \, w_j , \quad (7.2\text{-}48)$$

where the summation is over all the segments which are attached to the volume. The total heat transfer coefficient for the heater can then be found from Newton's law of cooling as

$$h_{tot}(0) = \frac{Q(0)}{A_{ht}(T_s - T_p)} \tag{7.2-49}$$

Here, A_{ht} represents the heat transfer area between the primary side and the remainder of the heater and T_p is the temperature on the primary side (which is just the temperature of the compressible volume). The Dittus-Boelter equation can now be used to calculate the primary side heat transfer coefficient $h_p(0)$,

$$h_p(0) = 0.023 \frac{k_p(0)}{D_{hp}} \left(\mathrm{Re}(0)\right)^{0.8} \left(P_f(0)\right)^{0.4} . \tag{7.2-50}$$

The variable k_p is the thermal conductivity of the primary side fluid, and D_{hp} the hydraulic diameter of the primary side. Since now both the total heat transfer coefficient and the primary side one are known, the coefficient h_s for the remainder of the heater can be found from the relationship

$$\frac{1}{h_s} = \frac{1}{h_{tot}} - \frac{1}{h_p} . \tag{7.2-51}$$

This coefficient will then stay fixed throughout the transient. This completes the initialization of the heater model.

During the transient, the heat source is treated explicitly, so the heater model coding consists of computing a new value for Q after the pressures, flows, and enthalpies have been updated. To do this, first the current primary side heat transfer coefficient is found from the Dittus-Boelter correlation, then Eq. 7.2-51 is used to update the total heat transfer coefficient. The new value of Q can then be found from Eq. 7.2-49.

7.2.3.4.2 Modelling the Enthalpy Distribution Along a Nonheated Segment

So far, all discussion of calculation of enthalpy has been limited to the enthalpy of fluid in compressible volumes or at the interface between a volume and a segment. However, the enthalpy distribution along a segment must also be computed. This section describes the model used to find the enthalpy distribution within a nonheated segment; Section 7.3 discusses the calculation of enthalpy along the heated segment in a superheater, and Section 7.4 describes how the enthalpy distribution is calculated in the heated segment sections of heaters.

The fundamental assumption of this model is that flow within each unheated segment is adiabatic, so that there is no exchange of heat with the pipe walls, pump impellers, etc. This assumption should be valid for many types of problems and allows the enthalpy distribution to be calculated from a simple, efficient algorithm in which enthalpy is transported from one compressible volume to another. The enthalpy at any point in a segment can be found just by tracking the movement of fluid through the segment over each timestep.

Two assumptions are made in order to initialize the enthalpy distribution along each segment. First, it is assumed that the temperature is constant along each subcooled liquid segment and that this temperature is equal to the temperature of the compressible volume at the segment inlet. Second, for two-phase and vapor segments, it is assumed that the enthalpy along the segment is constant and is equal to the enthalpy of the compressible volume at the segment inlet.

During the transient calculation, the algorithm first solves for segment flows and compressible volume enthalpies and pressures, then invokes the enthalpy transport model to update the segment enthalpy distributions. The enthalpy transport model begins by finding the average over the timestep of the fluid velocity in each segment from the expression

$$\bar{u} = \frac{w^{n+1/2}}{\overline{(\rho A)}} \tag{7.2-52}$$

where

$$\overline{(\rho A)} = \frac{\bar{\rho}}{L} \sum_j A_j \, L_j \, . \tag{7.2-53}$$

The summation is over all the elements in the segment, with A_j the cross sectional area of an element, L_j the element length, and L the length of the segment. It is assumed that the fluid which was in the segment at the start of the timestep has all travelled a distance $\bar{u}\Delta t$ over the timestep. The algorithm therefore shifts the enthalpy distribution by $\bar{u}\Delta t$, plus accounts for fluid which has entered the segment inlet and fluid which has left from the segment outlet. In the case of the first timestep in the transient, this procedure results in information about the enthalpy at three points: the inlet, the outlet, and at $\bar{u}_1\Delta t_1$, the point corresponding to fluid which was at the inlet at the start of the timestep. After the second timestep, the enthalpy will be known at four points along the segment: the inlet, the outlet, at $\bar{u}_2\Delta t_2$ from the inlet, and at $\left(\bar{u}_1\Delta t + \bar{u}_2\Delta t_2\right)$) from the inlet, assuming that this last point has not travelled so quickly as to pass out the segment outlet. The result is that the code tracks the progression of a set of points through each segment each timestep and interpolates between the points if enthalpy values are needed which fall between points (such as at the ends of the elements).

If fluid is moving fairly quickly through a segment, the number of points being tracked will remain small. However, if the flow becomes low enough, a situation could develop in which the algorithm is tracking an unnecessarily large number of points. Therefore, for each segment, a maximum is set on the number of points which can be tracked at one time, and a new point is not added at the end of a timestep if the point added most recently has not moved sufficiently far from the segment entrance.

In the vapor segments, simple enthalpy transport does not always provide an accurate model, since the enthalpy of a highly compressible fluid is sensitive to changes in pressure along the segment. Simple enthalpy transport might, for example, produce

very inaccurate results during a transient in which the vapor moved slowly relative to the changes in pressure with time. Therefore, in the vapor segments, a second algorithm is available which assumes that the enthalpy along the length of a segment is constant in space and is identical to the enthalpy of the fluid in the compressible volume at the segment entrance. The user can set a flag to choose between enthalpy transport or constant enthalpy in vapor segments.

7.2.3.5 Boundary Conditions

Often, it is desirable to perform calculations on only a portion of a power plant and to use boundary conditions to simulate the effect of the remainder of the plant. The balance-of-plant model has two types of boundary conditions available for this purpose: a flow boundary condition and a volume boundary condition. The flow boundary condition specifies flow and enthalpy as a function of time in a special flow segment attached to a compressible volume of the user's choice. The values of flow and enthalpy are either given by the user or are controlled by the plant control system. Multiple flow boundary conditions can be applied to the system. Flow boundary conditions are treated explicitly, and so they contribute to the combined mass and energy equations, Eqs. 7.2-37 and 7.2-44, only in the term

$$\Delta P = -\Delta t \sum_j w_j^n \, h_j^n \, \mathrm{sgn}\left(j, \ell\right), \tag{7.2-54}$$

which is the second term in the numerator. The summation over j must include not only all flow segments which are attached to volume ℓ but also any flow boundary condition attached to the volume.

A volume boundary condition is modelled as a compressible volume in which pressure, enthalpy, and quality as a function of time are either user-input or controlled by the plant control system. The volume can be attached to one or more flow segments. Multiple volume boundary conditions can be designated in a network. A volume boundary condition contributes an endpoint pressure to any flow segments to which it is attached and so affects terms a_1, a_2, and a_3 (Eqs. 7.2-19, -20, -21) in the momentum equation. It also provides inlet enthalpy and quality for any attached segments in which flow is directed out from the boundary condition.

Both flow and volume boundary conditions are updated at the start of each timestep.

7.2.4 Solution Procedure

The result of the discretization procedure described in Section 7.2.3 is a set of two equations: Eq. 7.2-17, which expresses the change in segment flow rate as a function of the changes in segment endpoint pressures, and Eq. 7.2-47, which expresses the change in compressible volume pressure as a function of the changes in the flows in each of the segments attached to the volume. These two equations can be combined into a single equation which has only changes in compressible volume pressures as variables. By substituting Eq. 7.2-17 in Eq. 7.2-47, the segment flows are eliminated, giving

$$\Delta P = -\Delta t \Bigg\{ Q_\ell^n + \sum_j w_j^n \left[h_j^n - h_\ell^n + \nu_\ell^n \, DHDN(\ell) \right] \mathrm{sgn}(j,\ell) + \sum_j \mathrm{sgn}(j,\ell) \Big[h_j^n - h_\ell^n + \nu_\ell^n \, DHDN(\ell) \Big] \cdot \Big[a_1(j) + \big(a_2(j) + \Delta t \left[\Delta P_{in}(j) - \Delta P_{out}(j) \right] \big) \Big] / \left[a_o(j) - a_3(j) \right] \Bigg\} / \, DENOM(\ell) \, . \tag{7.2-55}$$

If Eq. 7.2-55 is written for all L compressible volumes in a system, the result is a set of equations, each of the form

$$\sum_{J=1}^{L} c(I,J) \Delta P_J = d(I) \, . \tag{7.2-56}$$

The forms of the coefficients $c(I,J)$ and the source terms $d(I)$ in Eq. 7.2-56 are most clearly derived by separating out the contribution of each segment in Eq. 7.2-55. Consider a segment k, in which fluid flows from volume I to volume J. If Eq. 7.2-55 is written for volume I, the contribution of segment k to Eq. 7.2-55 can be expressed as the term

$$\Delta P_I(k) = -\Delta t \Big\{ -h_k^n(I) w_k^n + w_k^n \left[h_I^n - \nu_I^n \, DHDN(I) \right] - \left[h_k^n(I) - h_I^n + \nu_I^n \, DHDN(I) \right] \cdot \left[a_1(k) + a_2(k) + \Delta t \left[\Delta P_I - \Delta P_J \right] / \left(a_0(k) - a_3(k) \right) \right] \Big\} / \, DENOM(I) \, . \tag{7.2-57}$$

The term $h_k^n(I)$ is the enthalpy at the interface between segment k and volume 1. Equation 7.2-55 can then be rewritten as

$$\Delta P_1 = -\Delta t \, Q_I^n / \, DENOM(I) + \sum_k \Delta P_I(k) \tag{7.2-58}$$

The signs in Eq. 7.2-58 are consistent with the convention that a positive flow out of a volume is a flow in the negative direction.

Comparing Eqs. 7.2-56 and 7.2-58 shows the contributions from segment k to the coefficients $c(I,J)$ of the pressure changes to be

$$c_k(I,J) = -\Delta t \left(h_k^n(I) - h_I^n + \nu_I^n DHDN(I) \right) \cdot (-\Delta t) / \left[(a_0(k) - a_3(k)) \cdot DENOM(I) \right] \tag{7.2-59}$$

and

$$c_k(J,I) = -c_k(I,J) \tag{7.2-60}$$

while the contribution to the source term $d(I)$ is

$$\begin{aligned} d_k(I) = &-\Delta t\left\{-h_k^n(I)w_k^n + w_k^n\left(h_I^n - \nu_I^n DHDN(I)\right)\right. \\ &-\left(h_k^n(I) - h_I^n + \nu_I^n\, DHDN(I)\right)\left(a_1(k)+a_2(k)\right)/ \\ &\left.\left(a_0(k)-a_3(k)\right)\right\}/DENOM(I), \end{aligned} \tag{7.2-61}$$

and so Eq. 7.2-57 can be rewritten as

$$\Delta P_I(k) = -\Delta P_J\, c_k(I,J) - \Delta P_I\, c_k(I,J) + d_k(I)\ . \tag{7.2-62}$$

Equation 7.2-62 can be substituted into Eq. 7.2-58 with the result, after rearrangement,

$$\Delta P_I\left(1+\sum_k c_k(I,I)\right) + \sum_k \Delta P_{J(k)}\, c_k(I,J) = -\Delta t\, Q_I^n / DEMOM(I) + \sum_k d_k(I)\,. \tag{7.2-63}$$

Comparing Eqs. 7.2-56 and 7.2-63 shows that the coefficients of the pressure changes have the form

$$c(I,I) = 1 + \sum c_k(I,I) \tag{7.2-64}$$

and

$$\begin{aligned} c(I,J) &= \sum_{k\,:\,J(k)=J} c_k(I,J), \end{aligned} \tag{7.2-65}$$

(the range given for the sum in Eq. 7.2-65 is over all segments which run between volumes I and J), while the source term is given by

$$d(I) = -\Delta t\, Q_I^n / DENOM(I) + \sum_k d_k(I). \tag{7.2-66}$$

If Eq. 7.2-56 is written for all L compressible volumes, an LxL matrix equation is created which can be inverted and solved for all L volume pressure changes simultaneously. Once the pressure changes are known, the change in mass flow rate in each segment can be computed from Eq. 7.2-17, and the changes in volume enthalpy can be calculated from the equation of state. The explicit quantities, such as density and heat source, can then be updated.

Note that this procedure constitutes a simultaneous solution for the changes in volume pressure, volume enthalpy, and segment mass flow rate, not just for the changes in pressure. The procedure simply takes advantage of two facts: 1) each flow change is a function of endpoint pressure changes only (as expressed by the momentum equation), and therefore the flow changes can be updated one at a time once the pressure changes have been computed, and 2) the coupling between the changes in enthalpy in neighboring volumes can be eliminated by using the equation of state to express the change in enthalpy as a function of the change in pressure and the changes in the attached segment flows, and so the enthalpy changes can be updated one at a time once the changes in pressure and flow rate are known. The three steps of solving a matrix equation for the changes in pressure, then updating the flows, then updating the enthalpies comprise a simultaneous solution for all three variables.

7.2.5 Coupling Between the Balance-of-Plant Model and the Steam Generator Model

It is important to note that the balance-of-plant model does not include the water side of the steam generator. Instead, the steam generator is modelled separately and is explicitly coupled to the balance-of-plant model. By so doing, the steam generator can be represented without use of the momentum equation (see Section 7.3), thereby significantly reducing the number of implicitly coupled momentum cells in the balance of plant. This is particularly important in a systems analysis code, where a fully-implicit solution scheme can easily result in unacceptably long running times. The omission of a momentum equation in the steam generator requires the assumptions that (1) the pressure drop across the steam generator can be neglected and that (2) the coupling between the steam generator outlet and the remainder of the balance of plant is not very strong; these assumptions are valid in a wide range of operational and accident situations in nuclear power plants.

The coupling between the balance of plant and the steam generator is accomplished by having the steam generator provide a pressure at the subcooled/two-phase interface within the steam generator and a flow from the steam generator outlet into the outlet plenum. A detailed discussion of how the steam generator model calculates the interface pressure and outlet flow is given in Section 7.3. The balance-of-plant model simulates the evaporator subcooled/two-phase interface as a pseudo-compressible volume which serves as a boundary condition volume, with the volume pressure specified by the steam generator model. The coupling is completed by having the balance-of-plant model provide the subcooled region flow and the average steam generator pressure. The subcooled region is treated as one of the flow segments in the balance-of-plant network of segments and volumes, with the steam generator model providing a region-averaged enthalpy which is used to calculate the average liquid temperature and thermodynamic properties needed in the momentum equation. Thus, the balance-of-plant model can calculate the subcooled region flow at the same time that flows in the other flow segments are computed, and it can calculate the steam generator average pressure as the linear average of the pressures in the steam generator inlet and outlet plena.

The coupling between the balance-of-plant and steam generator models requires some time averaging to stabilize the rate of change of the steam generator pressure, as well as limits on the rate of change of the subcooled zone flow; neither constraint affects the accuracy of the overall calculation. A detailed explanation of these constraints is provided in Section 7.3.

7.2.6 Implementation of the Balance-of-Plant Model in SASSYS-1

The coding which implements the mathematical model described in the preceding sections can be divided into two main parts: a steady-state initializer and a transient solution algorithm. The calculational procedure followed in each part will be described now, and then the operation of the coding subroutine by subroutine will be outlined.

7.2.6.1 Steady-State Initialization

The job of the steady-state initializer is to derive the system parameters from the data which the user has entered. The parameters to be calculated include the following:

For volumes:	the density and enthalpy are computed from the equation of state.
For segments:	the length is computed from the element lengths, the endpoint enthalpies are derived from the equation of state, and the enthalpy transport arrays are set to steady-state values.
For elements:	the endpoint enthalpies are found from the equation of state, the orifice coefficient is calculated from the momentum equation, and the gravity head is computed from the average density (found from the equation of state) and the endpoint elevations.
For steam generators:	the inlet enthalpy is set from the inlet plenum enthalpy, and the steam generator pressure is computed as the average of the pressures in the inlet and outlet plena.
For heaters:	the heat transfer coefficients are initialized for the simple heater model; Section 7.4 discusses the initialization procedure for all other types of heaters. In all cases, the heat source term steady state value is computed.
For pumps:	the pump head is computed from the pump element endpoint pressures, and the corresponding pump speed is then determined through an iterative procedure identical to that used for the sodium-side pumps (see Chapter 5).

7.2.6.2 The Transient Solution Algorithm

This algorithm solves the difference equations described earlier at each timestep. The timestep size used is based on the size of the timestep used in the sodium-side calculations by the PRIMAR subroutine. A maximum value for the balance-of-plant timestep is defined as a user-specified fraction of the PRIMAR timestep, with the balance-of-plant timestep always less than or equal to the PRIMAR timestep. However, the balance-of-plant timestep is also limited by the rates of change of the segment flows

and the compressible volume pressures, as well as being limited by rates of change of the steam generator water and sodium flows, metal and sodium temperatures, water enthalpies, waterside void fractions, and waterside heat transfer coefficients. Therefore, depending upon transient conditions, the balance of plant may operate on a significantly smaller timestep than does the sodium loop. The balance of plant and the steam generator models always operate on the same timestep.

The calculation proceeds as follows:

1) For each steam generator, the feedwater enthalpy and flow and average pressure calculated by the balance-of-plant model the previous step are passed to the steam generator algorithm. If a superheater is associated with a steam generator, the superheater model algorithm is called first, then the steam generator model algorithm is used.

2) The steam generator outlet flow and enthalpy and the pressure difference between the subcooled/two-phase interface and the evaporator outlet are transferred to the balance-of-plant coding for each steam generator. For all superheaters, the superheater outlet enthalpy, average temperature, and average density are passed to the balance-of-plant model.

3) Now, the coefficients c(I,J) and source terms d(I) of Eq. 7.2-56 must be calculated. The first step is to compute the terms which depend only on conditions within a compressible volume and do not involve data from the segments. Primarily, this means computing the terms DHDN and DENOM in Eqs. 7.2-45 and 7.2-46.

4) Next, the momentum equation coefficients a_0 through a_3 must be found for each segment (see Eqs. 7.2-18 through 7.2-21).

5) The terms c(I,J) and d(I) can now be assembled by traversing the nodalization segment by segment and using Eqs. 7.2-64 through 7.2-66. The contributions from any flow boundary conditions, given by Eq. 7.2-54, are also included at this time.

6) The matrix equation resulting from step 5 is now solved for the compressible volume pressure changes by using Gauss-Jordan elimination.

7) Now that the changes in the volume pressures over the timestep are known, the updated pressures can be computed, and the updated segment flows can be found from Eq. 7.2-17.

8) The heat source terms for any heaters other than those represented by the simple model are updated now.

9) The new segment flows are used to update the compressible volume densities from Eq. 7.2-31. The changes in the compressible volume enthalpies can be computed from the changes in volume pressures and segment flows using Eq. 7.2-35 for single-phase volumes and Eq. 7.2-43 for two-phase volumes.

10) The enthalpy transport model is now used to calculate the current enthalpy distribution along each segment, except in segments where the user has opted for a uniform enthalpy distribution instead of enthalpy transport.

11) The new pump heads and speeds and the new gravity heads are now calculated. The heater source terms of any heaters represented by the simple heater model are also updated.

7.2.6.3 Code Operation

The calculational procedures just described are implemented by the set of subroutines and functions listed in Table 7.2-1, which includes both a brief description of the usage of each subroutine and identifies the calling subroutine except in the case of material property functions which are called from a number of different subroutines. The structure of the coding made up of these subroutines and functions is diagrammed in Figs. 7.2-1 and 7.2-2. The operation of this coding will now be discussed in some detail.

The progression of the calculation through the steady state initialization is diagrammed in Fig. 7.2-1. The calculational sequence moves from left to right and from top to bottom in the diagram. Subroutine SSPRM4 is an initialization subroutine used by the sodium-side PRIMAR-4 module which has been modified to call the initialization subroutines for the balance-of-plant module also. SSPRM4 begins by calling RENUM, which reads the balance-of-plant input information and rearranges the nodalization to the form that the code will actually use (see Section 7.2.7.1). For volumes for which pressures and temperatures are centered as input data, RENUM also computes the volume enthalpies, and for this task it needs function FINDH. This function uses a Newton-Raphson scheme to solve an equation-of-state for enthalpy as a function of temperature and pressure. FINDH is also used by a number of subroutines in the transient calculation. When RENUM stores information concerning the evaporator model, it uses subroutine MVPPSG to find the correct storage locations for each evaporator; similarly, when RENUM handles superheater information, it uses MVPPSH to store the data correctly for each superheater. The relief valve initializing routine SSRVW is also called from RENUM, as are subroutines SELSRT, which orders members of each component category from smallest to largest user number (this is done in case the user numbering is not consecutive), and PRNTST, which sets flags to invoke prints of just the parameters selected by the user for printing.

Table 7.2-1. Descriptions of the Balance-of-Plant Subroutines

ARF --

This subroutine is used to solve the transcendental equation needed to find heater water level in heaters which are right-circular cylinders oriented so the cylinder axis is parallel to the ground. It is called from WTRDRV.

CHVLW --

This subroutine implements the check valve model. It tests to see whether a check valve has met the criteria for closing (if the valve is open) or opening (if

the valve is closed) and sets the value of the orifice coefficient G2PW correctly before passing control to PIFLSG to compute the contribution of the valve to the segment moment equation. It is called from WTRDRV.

DTLM --

This function performs the log mean temperature difference calculation when the single-node version of the steam generator model is used. It is called from INIT and SGUNIT.

FINDH --

Function FINDH solves the equation of state for enthalpy as a function of temperature and pressure by using a Newton-Raphson scheme. This procedure is necessary because no correlation for enthalpy as a function of temperature and pressure is provided in the set of material properties expressions used in SASSYS.

HFlFUN --

This function computes saturated liquid water enthalpy.

HGlFUN --

This function computes saturated steam enthalpy.

INIT --

This subroutine initializes the evaporator of the steam generator model. It is called from SSSTGN.

INITS --

The superheater is initialized in this subroutine. It is called from subroutine SSSTGN.

MVPPSG --

The variables used in the steam generator model are not subscripted to accommodate more than one steam generator. Therefore, the data for each steam generator are stored in a single array and are transferred in and out as the calculation proceeds from steam generator to steam generator. The subroutine which performs this transfer for the evaporator variables is MVPPSG. It is called from RENUM and from INIT in the steady state and from TSBOP in the transient.

MVPPSH --

This subroutine operates just as MVPPSG does, but it transfers variables for the superheater model rather than the evaporator model. It is called from RENUM and INITS in the steady state and from WTRDRV in the transient.

NAHT --

The sodium heat transfer coefficient for a node within the evaporator is computed in this routine. It is called from INIT in the steady state and from

SGUNIT in the transient.

NAHTS --

The sodium heat transfer coefficient for a node within the superheater is computed in this routine. It is called from INITS in the steady state and from SHUNIT in the transient.

PIFLSG --

This is the subroutine which computes the contribution made to the momentum equation by a pipe element. It is called from WTRDRV.

PLTBOP --

This subroutine saves balance-of-plant data each main timestep for plotting. It is called in the steady state from SSBOP and in the transient from TSBOP.

PMPFLW --

PMPFLW calculates the contribution made by a pump element to the momentum equation of the segment in which the pump is located. It is called by WTRDRV.

PMPFNW --

This subroutine updates the speeds and heads of all pumps on the balance-of-plant side once the updated segment flows have been determined. It is called from WTRDRV.

PRNTST --

This subroutine sets print flags so that only the parameters selected by the user for printing will be printed by subroutine WTRPRT. It is called from RENUM.

PRSH2O --

PRSH2O is called only in the steady state and calculates the orifice coefficient and initial pressure drop for each element except for pumps, for which the orifice coefficient is defined to be zero. It is called from SSBOP.

RENUM --

This subroutine reads the fixed-point balance-of-plant data, generates the nodalization which the code will use internally, and reads the floating-point data. It is called in the steady state from SSPRM4.

REVLW --

This subroutine computes the fractional valve opening area as a function of pressure drop for a relief valve. A simple hysteresis curve is used to represent the opening area, so that the valve does not chatter when the pressure drop is near the point at which the valve opens or closes. The relief valve is modeled to open and close with a response time, which is the maximum valve opening time, to avoid numerical instabilities caused by the step changes in flow. It is called from TSRVW.

SELSRT --

This subroutine orders the members of each component category by user number, from smallest to largest; this allows the code to handle cases in which the user has not used consecutive numbers for members of one or more component categories. It is called from RENUM.

SFFUNW --

This function computes saturated liquid water entropy.

SGFUNW --

This function computes saturated steam entropy.

SGMOM --

This is the subroutine which calculates the momentum equation terms for the subcooled region in the evaporator and for the superheater. It is called from WTRDRV.

SGUNIT --

SGUNIT is the subroutine which computes temperatures and flows in the steam generator. It is also the subroutine which feeds information from the steam generator model to the balance-of-plant model. It is called from TSBOP.

SHIFT --

This subroutine updates beginning-of-timestep variables in the evaporator model. It is called from INIT in the steady state and from SGUNIT in the transient.

SHIFTS --

This subroutine updates beginning-of-timestep variables in the super-heater model. It is called from INITS in the steady state and from SHUNIT in the transient.

SHUNIT --

Temperatures along the superheater are computed by this routine. It is called from WTRDRV.

SSBOP --

This subroutine does the steady-state initialization for the balance-of-plant model. It is called from SSPRM4.

SSCFUN --

This function calculates the subcooled water entropy as a function of pressure and enthalpy.

SSHFUN --

This function calculates the superheated steam entropy as a function of pressure

and enthalpy.

SSHTRW --

Most of the initialization of any heaters is done in SSHTRW. SSHTRW computes the shell-side temperatures and/or the tube-side temperature distribution (along with the surface heat transfer area calibration factor). The heater heat source terms (and the heat source terms in the drain and/or the desuperheating region, if such regions are present) are calculated also in this subroutine. In addition, SSHTRW checks mass and energy conservation and finds the pseudo-heat conduction coefficient. It is called from SSBOP.

SSNZZL --

This subroutine performs the steady-state initialization for the nozzle model. SSNZZL computes the isentropic enthalpy and the fluid density following the isentropic expansion. The steady-state nozzle velocity is calculated, and the nozzle flow area is calibrated in this subroutine. It is called from SSBOP.

SSPMPW --

The steady-state initialization of the pumps in the balance of plant is done in SSPMPW. It is called from SSBOP.

SSPRM4 --

SSPRM4 is a PRIMAR-4 subroutine which is also used to call the steady state subroutines RENUM and SSBOP which initialize the balance-of-plant model. It is called from PRIMAR-4 driver subroutine SSTHRM.

SSRVW --

This subroutine calibrates the relief valve flow area for a fully open valve according to the relief valve capacity. This is done in the steady-state balance-of-plant, when the flow through the relief valve is normally zero. It is called from RENUM.

SSTRBN --

The steady-state initialization of the turbine stage is done in this subroutine. SSTRBN checks the conservation of mass and energy in the turbine stage. It also computes the turbine torque and sets the generator torque. It is called from SSBOP.

TRNSPT --

TRNSPT tracks the transport of enthalpy through each segment in the balance of plant. It is called from subroutine WTRDRV.

TSBOP --

This is the driver subroutine which calls the steam generator model and the balance-of-plant model. It also saves waterside plot data and calls WTRPRT to print waterside output. It is called from TSSTGN.

TSHTRW --

The transient calculation of heater temperatures and heat source are done in TSHTRW. This subroutine updates the heater shell-side temperature and/or the tube-side temperature distribution. The heater heat source terms (and the heat source terms in the drain and/or desuperheating regions, if such regions are present) are also updated in TSHTRW. It is called from WTRDRV.

TSNZZL --

The transient calculation of the nozzle velocity, the isentropic fluid enthalpy, the fluid density following the isentropic expansion, and the flow rate is done in this subroutine. It also generates the coefficients of the nozzle momentum equation for the matrix elements. It is called from WTRDRV.

TSRVW --

This subroutine calls REVLW to check if the relief valve is open or not. It the relief valve is open, TSRVW generates the coefficients of the relief valve momentum equation for the matrix elements and later is called again from WTRDRV to calculate the flow rate; otherwise TSRVW is bypassed and returned to the calling subroutine WTRDRV.

TSTRBN --

This subroutine updates the turbine stage parameters in the transient. TSTRBN calculates the turbine stage work term, updates the turbine torque, and adjusts the rotor angular velocity. It is called from WTRDRV.

VALVEW --

The orifice coefficient used for a standard valve is computed in this subroutine. It is called from TSBOP.

WTRDRV --

WTRDRV is the transient driver for the balance-of-plant calculation. It is in WTRDRV that the updated balance-of-plant parameters are computed. It is called from TSBOP.

WTRPRT --

This subroutine prints the current values for the balance-of-plant parameters. The frequency with which it is called is at the user's discretion. It is called from TSBOP.

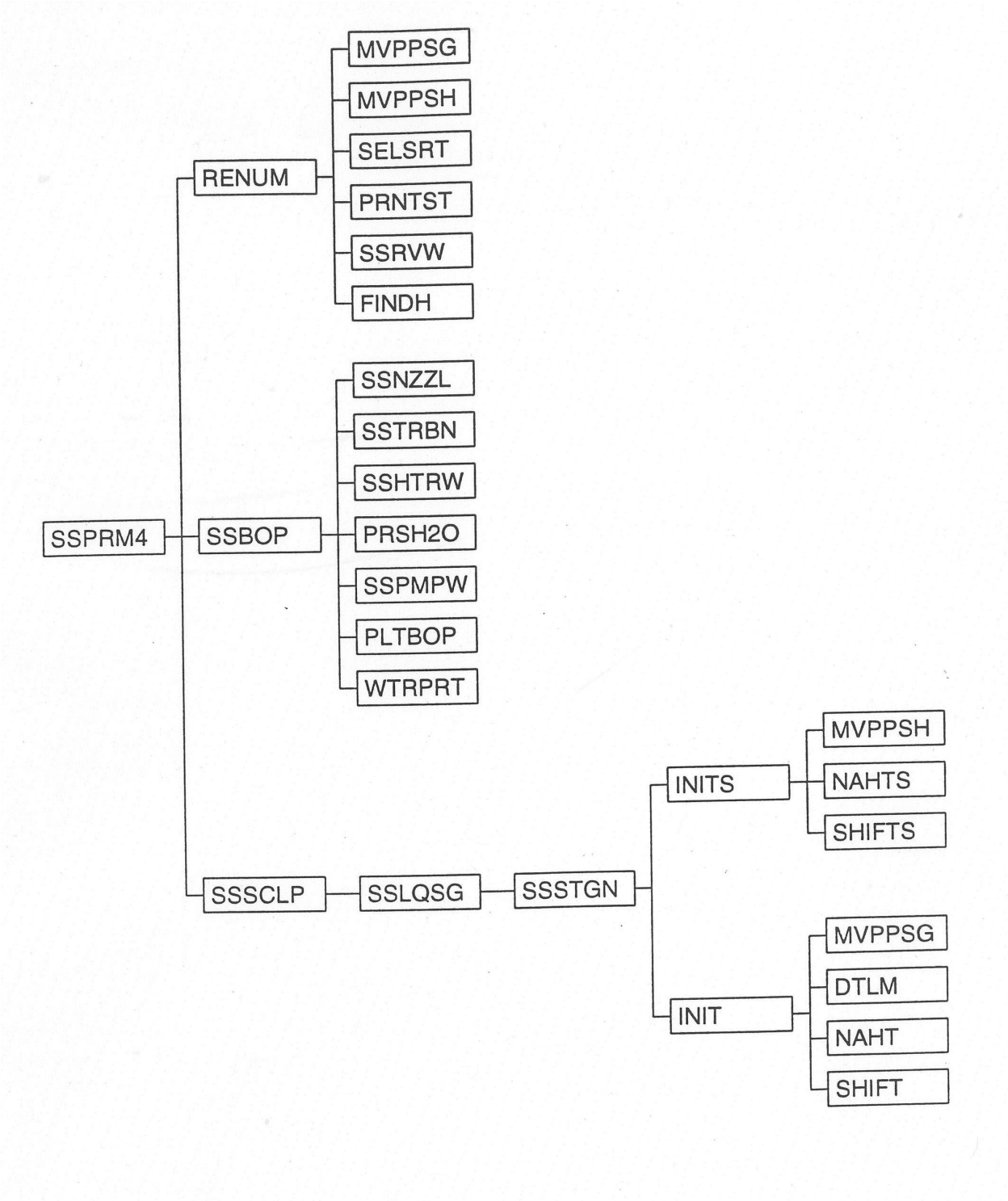

Figure 7.2-1. Steady-State Program Structure

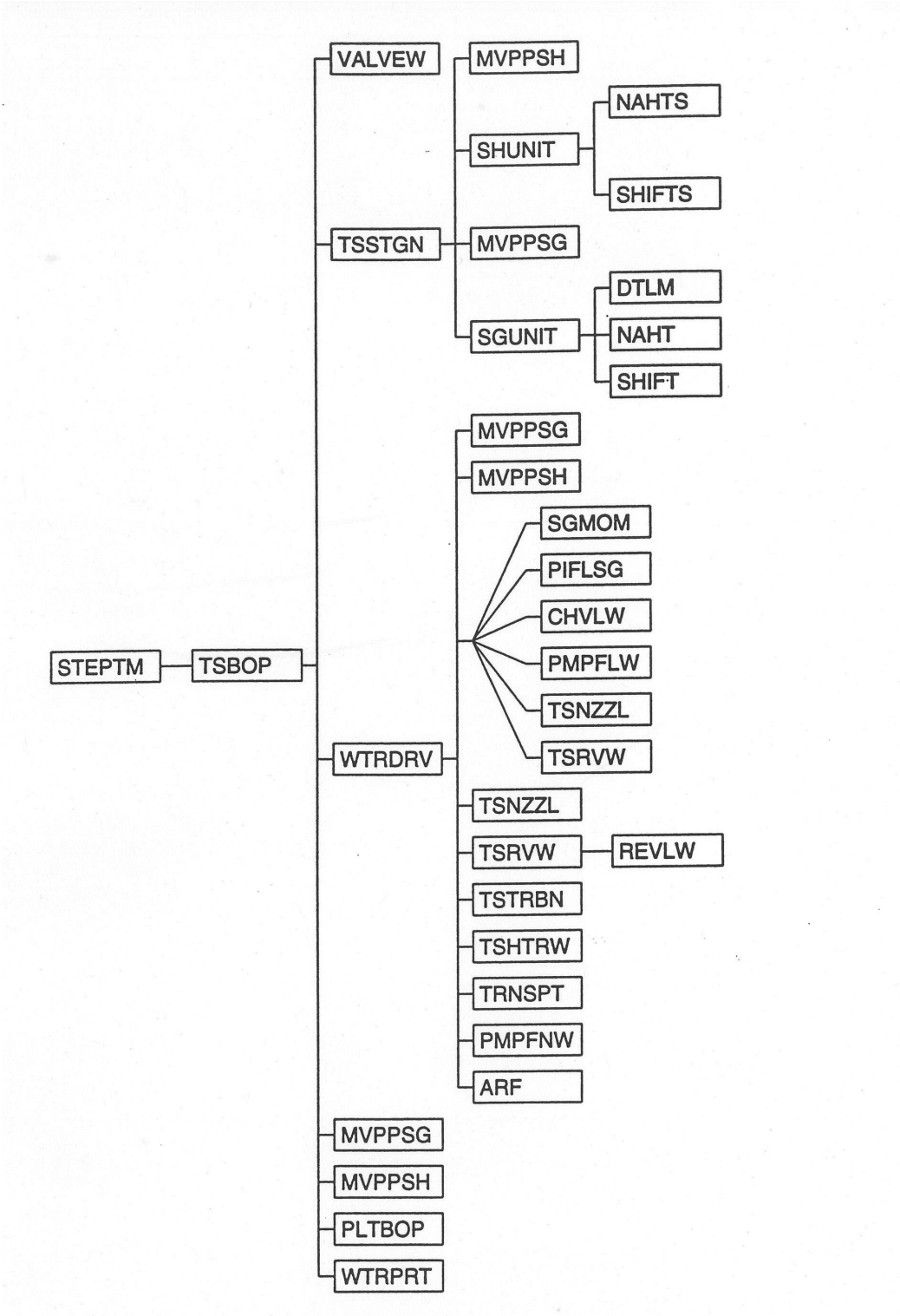

Figure 7.2-2. Transient Program Structure

Once RENUM completes its work, SSPRM4 moves on to call SSBOP to do the remainder of the steady-state balance-of-plant initialization. This is the subroutine in which the steady-state enthalpies, gravity heads, segment lengths, etc. are computed. All the calculations necessary to complete the steady-state initialization of the balance of plant are performed in SSBOP except the initialization of the nozzles, which is done in SSNZZL; the initialization of the turbine, which is done in SSTRBN; the initialization of the heaters, which is done in SSHTRW; the calculation of the element orifice coefficients, which is done in PRSH2O, and the calculation of the pump speed and torque, which is performed in SSPMPW. Finally, SSBOP calls PLTBOP to save steady-state data for plotting.

After the balance of plant has been initialized, SSPRM4 calls SSSCLP, a sodium-side subroutine which in turn calls another sodium-side routine, SSLQSG, which then calls SSSTGN, the steam generator initialization driver. Both the superheater and evaporator models are initialized from this subroutine with calls to INITS and INIT, respectively. Section 7.3 discusses these routines in detail.

With the steady-state initialization completed, the transient calculation can begin. Figure 7.2-2 outlines the progression of the calculation through the coding. The PRIMAR-4 subroutine STEPTM calls subroutine TSBOP, which is the driver for the waterside transient calculation. After updating several parameters to the current sodium-side timestep, TSBOP calls VALVEW to update the condition of all standard valves. The code then begins to operate on the balance-of-plant/steam generator timestep. First, subroutine TSSTGN, the steam generator transient driver, is called. If there are any superheaters in the problem, TSSTGN calls SHUNIT to perform the heat transfer calculation within each superheater. Similarly, if there are any evaporators or once-through steam generators, TSSTGN calls SGUNIT for each one, then updates the parameters which constitute the evaporator/balance-of-plant interface. Both SHUNIT and SGUNIT are discussed in detail in Section 7.3.

The next step for TSBOP is to call WTRDRV, the balance-of-plant driver, to compute the balance-of-plant parameters. WTRDRV has the job of assembling the matrix equation for the compressible volume pressure changes, solving for the pressure changes, and then solving for the remaining balance-of-plant parameters. While most of this work is performed in WTRDRV itself, there are a number of subroutines which contribute to the calculation, as can be seen in Fig. 7.2-2. The momentum equation coefficients for incompressible flow elements are computed by SGMOM for superheaters and for the subcooled region of each evaporator; by PIFLSG for pipes; by CHVLW for check valves; and by PMPFLW for pumps. For compressible flow elements, the momentum equation contributions are computed by TSNZZL for nozzles and by TSRVW for relief valves. Most calculations related to heaters other than those simulated by the simple heater model are performed by TSHTRW; simple heater model calculations take place in WTRDRV. Enthalpy transport is done by a call to TKNSPT, and PMPFNW updates pump heads and speeds. Subroutine ARF is called in conjunction with finding the new water level in some types of heaters.

Once the balance-of-plant calculations for a timestep are completed, TSBOP checks to see if the end of a sodium-side PRIMAR timestep has been reached. If so, TSBOP calls

PLTBOP to save plot data and calls WTRPRT to provide a printout of the waterside parameters. Both PLTBOP and WTRPRT can be called less frequently than once each PRIMAR timestep by setting the frequency of each call through input. If the end of a PRIMAR timestep has not been reached, TSBOP increments the balance-of-plant/steam generator timestep and begins another series of calls to TSSTGN and WTRDRV.

7.2.6.4 Data Input

The input data variable names are defined in Appendix 7.1, which also lists many of the balance-of-plant variables that do not represent input quantities. A complete line-by-line description of the input data is presented in Appendix 2.2.

7.2.7 Creating a Plant Nodalization

The first step in analyzing a particular power plant using the models discussed above is to discretize the plant layout into a network composed of the component models available in SASSYS. The elements of the network (volumes, segments, etc.) must be assigned numbers for use by the code, and there are a few simple rules governing how the numbering is done, as discussed below in Section 7.2.7.1. There are also several features o£ the code which can help simplify the input data required and reduce the size of the problem; these are described in Sections 7.2.7.2 through 7.2.7.4.

7.2.7.1 Rules About Numbering Plant Components

Designing a nodalization for a plant layout involves going through the layout and deciding how best to simulate the plant using the component models available in the code. The plant is thereby reduced to a network of compressible volumes and flow segments, with the segments further divided into flow elements.

Once this network has been created, the nodalization is completed by numbering the volumes, segments and elements. The process of numbering is easy, as there are very few rules which must be followed in order to assemble a nodalization which SASSYS will accept. The balance-of-plant coding was designed to minimize numbering restrictions, primarily to make it easier for the user to add on to an existing nodalization. The current coding requires only that the user assign numbers in the following ranges:

For compressible volumes -- between 1 and 100

For segments -- between 1 and 100

For elements -- between 1 and 200

For pumps -- between 1 and 10

For volume boundary condition tables -- between 1 and 10

For flow boundary condition tables -- between 1 and 10

For standard valves -- between 1 and 40

For check valves -- between 1 and 40

For supersegments -- between 1 and 10

For heaters -- between 1 and 20

For legs of the balance of plant -- between 1 and 10

Steam generators and superheaters must be numbered consecutively beginning with 1 in order to be consistent with the sodium side coding. All members of a category (e.g., all segments) must be assigned unique numbers, but the same number may be used in more than one category (so there can be a segment 6 and an element 6, for example). The numbers used do not have to be consecutive, which makes it easy to add elements within a segment or add new volumes and segments to the entire system. An existing nodalization can be expanded with no renumbering of any item in the original nodalization. Members of a particular category may be assigned any numbers convenient for the user; there is no need to assign the number 1 to some category member.

This very flexible way of handling the nodalization is made possible by a section of the code which performs a renodalization internally once all the data concerning the nodalization set up by the user have been read. The user never sees the internal nodalization; when data are printed out or saved for plotting, they are numbered according to the user's nodalization. However, all the calculations performed by the code are done with the internal nodalization. The code simply renumbers the members of each category according to the order in which information was entered in the data deck (for example, if the user enters data for segment 8 first, then volume 3, then volume 15, then segment 4, the code will assign segment 8 the number 1, segment 4 the number 2, volume 3 the number 1, and volume 15 the number 2). The only exception to this is the elements; the code goes segment by segment (following the internal nodalization segment numbers) and renumbers the elements consecutively within each segment. Ordering the elements consecutively within a segment allows the program to operate more efficiently.

The following discussion will give a description of how subroutine RENUM manipulates the fixed-point input data to create a new nodalization in which each type of component is consecutively numbered starting at number one. There is also extensive documentation of this process within RENUM in the form of comment cards, and anyone with a need to understand this section of the coding in detail should refer to these comment cards.

Once all the fixed-point data are read in, and before any floating-point data are entered, RENUM performs the renodalization. Part of the renodalization process is the creation of arrays which translate between the user's numbering scheme and the scheme resulting from the renodalization. The floating-point data are not entered until after these translator arrays are created so that all floating-point arrays can be automatically ordered according to the renodalization numbering scheme as the data are read from the input file.

The goal of the renodalization is to renumber all components so that the calculations performed in solving the mass, momentum, and energy equations can be executed as efficiently as possible. If the problem is not divided into two or more legs, components of each type are simply numbered in the order in which they were entered

in the fixed-point data block (so that, for example, the first element entered becomes element 1, the first volume entered becomes volume 1, etc.). If the problem is divided into two or more legs, components of each type are grouped by leg, with all components of a given type numbered consecutively within a leg in the order in which they were read in the fixed-point data block. The user must specify the order in which legs are to be arranged through the variable LEGORD.

As the fixed-point data are entered, RENUM keeps count of the total number entered of each component type. The first renodalization task it performs is to add the subcooled region of each steam generator to the total number of flow segments which were read in through input. The code then turns to the compressible volume fixed-point data. These are stored in a temporary array at the time the data are read. RENUM now marches through volume by volume, separating volume boundary conditions from the rest and initializing boundary condition variables both for volumes which are volume boundary conditions and volumes which are attached to flow boundary condition segments. The fixed-point volume data are stored in the correct permanent arrays in the order in which the volumes were read in.

The legs of the loop are now renumbered beginning at one in the order specified by the user in array LEGORD. The array LEGBCK, which translates the user's number for a particular leg into the number assigned by the code, is generated; LEGORD is the translator array from the code numbering to the user's numbering. Once the legs are reordered, the compressible volumes (excluding volume boundary conditions) can be renumbered so that the volumes in leg 1 are numbered consecutively beginning with the number one, in the order in which they were entered in the fixed-point data input; the volumes in leg 2 are ordered consecutively following those in leg 1, etc. The arrays NCVIN and NCVOUT, which mark the first and last volumes in each leg, are set at this time, and the arrays NCVBCK, which translates from the user's numbering of volumes to the code's numbering, and NCVTRN, which translates from the code's numbering to the user's numbering, are both rearranged to be consistent with the renumbering of the volumes by leg. The remaining fixed-point volume input arrays, NTPCVW, NCVBCW, NLGCVW, and NQFLG are also rearranged.

At this point, the code turns to the flow boundary conditions and to the outlet flows passed by the evaporator model to the balance-of-plant coding. The flow boundary condition segments are numbered consecutively leg by leg, and the array JCVW, which specifies the numbers of the compressible volumes at the segment endpoints, is set for each boundary condition segment. The arrays ISGIN and ISGOUT, which designate the first and last boundary condition segments in each leg, are also set at this time. This entire process is then repeated for the segments representing each evaporator outlet flow.

The boundary condition volumes and the evaporator subcooled/two-phase interfaces are next. The code treats the interfaces as additional boundary condition volumes, with the evaporator model providing the thermodynamic parameters at each interface. RENUM first numbers the boundary condition volumes consecutively, with the numbers beginning immediately after the remaining volumes, then numbers the subcooled/two-phase interface in each evaporator in the order of numbering of the

evaporators. The total number of volumes in the problem, then, is the sum of the number of interior volumes, plus the number (if any) of boundary condition volumes, plus the number of evaporator subcooled/two-phase interfaces.

After testing to see that the total numbers of volumes, segments, elements, and pumps do not exceed the dimensions of the arrays associated with these components, the code reorders several fixed-point arrays of volume-related parameters, including JCVW, NLGCVW, NBCCVF, NBCCVP, and ICVSGN. JCVW is also set for the evaporator outlet flow segments at this point. RENUM then moves on to renumbering the segments, grouping them by leg as was done for the volumes. ISGIN and ISGOUT are set here, too, to flag the first and last segment in each leg. Once the segments are renumbered, the code revises all fixed-point segment-related arrays (such as NODMAX, the maximum number of enthalpy transport nodes allowed in a segment) so that these arrays reflect the revised segment numbering rather than the user's original numbering. The elements can now be renumbered, and this is done segment by segment, with elements numbered consecutively within a segment.

The final step in creating the revised nodalization is to generate for each volume the arrays NSEGCV, ISEGCV, and ISGNCV, which give, respectively, the number of segments attached to the volume, the numbers of those segments, and the direction of flow in each attached segment. RENUM then proceeds to read in the balance-of-plant floating-point data.

7.2.7.2 Supersegments

Frequently, the best way to initialize regions containing superheated vapor is to assume that the enthalpy is constant throughout the region. However, the input data available are usually in terms of pressures and temperatures, not enthalpy, and so setting the enthalpy constant in all the volumes and segments making up a region can require some extra calculation on the part of the user and can also result in some input data inconsistencies if the user does not have available the same equation-of-state functions as are used by the code. This difficulty is easily resolved by making use of an input device called a supersegment. A supersegment is a chain of compressible volumes and flow segments, beginning and ending with a volume. The code sets the steady-state enthalpy throughout the chain, up to but not including the terminating volume, to the value of the enthalpy in the volume at the entrance to the supersegment. Up to ten supersegments can be assigned to a nodalization, and a volume can be the terminus of more than one supersegment. Supersegments provide an option which can simplify input data preparation for the user.

7.2.7.3 Legs of the Nodalization

A leg of the nodalization is the set of all volumes and segments contained between two boundary conditions on the water side. A boundary condition in this case can be a flow or volume boundary condition, or it can be an interface between a balance-of-plant component and the steam generator. Any nodalization of a plant can be considered a single leg, but in some cases, it is possible to break the plant up into more than one leg. This has the advantage of reducing the dimension of the matrix equations which must be solved for the changes in volume pressures (i.e., two or more smaller matrix

equations are solved rather than one large one). Such a reduction can be very important if the code is run on a scalar machine; because the code vectorizes well, reducing the size of the matrix is of much less importance if a vector machine is used.

As an example of how to divide a problem into more than one leg, consider a case in which the balance of plant is modelled as beginning at a volume boundary condition, proceeding through a series of pumps, heaters, pipes, and valves up to a steam generator, then finishing past the steam generator with more piping ending in another volume boundary condition. This problem can be split into two legs: one from the inlet volume boundary condition to the subcooled/two-phase interface inside the steam generator, and one from the steam generator outlet plenum to the outlet volume boundary condition. Modelling the problem as two legs instead of one involves slightly more fixed-point input data but may result in significant savings in running time. A decision to try to divide a problem into multiple legs should be based on whether or not the added complexity in the nodalization is justified by any savings in running time; this will depend in part upon the machine being used. For some large problems being run on scalar machines, breaking the problem into legs may be the only cost-effective way to run a transient.

7.2.7.4 Multiplicity

Sometimes, the size of a plant nodalization can be reduced by taking advantage of symmetries which exist at least for some types of transients. The SASSYS code is equipped to take advantage of symmetries by use of a parameter called multiplicity. The operation of multiplicity in the code is best explained by a simple example.

Suppose a plant has two pumps operating in parallel, as in Fig. 7.2-3. Now, some types of problems, the two pumps may behave very differently (e.g., one pump may trip and coast down while the other continues to operate), and so the momentum equation must be solved separately within each segment. However, in other problems, the pumps may operate identically, and so it would be a duplication of effort to solve the momentum equation in each segment. This is where multiplicity comes in. The two pump segments can be replaced by one segment so long as a proper accounting of the flows at the pump header and manifold is done. In this case, the correct flow contribution to each compressible volume is made by defining a multiplicity factor of two and multiplying the segment flow by this factor when solving the conservation equations. A multiplicity factor is needed at each end of any segment, since, in general, duplicate branches of a system can contain more than one segment, and so a factor of two might be needed at one end of a segment while a factor of one might be needed at the other end.

The real value of using multiplicity comes not in a simple case, such as the pump configuration of this example, but in cases involving major branches of the balance of plant. Computing time can be reduced significantly, for instance, in the case of a plant which has two steam generators and therefore two identical branches from the feedwater pump manifold to the high-pressure turbine. In some transients, these two branches will operate identically, and so the use of multiplicity can cut the computing time nearly in half. The use of multiplicity is optional, but it is usually worthwhile to

see if a particular transient can benefit from the use of multiplicity and to reconfigure the plant (and therefore the nodalization) so as to eliminate duplicate branches.

Remember, one branch is a duplicate of another only if both have the same physical configuration and they can be expected to operate identically throughout the transient. Only then can multiplicity be applied.

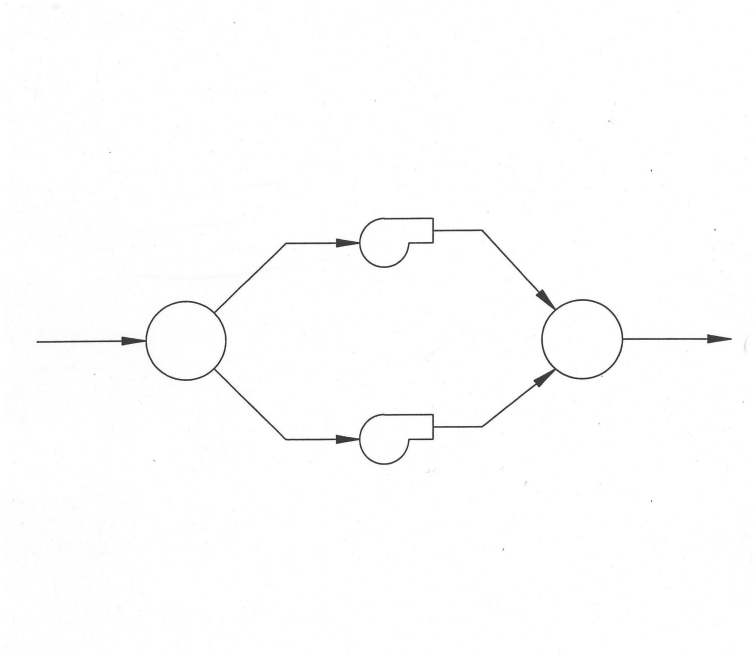

Figure 7.2-3. Exampled Problem for Demonstrating Multiplicity

7.3 Steam Generator Model

7.3.1 Once-Through Steam Generator

In an once-through steam generator subcooled feedwater enters the bottom on the water side and superheated steam comes out the top (see Fig. 7.3-1). Considering that there is a transition boiling zone, the water side is naturally divided into three regions. Figure 7.3-2 shows a detailed schematic of the once-through steam generator. The top of the subcooled zone and the bottom of the boiling zone is defined by the point of saturated liquid enthalpy. The top of the boiling zone and the bottom of the superheated vapor zone is defined by the point of saturated vapor enthalpy. This is the situation during normal steady-state operation. Various transient conditions can produce any situation from a steam generator filled with subcooled water to total dry-out on the water side. The current model can calculate this whole spectrum of conditions with one proviso: there must always be a subcooled liquid region of some finite length at the inlet of the steam generator; but this length can be extremely small. Another way of stating this assumption is that there is no provision for two-phase fluid or superheated vapor in the inlet plenum of the steam generator. Going to the other end of the spectrum of transient cases, the complete disappearance of both the boiling and superheated vapor zones can be calculated. If, however, there is a superheated

vapor zone, there must, of course, be a boiling zone. Each of the three zones, therefore, is treated as a separate calculation with its own node structure and providing boundary conditions for the adjacent region or regions even as each zone length changes during the transient.

The steam generator is, of course, one module in the balance-of-plant sequence. As far as the system is concerned, it represents a pressure drop and a momentum source or sink from a hydrodynamic point of view. The balance-of-plant calculation produces pressures at the inlet and outlet plena of the steam generator as well as the mass flow into the steam generator. As will be shown later, the steam generator model itself calculates outlet flows from the steam generator. The steam generator provides the balance-of-plant momentum equation with an estimate of the pressure drop across the steam generator. This will be discussed later.

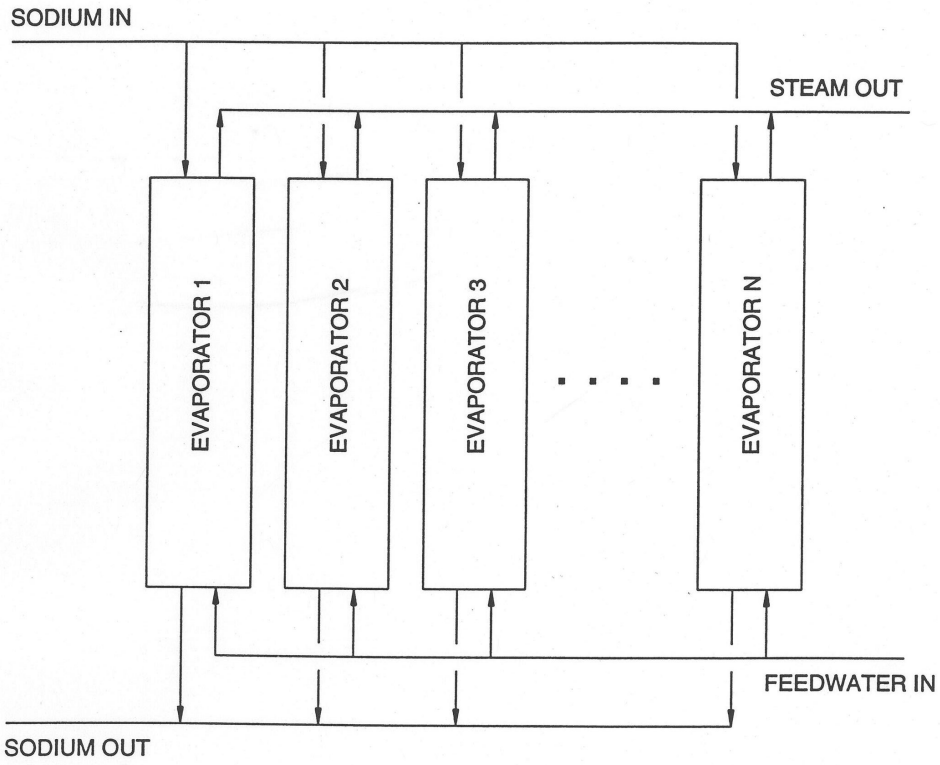

Figure 7.3-1. Once-Through Steam Generator

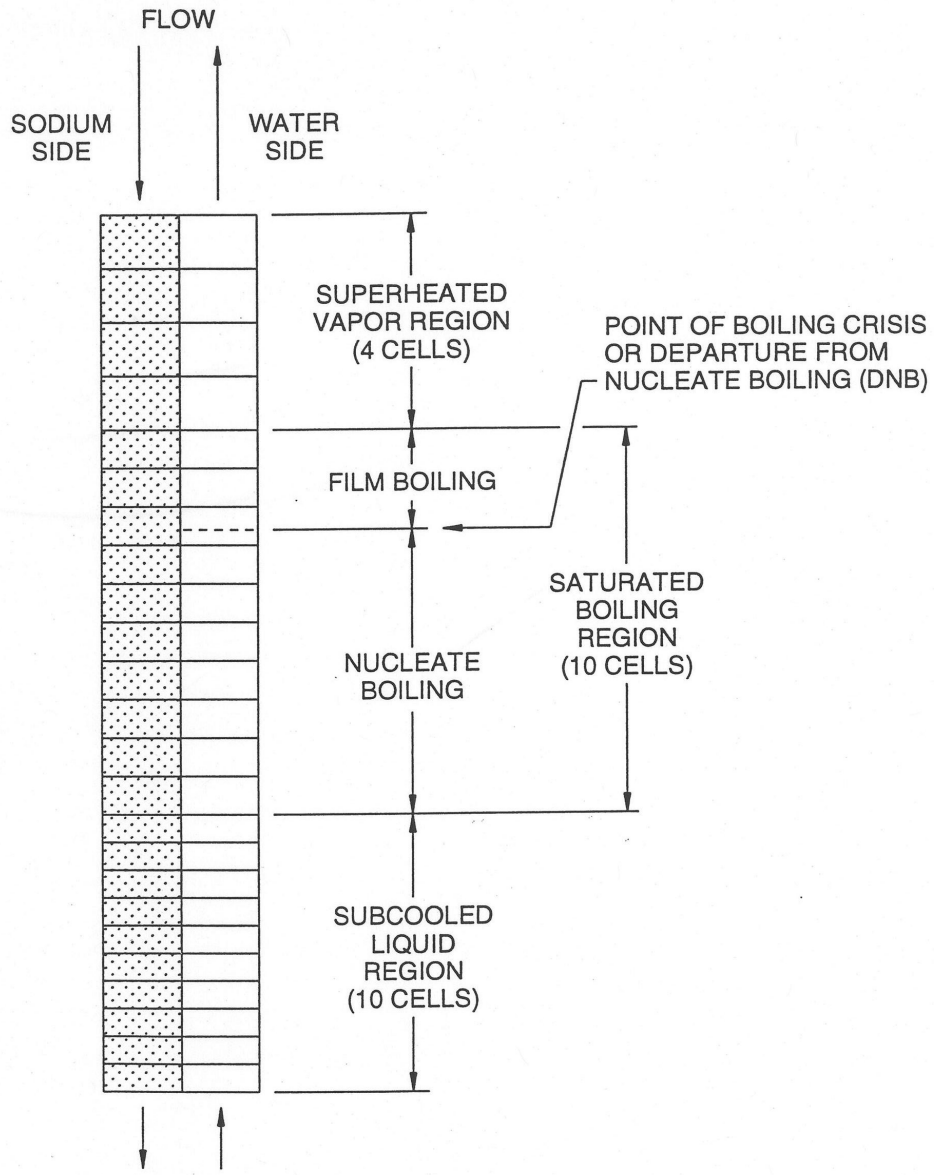

Figure 7.3-2. Schematic of Once-Through Steam Generator

There are two main points to emphasize here, however. First, the inlet and outlet pressures provided by the balance-of-plant momentum equation are simply averaged and this average pressure is used at each time step by the steam generator to calculate properties. Thus no account is taken of the variation of pressure across the steam generator for the purpose of calculating properties. For many and probably most transient calculations of interest, this pressure variation is small and, although not trivial, can be safely neglected in the total context of the calculation. There are some transients, however, involving large pressure reductions downstream of the steam generator, which would produce a significant pressure variation across the steam generator, the neglect of which could lead to some level of inaccuracy.

The second point to emphasize is, given the estimate of the pressure drop across the steam generator, the inlet flow is provided as a boundary condition for the steam generator. There is no momentum equation coupled to the mass and energy conservation equations which characterize the regions in the steam generator to produce velocities. Instead the mass flows above the subcooled zone result from the mass and energy equations alone (as shown below), given the inlet flow as a driving function.

The subcooled liquid and superheated vapor zones each have their own heat transfer regime. The boiling zone has two heat transfer regimes separated at the boiling crisis or departure-from-nucleate-boiling (DNB) point. No smoothing or intermediate regimes are used between these four regimes. This provides of course calculation convenience. Heat transfer phenomena in a steam generator are much more complicated. The adequacy of this heat transfer scheme will be judged by benchmarking against experimental data. The DNB point is crucial to properly characterizing the boiling zone. But tracking the point produces calculation difficulties. This will be explained in some detail later. Suffice it to say here that the DNB point is assumed to be at the intersection of two curves, one representing the local heat flux at the tube wall and the other representing the heat flux required for the boiling crisis to occur. In this way, the point of maximum boiling heat flux is tracked. This DNB point is tracked continuously within the node structure of the boiling zone and the heat flux in the cell where the DNB point is a prorated average of the two boiling heat transfer regimes since the volumetric heat flux is always calculated on a cell-average basis. Depending on the fineness of the node structure, this produces some amount of inaccuracy and approximation to the real physical situation.

The following are general forms of the continuity and of the enthalpy form of the energy conservation equation in one dimension:

$$\frac{\partial \rho}{\partial t} = -\frac{\partial G}{\partial z} \tag{7.3-1}$$

$$\frac{\partial (\rho h)}{\partial t} = -\frac{\partial (Gh)}{\partial z} + Q - (\tau : \nabla v) + \frac{\partial P}{\partial t} + v\frac{\partial P}{\partial z} \tag{7.3-2}$$

Q is a volumetric heat source, $-(\tau : \nabla v)$ represents viscous dissipation and $v(\partial P/\partial z)$ is a work-energy conversion term (representing feedwater pump work, for example). The viscous dissipation term will be dropped for this application because it is small compared to other terms. The work term will also be neglected for the same reason although it is possible that in certain extreme conditions the term could be of some significance. The general energy equation thus becomes,

$$\frac{\partial (\rho h)}{\partial t} = -\frac{\partial (Gh)}{\partial z} + Q + \frac{\partial P}{\partial t} \tag{7.3-3}$$

Incompressible flow is assumed in the subcooled liquid zone. The balance-of-plant momentum equation provides the inlet mass flow, as stated above and thus the mass flow for the whole zone (ΔG=0). Therefore no continuity equation is needed to characterize the region. The enthalpy level and shape and the subcooled region length are all that need be solved for with a coupled set of nodal energy conservation equations. The boundary conditions for flow are the constant mass flow and for energy, the inlet enthalpy and the saturated liquid enthalpy unless the zone reaches the top of the steam generator in which case the region length is known and the outlet enthalpy is calculated. Since is assumed to be zero, the LHS of the energy equation (7.3-3) can be simplified. The density changes over the transient as a result of changes in pressure and enthalpy but these changes are taken into account by updating the density at the end of each time step in the transient after new enthalpies and pressures are obtained.

In the boiling region, compressible flow is calculated with sets of nodal mass and energy conservation equations. The equations are formulated in terms of the void fraction instead of density and enthalpy. This is conveniently done since saturation conditions are always assumed and a no slip condition between phases is assumed; and also because saturation properties are functions of pressure alone. Thus simultaneous nodal continuity and energy equations are used to solve for mass flows and void fractions. The boundary conditions at the bottom of the zone are the single-phase liquid flow and the saturated liquid enthalpy (i.e. void fraction zero). At the top of the zone, there is either the saturated vapor enthalpy (i.e. void fraction 1.0) or, if the boiling zone extends all the way to the top of the steam generator, then the void fraction is a free variable and only lower boundary conditions are required. When the zone does not extend to the top of the steam generator, then the upper boundary condition of the saturated vapor enthalpy is used by requiring that the length of the zone be adjusted until the upper boundary condition is satisfied.

Compressible flow is also assumed in the superheated vapor region. The boundary conditions at the bottom of the zone are the saturated vapor enthalpy and the mass flow calculated at the top of the boiling zone. Since the length of the zone is known, simultaneous nodal mass and energy equations are used to solve for enthalpies and mass flows all the way to the top of the steam generator.

On the sodium side, there is no change of phase and consequently the liquid can be adequately treated with incompressible flow. There is a calculation of the sodium flow external to the steam generator calculation so that, as far as the steam generator is concerned, the mass flow is given. Therefore no continuity equation is required. Besides the mass flow, the only boundary condition required is the inlet sodium temperature at the top of the steam generator. Only the nodal energy equation is required to solve for the enthalpy shape on the sodium side. In addition, given the relatively stable and low pressure conditions on the sodium side, the pressure term in the energy equation (7.3-3) can be safely neglected.

The heat capacity of the tube wall separating the water and the sodium must be taken into account. Therefore its effect on the heat transfer from the sodium to the water is treated by means of a wall temperature calculation. With no convective or

pressure terms the energy equation (7.3-3) becomes much simplified. Also, the density is assumed to be temperature independent which further facilitates the solution.

7.3.2 Recirculation-Type Steam Generator

Figure 7.3-3 depicts a steam generator which consists of several evaporators, several superheaters, a steam drum and a recirculation loop. Subcooled water is pumped into the bottom of the evaporator. Within the evaporator the water boils and a two-phase fluid, typically of very high quality, leaves the top of the evaporator and enters the steam drum. One exit line from the steam drum transports saturated steam to the bottom of the superheater where more heat is added so that highly superheated steam leaves the top available for the turbines. The other exit line from the steam drum transports saturated liquid to the pump but before reaching the pump it is mixed with feedwater. This mixture is substantially subcooled, therefore, and is pumped back to the evaporator to complete the cycle.

The modeling of the evaporator can be done with the once-through steam generator model which is designed to model any situation from a liquid-filled steam generator to the normal operating condition for a once-through type with superheated vapor exiting the top. Thus the physical modeling assumptions of the previous section apply to the evaporator.

The modeling of the superheater is different, however, than the super-heated vapor zone of the previous section. Without elaborating on the details, it is sufficient here to say that the momentum equation of the balance-of-plant model is much more tractable if the assumption of incompressible flow is made for the superheater. Since the superheater operates at quite high pressures, this incompressibility assumption is probably adequate in most transient conditions. There may, however, be certain conditions when the pressure in the superheater is greatly reduced when inaccuracies may result from this assumption. A study of this effect would have to be undertaken to decide the issue and it has not been done so far. The lower boundary condition besides the given mass flow is the inlet enthalpy (i.e. the saturated vapor enthalpy). Thus the enthalpy shape is determined given these conditions. The density is updated each time step during the transient after new enthalpies and pressures have been determined.

The steam drum is modeled as a zero-dimensional reservoir in the sense that perfect mixing of all incoming fluid and the pre-existing separated two phases is presumed. There is one proviso here, however: the liquid level must be tracked so that appropriate action can be taken when liquid may enter the pipe to the superheater or vapor may enter the pipe to the recirculation pump.

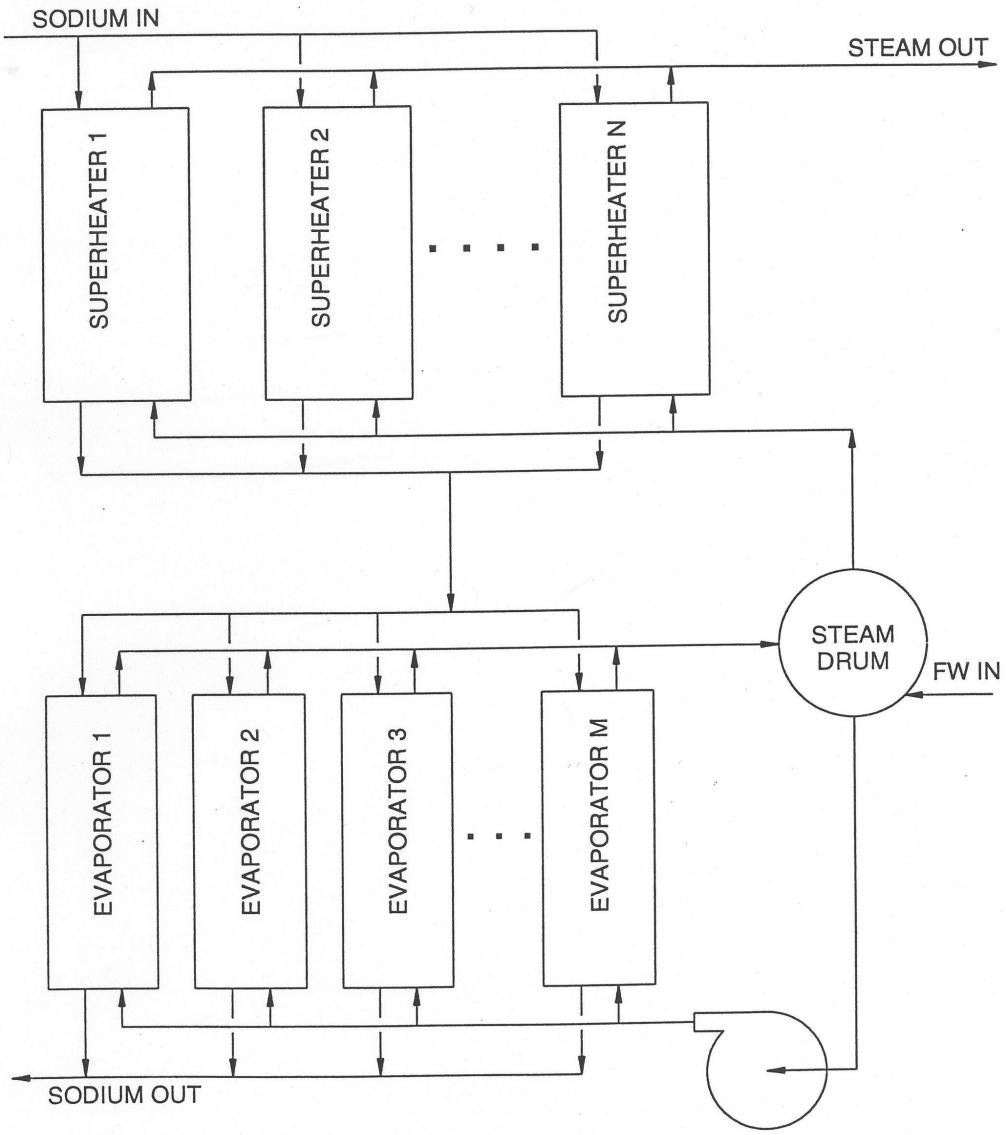

Figure 7.3-3. Steam Generator with Separate Evaporator and Superheaters and Recirculation Loop

7.3.3 Numerical Solution Methods

7.3.3.1 Once-Through Steam Generator

7.3.3.1.1 General Forms of the Conservation Equations

Before the individual solution methods for each water side region and the sodium side can be considered, general forms of the continuity and energy equations must be developed. Equations will be given for one node of the multi-node system of equations. Integration of the continuity Eq. 7.3-1 over the length of one cell from Z_i to Z_{i+1} gives,

$$\int_{Z_i}^{Z_{i+1}} \frac{\partial}{\partial t} \rho dz = -\int_{Z_i}^{Z_{i+1}} \frac{\partial}{\partial z} G dz \tag{7.3-4}$$

According to Leibnitz's Theorem,

$$\int_{Z_i}^{Z_{i+1}} \frac{\partial}{\partial t} \rho dz = \frac{d}{dt} \int_{Z_i}^{Z_{i+1}} \rho dz - \rho_{i+1} \dot{Z}_{i+1} + \rho_i \dot{Z}_i \tag{7.3-5}$$

Equation 7.3-4 becomes,

$$\frac{d}{dt} \int_{Z_i}^{Z_{i+1}} \rho dz - \rho_{i+1} \dot{Z}_{i+1} + \rho_i \dot{Z}_i = -\int_{Z_i}^{Z_{i+1}} \frac{\partial}{\partial z} G dz \tag{7.3-6}$$

Therefore,

$$\frac{d}{\mathrm{dt}} \{\overline{\rho}_i \Delta Z_i\} - \rho_{\mathrm{i+1}} \dot{Z}_{\mathrm{i+1}} + \rho_{\mathrm{i}} \dot{Z}_{\mathrm{i}} = -\Delta \mathrm{G_i} \tag{7.3-7}$$

Donor-cell differencing is used to enhance numerical stability. In order to write the equation in donor-cell form, let ρ_{i+1} replace the average value over the interval, $\overline{\rho}_i$ and simplify,

$$\dot{\rho}_{i+1} \Delta Z_i - \Delta \rho_i \dot{Z}_i = -\Delta G_i \tag{7.3-8}$$

Integration of the enthalpy form of the energy Eq. 7.3-3 from Z_i to Z_{1+1} gives,

$$\int_{Z_i}^{Z_{i+1}} \frac{\partial}{\partial t} (\rho h) dz = -\int_{Z_i}^{Z_{i+1}} \frac{\partial}{\partial z} (Gh) dz + \int_{Z_i}^{Z_{i+1}} Q dz + \int_{Z_i}^{Z_{i+1}} \frac{\partial}{\partial z} P dz \tag{7.3-9}$$

According to Leibnitz's theorem,

$$\int_{Z_i}^{Z_{i+1}} \frac{\partial}{\partial t}(\rho h)dz = \frac{\mathrm{d}}{\mathrm{dt}} \int_{Z_i}^{Z_{i+1}} (\rho h)dz - (\rho h)_{\mathrm{i+1}} \dot{Z}_{\mathrm{i+1}} + (\rho h)_{\mathrm{i}} \dot{Z}_{\mathrm{i}} \tag{7.3-10}$$

$$\int_{Z_i}^{Z_{i+1}} \frac{\partial}{\partial t} P dz = \frac{d}{dt} \int_{Z_i}^{Z_{i+1}} P dz - P_{i+1} \dot{Z}_{i+1} + P_i \dot{Z}_i \tag{7.3-11}$$

Equation (7.3-9) becomes

$$\begin{aligned} \frac{d}{dt} \int_{Z_i}^{Z_{i+1}} (\rho h) dz - (\rho h)_{i+1} \dot{Z}_{i+1} + (\rho h)_i \dot{Z}_i = - \int_{Z_i}^{Z_{i+1}} \frac{\partial}{\partial z}(Gh) dz + \int_{Z_i}^{Z_{i+1}} Q dz \\ + \frac{d}{dt} \int_{Z_i}^{Z_{i+1}} P dz - P_{i+1} \dot{Z}_{i+1} + P_i \dot{Z}_i \end{aligned} \tag{7.3-12}$$

Therefore,

$$\begin{aligned} \frac{d}{dt}\left\{\left(\overline{\rho h}\right)_i \Delta Z_i\right\} - (\rho h)_{i+1} \dot{Z}_{i+1} + (\rho h_i) \dot{Z}_i = -\Delta(Gh)_i + Q_i \Delta Z_i \\ + \frac{d}{dt}\left\{\overline{P}_i \Delta Z_i\right\} - P_{i+1} \dot{Z}_{i+1} + P_i \dot{Z}_i \end{aligned} \tag{7.3-13}$$

In order to write Eq. 7.3-13 in donor-cell form, let $(\rho h)_{i+1}$ replace the average value over the interval $[\rho h]_i$, let P_{i+1} replace $\overline{P}_i$, and simplify,

$$\left(\rho \dot{h}\right)_{i+1} \Delta Z_i - \Delta(\rho h)_i \dot{Z}_i = -\Delta(Gh)_i + Q_i \Delta Z_i + \dot{P}_{i+1} \Delta Z_i - \Delta P_i \dot{Z}_i \tag{7.3-14}$$

As discussed before, the pressure variation across the steam generator is neglected, i.e., $\Delta P_i = 0$, and Eq. 7.3-14 becomes

$$\left(\rho \dot{h}\right)_{i+1} \Delta Z_i - \Delta(\rho h)_i \dot{Z}_i = -\Delta(Gh)_i + Q_i \Delta Z_i + \dot{P} \Delta Z_i \tag{7.3-15}$$

Each of the three regions on the water side is divided into a fixed number of cells. Since the region lengths vary during the transient, the cell lengths also vary and are thus a constant fraction of the varying region length. Thus $\Delta Z_i = \frac{1}{n} \cdot Z_x$ where Z_x is the current length of region *x* and *n* is the number of cells in region *x*. Therefore the subscript *i* can be dropped for ΔZ_i in equations for a given region. On the sodium side, the same node structure is used as on the water side in order to simplify the calculation,

although the precise node structure on the sodium side is not nearly as important as on the water side since there is no change of phase and properties thus calculated parameters change gradually and smoothly over the length of the steam generator.

All spatially variable parameters except two are evaluated at the cell boundary so that there are n+1 values needed to characterize a region, where n is the number of cells in the region. The two exceptions are the tube wall enthalpy and the heat flux. The volumetric heat source is most conveniently calculated on a cell-average basis so that n cells exactly encompass the whole of the heat transfer for a given region. If the heat source were calculated at the cell edge, then half-cells would have to be used at the ends of a region where the heat transfer coefficients change form. In order to calculate the temperature gradients for the heat flux, linear averages over the cell length are computed from the cell-edge values for water and sodium. However, there is no need to calculate the tube wall temperature at the cell edge and a cell-centered value is most convenient for the heat flux calculation. Other parameters such as enthalpies, void fractions, mass fluxes, etc. are most conveniently calculated at the cell-edge since this is where the boundary conditions are defined.

7.3.3.1.2 Subcooled Liquid Region

In the subcooled region, the mass flow is assumed to be uniform throughout the zone due to incompressible flow. Each time step during the transient an updated inlet mass flow is provided to the steam generator from the explicitly-coupled momentum equation. Therefore no continuity equation is required. The coupled set of nodal energy conservation equations are used to determine the length of the zone and the nodal enthalpies simultaneously using the inlet enthalpy and the saturated liquid enthalpy as boundary conditions. Or, alternatively, when liquid fills the steam generator and the zone length is known, the outlet enthalpy is instead determined.

Using Eq. 7.3-15 and setting $\dot{\rho}$ = 0 because of the incompressible flow, and recalling that ΔZ_i is invarient within a zone, the following results for node *i*,

$$\dot{h}_{i+1}\,\rho_{i+1}\,\Delta Z-\Delta\left(\rho h\right)_i\dot{Z}_i=-\Delta\left(Gh\right)_i+Q_i\,\Delta Z+\dot{P}\Delta Z \tag{7.3-16}$$

The following is Eq. 7.3-16 in finite difference form,

$$\begin{aligned}&h_{i+1}^{k+1}\frac{1}{\Delta t}\rho_{i+1}^{k}\frac{1}{n}Z_{SC}^{k}-h_{i+1}^{k}\frac{1}{\Delta t}\rho_{i+1}^{k}\frac{1}{n}Z_{SC}^{k+1}-\bar{\rho}_i^{k}\left(h_{i+1}^{k}-h_i^{k}\right)\frac{i-1}{n}\\&\cdot\frac{1}{\Delta t}\left(Z_{SC}^{k+1}-Z_{SC}^{k}\right)=-G^{k+1}\left(h_{i+1}^{k+1}-h_i^{k+1}\right)+Q_i^{k}\frac{1}{n}Z_{SC}^{k+1}+\dot{P}\frac{1}{n}Z_{SC}^{k+1}\end{aligned} \tag{7.3-17}$$

There are several points to note concerning Eq. 7.3-17. The ΔZ in the first term on the LHS is treated semi-implicitly in time since h_{i+1}^{k+1} is multiplied by Z_{SC}^{k}, the value at the beginning of the time step and h_{i+1}^{k+1} is multiplied by Z_{SC}^{k+1}, the value at the end-of-step which needs to be determined. h_{i+1}^{k+1} cannot be multiplied by the end-of-step value without making the equation set non-linear. Making the term semi-implicit as opposed

to fully explicit has been found to enhance stability in the calculation. The next point is that the density is entirely explicit in time. It is updated at the end of every time step as enthalpy and pressure change. This is consistent with the assumption of incompressibility as density changes slowly and gradually over time. Note also the use of $\bar{\rho}_i^k$ in the third term on the LHS of Eq. 3-17. $\Delta\rho h_i$ becomes $\rho\Delta h_i$ in order to preserve the proper sign of the term. Using $\bar{\rho}_i^k$ which is 0.5 $\left(\rho_{i+1}^k + \rho_i^k\right)$, introduces only a small error so long as the mesh structure is not too coarse. Δh_i must be explicit in time because it is multiplied by Z_{SC}^{k+1} and the equation must be kept linear. G^{k+1} in the convective term implies that the inlet mass flow is updated before the steam generator solution begins. The volumetric heat source is totally explicit since the temperatures used in calculating the ΔT and the properties contained in the heat transfer correlation (see Appendix 7.2) cannot be made implicit without making the equation insoluble.

Rearranging Eq. 7.3-17 according to coefficients there are n equations of the following form,

$$\begin{aligned}
&\left[-G^{k+1}\right]\cdot h_i^{k+1} + \left[\frac{1}{\Delta t}\rho_{i+1}^k \frac{1}{n} Z_{SC}^k + G^{k+1}\right]\cdot h_{i+1}^{k+1} \\
&\quad + \left[-h_{i+1}^k \frac{1}{\Delta t}\rho_{i+1}^k \frac{1}{n} - \bar{\rho}_i^k \left(h_{i+1}^k - h_i^k\right)\frac{i-1}{n}\frac{1}{\Delta t} - Q_i^k \frac{1}{n} - \dot{P}\frac{1}{n}\right]\cdot Z_{SC}^{k+1} \\
&\quad = -\rho_i^{-k}\left(h_{i+1}^k - h_i^k\right)\frac{i-1}{n}\frac{1}{\Delta t} Z_{SC}^k
\end{aligned} \tag{7.3-18}$$

Equation (7.3-18) can be written as,

$$a_i h_i + b_i h_{i+1} + c_i Z_{SC} = d_i \tag{7.3-19}$$

In the case where the liquid region does not reach the top of the steam generator, h_1 and h_{n+1} are known, since they are the inlet enthalpy and h_f. h_2 - h_n and Z_{SC} are unknown (n unknowns) and are solved for as follows. (The superscript k+1 is dropped as unnecessary.)

From the first equation of the equation set (7.3-19), solve for h_2, then for h_3 from the second equation and so on,

$$\begin{aligned}
h_2 &= e_1 + f_1 Z_{SC};\ e_1 = \frac{d_1 - a_1 h_1}{b_1},\ f_1 = -\frac{c_1}{b_1} \\
h_3 &= e_2 + f_2 Z_{SC};\ e_2 = \frac{d_2 - a_2 e_1}{b_2},\ f_2 = -\frac{c_2 + a_2 f_1}{b_2} \\
h_{i+1} &= e_i + f_i Z_{SC};\ e_i = \frac{d_i - a_i e_{i-1}}{b_i},\ f_i = -\frac{c_i + a_i f_{i-1}}{b_i}
\end{aligned} \tag{7.3-20}$$

Finally, in the equation for h_{n+1}, Z_{SC} can be solved for since h_{n+1} is known. Then each of h_2 - h_n can be solved for since they are all functions of only Z_{SC} in the equation set (7.3-20).

If the steam generator is filled with liquid, then the outlet enthalpy is unknown and there are n equations with h_2 - h_{n+1} as the unknowns. Eq. 7.3-16 becomes the following in finite difference form (the zone length, now constant as the length of the steam generator, is denoted simply as Z_{SC}),

$$\frac{1}{\Delta t}\rho_{i+1}^{k}\frac{1}{n}Z_{SC}\left(h_{i+1}^{k+1}-h_{i+1}^{k}\right)=-G^{k+1}\left(h_{i+1}^{k+1}-h_{i}^{k+1}\right)+\frac{1}{n}Z_{SC}\left(Q_{i}^{k}+\dot{P}\right) \tag{7.3-21}$$

The following equations are simply solved from the bottom to the top of the steam generator successively,

$$h_{i+1}^{k+1}=\frac{\frac{1}{\Delta t}h_{i+1}^{k}\rho_{i+1}^{k}\frac{1}{n}Z_{SC}+G^{k+1}h_{i}^{k+1}+Q_{i}\frac{1}{n}Z_{SC}+\dot{P}\frac{1}{n}Z_{SC}}{\frac{1}{\Delta t}\rho_{i+1}^{k}\frac{1}{n}Z_{SC}+G^{k+1}} \tag{7.3-22}$$

7.3.3.1.3 Boiling Region

In the boiling zone, the fluid is treated as compressible. Simultaneous nodal equations are solved for void fraction, mass flow and region length. Boundary conditions are the saturated liquid enthalpy and subcooled region mass flow at the bottom of the boiling zone and either the saturated vapor enthalpy at the top of the zone or, if there is no superheated vapor zone, the region length is defined and the outlet enthalpy is determined. Only the pressure and the volumetric heat source are treated explicitly in time. The void fraction, the mass flow and the region length are all treated in fully implicit fashion. An iterative method is used to solve for the region length. The current value of the region length is held constant for each pass in the iteration while nodal void fractions and mass flows are calculated from the mass and energy equations. When the uppermost void fraction in the boiling zone is computed at the end of an iteration, its value is compared to 1.0 and the region length is adjusted appropriately and the iterative process continues until convergence. When the boiling zone extends to the top of the steam generator, the same method is used but there is no iteration since the region length is known.

First, a number of definitions and identities concerning a two-phase fluid must be reviewed. ρ_f and h_f are the saturated liquid density and enthalpy respectively. ρ_g and h_g are the saturated vapor density and enthalpy. $\rho_{fg} = \rho_g - \rho_f$. $h_{fg} = h_g - h_f$. The density of the two-phase mixture is, with α denoting the void fraction,

$$\rho=\alpha\rho_{fg}+\rho_{f} \tag{7.3-23}$$

The enthalpy of the two-phase mixture is, with χ denoting the quality,

$$h = \chi h_{fg} + h_f \tag{7.3-24}$$

Since homogeneous flow is assumed in the two-phase zone,

$$\chi = \frac{\alpha\rho_g}{\rho} = \frac{\alpha\rho_g}{\rho_f + \alpha\rho_{fg}} \tag{7.3-25}$$

Defining $(h\rho)_{fg}$ as $h_g\rho_g - h_f\rho_f$, Eqs. 7.3-23, -24, and -25 imply,

$$(h\rho) = h_f\ \rho_f + \alpha(h\rho)_{fg} \tag{7.3-26}$$

The general continuity Eq. 7.3-8 is written in terms of the nodal void fraction, α,

$$\left(\dot{\alpha}_{i+1}\rho_{fg} + \alpha_{i+1}\dot{\rho}_{fg} + \dot{\rho}_f\right)\Delta Z - \left(\alpha_{i+1} - \alpha_i\right)\rho_{fg}\dot{Z}_i = -\Delta G_i \tag{7.3-27}$$

The finite difference form of Eq. 7.3-27 is,

$$\begin{aligned}&\left[\frac{1}{\Delta t}\left(\alpha_{i+1}^{k+1} - \alpha_{i+1}^{k}\right)\rho_{fg}^{k} + \alpha_{i+1}^{k+1}\ \dot{\rho}_{fg}^{k} + \dot{\rho}_f^{k}\right]\frac{1}{n}Z_{TP}^{k+1} \\ &- \left(\alpha_{i+1}^{k+1} - \alpha_i^{k+1}\right)\rho_{fg}^{k}\left[\frac{i-j}{n}\ \frac{1}{\Delta t}\left(Z_{TP}^{k+1} - Z_{TP}^{k}\right) + \dot{Z}_{SC}\right] = -\left(G_{i+1}^{k+1} - G_i^{k+1}\right)\end{aligned} \tag{7.3-28}$$

Rearranging Eq. 7.3-28 according to coefficients of α_{i+1}^{k+1} and G_{i+1}^{k+1} the following results,

$$\begin{aligned}&\left\{\frac{1}{\Delta t}\rho_{fg}^{k}\frac{1}{n}Z_{TP}^{k+1} + \dot{\rho}_{fg}^{k}\frac{1}{n}\ Z_{TP}^{k+1} - \rho_{fg}^{k}\left[\frac{i-j}{n}\frac{1}{\Delta t}\left(Z_{TP}^{k+1} - Z_{TP}^{k}\right) + \dot{Z}_{SC}\right]\right\}\cdot\alpha_{i+1}^{k+1} \\ &+ G_{i+1}^{k+1} + \left\{-\frac{1}{\Delta t}\alpha_{i+1}^{k}\rho_{fg}^{k}\frac{1}{n}\ Z_{TP}^{k+1} + \dot{\rho}_f^{k}\frac{1}{n}Z_{TP}^{k+1} + \alpha_i^{k+1}\rho_{fg}^{k}\left[\frac{i-j}{n}\frac{1}{\Delta t}\right.\right. \\ &\left.\left.\cdot\left(Z_{TP}^{k+1} - Z_{TP}^{k}\right) + \dot{Z}_{SC}\right] - G_i^{k+1}\right\} = 0\end{aligned} \tag{7.3-29}$$

Equation 7.3-29 can be written as,

$$a \cdot \alpha_{i+1}^{k+1} + G_{i+1}^{k+1} + c = 0 \tag{7.3-30}$$

Writing the general energy Eq. 7.3-15 in terms of α results in the following,

$$\left[\dot{\alpha}_{i+1}\left(h\rho\right)_{fg}+\alpha_{i+1}\left(h\dot{\rho}\right)_{fg}+\left(h\dot{\rho}\right)_{f}\right]\Delta Z-\left(\alpha_{i+1}-\alpha_{i}\right)\left(h\rho\right)_{fg}\dot{Z}_{i} =-\Delta\left(Gh\right)_{i}+Q_{i}\Delta Z+\dot{P}\Delta Z \tag{7.3-31}$$

The finite difference form of Eq. 7.3-31 is,

$$\begin{aligned}&\left[\frac{1}{\Delta t}\left(\alpha_{i+1}^{k+1}-\alpha_{i+1}^{k}\right)\left(h\rho\right)_{fg}^{k}+\alpha_{i+1}^{k+1}\left(h\dot{\rho}\right)_{fg}^{k}+\left(h\dot{\rho}\right)_{f}^{k}\right]\frac{1}{n}Z_{TP}^{k+1}-\left(\alpha_{i+1}^{k+1}-\alpha_{i}^{k+1}\right)\\&\left(h\rho\right)_{fg}^{k}\left[\frac{i-j}{n}\frac{1}{\Delta t}\left(Z_{TP}^{k+1}-Z_{TP}^{k}\right)+\dot{Z}_{SC}\right]=-\left[G_{i+1}^{k+1}\left(h_{f}^{k}+\frac{\alpha_{i+1}^{k+1}\rho_{g}^{k}h_{fg}^{k}}{\rho_{f}^{k}+\alpha_{i+1}^{k+1}\rho_{fg}^{k}}\right)+\right.\\&\left.G_{i}^{k+1}\left(h_{f}^{k}+\frac{\alpha_{i}^{k+1}\rho_{g}^{k}h_{fg}^{k}}{\rho_{f}^{k}+\alpha_{i}^{k+1}\rho_{fg}^{k}}\right)\right]+Q_{i}^{k}\frac{1}{n}Z_{TP}^{k+1}+\dot{P}\frac{1}{n}Z_{TP}^{k+1}\end{aligned} \tag{7.3-32}$$

Rearranging Eq. 7.3-32 according to coefficients of α_{i+1}^{k+1} and G_{i+1}^{k+1}, the following results,

$$\begin{aligned}&\left\{\frac{1}{\Delta t}\left(h\rho\right)_{fg}^{k}\frac{1}{n}Z_{TP}^{k+1}+\left(h\dot{\rho}\right)_{fg}^{k}\frac{1}{n}Z_{TP}^{k+1}-\left(h\rho\right)_{fg}^{k}\left[\frac{i-j}{n}\frac{1}{\Delta t}\left(Z_{TP}^{k+1}-Z_{TP}^{k}\right)+\dot{Z}_{SC}\right]\right\}\\&\cdot\alpha_{i+1}^{k+1}+G_{i+1}^{k+1}\left(h_{f}^{k}+\frac{\alpha_{i+1}^{k+1}\rho_{g}^{k}h_{fg}^{k}}{\rho_{f}^{k}+\alpha_{i+1}^{k+1}\rho_{fg}^{k}}\right)+\left\{-\alpha_{i+1}^{k}\frac{1}{\Delta t}\left(h\rho\right)_{fg}^{k}\frac{1}{n}Z_{TP}^{k+1}\right.\\&+\left(h\dot{\rho}\right)_{f}^{k}\frac{1}{n}Z_{TP}^{k+1}+\alpha_{i}^{k+1}\left(h\rho\right)_{fg}^{k}\left[\frac{i-j}{n}\frac{1}{\Delta t}\left(Z_{TP}^{k+1}-Z_{TP}^{k}\right)+\dot{Z}_{SC}\right]\\&\left.-G_{i}^{k+1}\left(h_{f}^{k}+\frac{\alpha_{i}^{k+1}\rho_{f}^{k}h_{fg}^{k}}{\rho_{f}^{k}+\alpha_{i}^{k+1}\rho_{fg}^{k}}\right)-Q_{i}^{k}\frac{1}{n}Z_{TP}^{k+1}-\dot{P}\frac{1}{n}Z_{TP}^{k+1}\right\}=0\end{aligned} \tag{7.3-33}$$

If a' and c' represent the coefficient of α_{i+1}^{k+1} and the constant term respectively, Eq. 7.3-33 becomes,

$$a'\cdot\alpha_{i+1}^{k+1}+G_{i+1}^{k+1}\left(h_{f}^{k}+\frac{\alpha_{i+1}^{k+1}\rho_{g}^{k}h_{fg}^{k}}{\rho_{f}^{k}+\alpha_{i+1}^{k+1}\rho_{fg}^{k}}\right)+c'=0 \tag{7.3-34}$$

When the mass Eq. 7.3-30 is substituted into Eq. 7.3-34, a quadratic in α_{i+1}^{k+1} results,

$$\begin{aligned}\left(\alpha_{i+1}^{k+1}\right)^{2}&\left[a'\rho_{fg}^{k}-ah_{f}^{k}\rho_{fg}^{k}-a\rho_{g}^{k}h_{fg}^{k}\right]+\alpha_{i+1}^{k+1}\left[a'\rho_{f}^{k}-c\rho_{fg}^{k}h_{f}^{k}\right.\\&\left.-c\rho_{g}^{k}h_{fg}^{k}+c'\rho_{fg}^{k}-ah_{f}^{k}\rho_{f}^{k}+\left[c'\rho_{f}^{k}-ch_{f}^{k}\rho_{f}^{k}\right]=0\right.\end{aligned} \tag{7.3-35}$$

Several points need to be noted here. An inspection of Eqs. 7.3-28 and 7.3-32 shows that both α_{i+1} and G_{i+1} are totally implicit in time. It cannot be emphasized enough how much this feature of the boiling zone numerical solution enhances the stability of the calculation compared to other numerical schemes which are semi-implicit in time which were also tried. In order to preserve a linearized set of equations, it is necessary that the void fractions and mass flows be semi-implicit in time and this has a strong tendency to produce instabilities. The only quantities which are explicit in time are the saturation properties which are functions of pressure alone and the volumetric heat source term. Saturation properties are very well behaved functions of time since pressure tends to be a relatively stable function of time in most transients and the saturation properties are not as sensitive to changes in pressure as other quantities are sensitive to changes over time.

The last point concerns the k+1 superscript on Z_{TP}, the length of the two-phase zone. What this indicates, as noted above, is that the current value of the zone length in the iterative process is used in Eqs. 7.3-30 and 7.3-35. Equation 7.3-35 is solved for α_{i+1}^{k+1} and then G_{i+1}^{k+1} is obtained from the continuity Eq. 7.3-30 for each node. At first, the value of Z_{TP} from the last time step (i.e. Z_{TP}^{k}) is used to solve for α_{i+1}^{k+1} and G_{i+1}^{k+1} over the whole mesh starting at the bottom (i=1) where α_{i}^{k+1} and α_{i}^{k+1} (=0.) are the known boundary conditions. The solution then proceeds upwards until α_{i+1}^{k+1} is calculated. α_{i+1}^{k+1} compared to 1.0 and if it is greater than 1.0, Z_{TP} is reduced for the next iteration and if it is less than 1.0, Z_{TP} is increased. The search on Z_{TP} continues until α_{i+1}^{k+1} is sufficiently close to 1.0. If the boiling zone extends to the top of the steam generator, the same procedure is used, but no iteration on Z_{TP} is necessary since Z_{TP} is a fixed, known value.

7.3.3.1.4 Superheated Vapor Region

A compressible treatment of the vapor is used above the boiling zone and simultaneous nodal mass and energy equations are solved for nodal enthalpies and mass flows since the region length is known, being the remainder of the steam generator length after computing new subcooled and boiling zone lengths. The nodal densities and enthalpies are treated partially explicitly in time. Boundary conditions are the saturated vapor enthalpy and the mass flow at the bottom of the zone. The solution proceeds upwards to the top of the steam generator.

Since there is an expression for ρ as a function of enthalpy and pressure,

$$\dot{\rho} = \frac{\partial \rho}{\partial h}\frac{\partial h}{\partial t} + \frac{\partial \rho}{\partial P}\frac{\partial P}{\partial t} \tag{7.3-36}$$

By substituting Eq. 7.3-36 into the mass Eq. 7.3-8, an expression for G_{i+1} as a function of h_{i+1} results,

$$G_{i+1} = G_i - \left[\frac{\partial \rho}{\partial h} \dot{h}_{i+1} + \frac{\partial \rho}{\partial P} \dot{P} \right] \Delta Z + \Delta \rho_i \dot{Z}_i \tag{7.3-37}$$

Next, Eq. 7.3-36 is substituted into Eq. 7.3-15, the following results

$$\begin{aligned} &\left[\frac{\partial \rho}{\partial h} \dot{h}_{i+1} + \frac{\partial \rho}{\partial P} \dot{P} \right] h_{i+1} \Delta Z + \rho_{i+1} \dot{h}_{i+1} \Delta Z - \Delta(\rho h)_i \dot{Z}_i \\ &\quad = - G_{i+1} h_{i+1} + G_i h_i + Q_i \Delta Z + \dot{P} \Delta Z \end{aligned} \tag{7.3-38}$$

Now, substituting the expression for G_{i+1} which results from the continuity Eq. 7.3-37 into the energy Eq. 7.3-38 and simplifying,

$$\rho_{i+1} \dot{h}_{i+1} \Delta Z + \rho_i h_i \dot{Z}_i = - G_i h_{i+1} + \rho_i h_{i+1} \dot{Z}_i + G_i h_i + Q_i \Delta Z + \dot{P} \Delta Z \tag{7.3-39}$$

The finite difference form of Eq. 7.3-39 is,

$$\begin{aligned} &\frac{1}{\Delta t} \left(h_{i+1}^{k+1} - h_{i+1}^{k} \right) \rho_{i+1}^{k} \frac{1}{n} Z_{SH}^{k+1} + h_i^{k+1} \rho_i^{k+1} \frac{i-j}{n} \dot{Z}_{SH}^{k+1} = - G_i^{k+1} h_{i+1}^{k+1} + h_{i+1}^{k+1} \rho_i^{k+1} \frac{i-j}{n} \dot{Z}_{SH}^{k+1} \\ &\quad + G_i^{k+1} h_i^{k+1} + Q_i^{k} \frac{1}{n} Z_{SH}^{k+1} + \dot{P} \frac{1}{n} Z_{SH}^{k+1} \end{aligned} \tag{7.3-40}$$

Equation 7.3-40 is entirely implicit in enthalpy, mass flow and zone length. However, it is necessary to use the beginning-of-step value of ρ_{i+1} since density is a complicated function of enthalpy and pressure and there is no way to incorporate this function in Eq. 7.3-40 and preserve linearity. ρ_i, however, is entirely implicit since the solution proceeds upwards in the mesh and ρ_i can be updated as the solution proceeds along the mesh. By solving for h_{i+1}^{k+1}, the following results,

$$h_{i+1}^{k+1} = \frac{h_i^{k+1} \left(G_i^{k+1} - \rho_i^{k+1} \frac{i-j}{n} \dot{Z}_{SH}^{k+1} \right) + \frac{1}{n} Z_{SH}^{k+1} \left(\frac{1}{\Delta t} h_{i+1}^{k} \rho_{i+1}^{k} + Q_i^{k} + \dot{P}^{k} \right)}{G_i^{k+1} + \frac{1}{\Delta t} \rho_{i+1}^{k} \frac{1}{n} Z_{SH}^{k+1} - \rho_i^{k+1} \frac{i-j}{n} \dot{Z}_{SH}^{k+1}} \tag{7.3-41}$$

The finite-difference form of Eq. 7.3-37 is,

$$G_{i+1}^{k+1} = G_i^{k+1} - \left[\frac{\partial \rho}{\partial h} \frac{\left(h_{i+1}^{k+1} - h_{i+1}^{k} \right)}{\Delta t} + \frac{\partial \rho}{\partial P} \cdot \dot{P} \right] \frac{1}{n} Z_{SH}^{k+1} + \left(\rho_{i+1}^{k+1} - \rho_i^{k+1} \right) \dot{Z}_{SH} \tag{7.3-42}$$

After obtaining h_{i+1}^{k+1} from Eq. 7.3-41, ρ_{i+1}^{k+1} is calculated as a function of h_{i+1}^{k+1} and P^{k+1} and these are used to calculate G_{i+1}^{k+1} in Eq. 7.3-42. It should be noted that the

partial derivatives of density with respect to enthalpy and pressure are evaluated with the h_{i+1}^{k+1} and ρ_{i+1}^{k+1} just calculated. Starting at the bottom of the mesh, G_1^{k+1} and h_1^{k+1} (=h_g) are known and each parameter is solved for at the top of the cell at the i+1 location according to the above procedure up to the top of the steam generator.

7.3.3.1.5 Sodium Side Calculation

Incompressible flow is assumed on the sodium side because it is always in the liquid phase. Therefore there is no continuity equation. Also, since the sodium side is at relatively low pressure and has a stable pressure history, the pressure terms in the energy Eq. 7.3-13 are neglected. Next, since the sodium flows downward, in order to donor-cell the energy equation, $\left(\overline{\rho h}\right)_i$ is set equal to $\left(\rho h\right)_i$. Lastly, it is convenient to assume that G is positive for downward-flowing sodium which means that $-\Delta\left(Gh\right)_i$ becomes $-G\left[h_i - h_{i+1}\right]$. Thus Eq. 7.3-13 becomes,

$$\left(\rho\dot{h}\right)_i \Delta Z - \left[\left(\rho h\right)_{i+1} - \left(\rho h\right)_i\right]\dot{Z}_{i+1} = -G\left(h_i - h_{i+1}\right) + Q_i \Delta Z \tag{7.3-43}$$

Assuming $\dot{\rho}$ = 0 because of incompressible flow and rewriting Eq. 7.3-43 in terms of temperature (and neglecting the $\dot{c}_p$ term as unimportant), the following results,

$$\overline{\rho}_i \overline{c}_{p,i} \dot{T}_i \Delta Z - \overline{\rho}_i \overline{c}_{p,i}\left(T_{i+1} - T_i\right)\dot{Z}_{i+1} = -G\overline{c}_{p,i}\left(T_i - T_{i+1}\right) + Q_i \Delta Z \tag{7.3-44}$$

The $\overline{c}_{p,i}$ and the $\overline{\rho}_i$ are computed using the sodium temperature at the cell-center. (This is a slight inaccuracy but, given the fact that liquid sodium properties are so well-behaved and change so gradually, it is of small consequence.) The finite difference form of Eq. 7.3-44 is,

$$\frac{\overline{\rho}_i^k}{\Delta t}\left(T_i^{k+1} - T_i^k\right)\Delta Z^{k+1} - \overline{\rho}_i^k\left(T_{i+1}^{k+1} - T_i^k\right)\dot{Z}_{i+1}^{k+1} = -G^{k+1}\left(T_i^{k+1} - T_{i+1}^{k+1}\right) + \frac{\Delta Z^{k+1}}{\overline{c}_{p,i}} Q_i^k \tag{7.3-45}$$

Note that the $\overline{\rho}_i$ and the $\overline{c}_{p,i}$ are computed with beginning-of-step temperatures and that the ΔZ and $\dot{Z}_{i+1}$ are the end-of-step quantities just calculated in the water side calculation. Q_i is, of course, explicit in time as usual and the mass flow provided by the external sodium loop calculation is the new end-of-time-step value. If Eq. 7.3-45 is now solved for T_i^{k+1}, the following results,

$$T_i^{k+1} = \frac{T_{i+1}^{k+1}\left(G^{k+1} + \overline{\rho}_i^k \dot{Z}_{i+1}^{k+1}\right) + T_i^k \dfrac{\Delta Z^{k+1}}{\Delta t}\overline{\rho}_i^k + \dfrac{\Delta Z^{k+1}}{\overline{c}_{p,i}} Q_i^k}{\dfrac{\Delta Z^{k+1}}{\Delta t}\overline{\rho}_i^k + \overline{\rho}_i^k \dot{Z}_{i+1}^{k+1} + G^{k+1}} \tag{7.3-46}$$

Starting at the top of the steam generator, with the new inlet sodium temperatures at the end of the time step, the calculation proceeds downward to the bottom of the mesh.

7.3.3.1.6 Wall Temperature Calculation

The heat capacity of the tube wall must be taken into account during the transient. Since there is no convective term in the energy equation, central differencing is used. This means that $\left(\overline{\rho h}\right)_i = \frac{1}{2}\left[\left(\rho h\right)_{i+1} + \left(\rho h\right)_i\right]$ in Eq. 7.3-13 which becomes,

$$\frac{d}{dt}\left\{\frac{1}{2}\left[\left(\rho h\right)_{i+1} + \left(\rho h\right)_i\right]\Delta Z\right\} - \left(\rho h\right)_{i+1}\dot{Z}_{i+1} + \left(\rho h\right)_i \dot{Z}_i = Q_i\,\Delta Z \tag{7.3-47}$$

Eq. 7.3-47 is written in terms of temperature and both ρ and c_p are assumed to be temperature independent. This results in the following,

$$\begin{aligned}\frac{d}{dt}\left\{\frac{1}{2}\left(T_{i+1}+T_i\right)\right\}\Delta Z + \frac{1}{2}\left(T_{i+1}+T_i\right)\left(\dot{Z}_{i+1}-\dot{Z}_i\right) - T_{i+1}\dot{Z}_{i+1} \\ + T_i\dot{Z}_i = \frac{\Delta Z}{\rho c_p}Q_i\end{aligned} \tag{7.3-48}$$

Since the wall temperature is tracked at the cell center, not the cell edge, the quantity desired is $\overline{T}_i = \frac{1}{2}(T_{i+1} + T_i)$. Thus Eq. 7.3-48 becomes, after simplification,

$$\dot{\overline{T}} = \frac{1}{\rho c_p}Q_i^k + \frac{1}{2}\frac{1}{\Delta Z^{k+1}}\left(T_{i+1}^k - T_i^k\right)\cdot\left(\dot{Z}_{i+1}^{k+1} + \dot{Z}_i^{k+1}\right) \tag{7.3-49}$$

The heat source is explicit in time and the ΔZ and $\dot{Z}$ terms are the end-of-step values from the water side calculation. The difficulty with this equation is calculating the cell-edge values T_{i+1} and T_i since the wall temperatures are tracked at the cell center. Therefore interpolated or extrapolated estimates of the cell-edge values are formed from the cell-center temperatures.

7.3.3.1.7 Calculation of Boiling Crisis Point

The point of boiling crisis, or DNB point, in the boiling zone is computed by tracking the continuously varying intersection of two functions which is a point within the node structure. The first function represents the required heat flux for the boiling crisis to occur and the second is the actual local heat flux at the wall surface.

The DNB heat flux correlation [7-3] is as follows,

$$F_D = 7.84 \cdot 10^8 \left[\chi h_{fg} \rho_g / \rho_f \sqrt{\frac{G}{1355}} \right]^{-0.667} \quad (7.3\text{-}50)$$

This correlation is evaluated at each cell center in the boiling zone using the local quality. The inlet mass flux G is used instead of the local mass flux to enhance numerical stability although the original correlation used the local flow.

An expression for the wall surface heat flux is obtained as follows. There is a correlation for the heat transfer coefficient at the tube wall surface but the wall surface temperature is unknown, although the mid-wall temperature and the water temperature at saturation are known. Without going into the details of the correlation here (see Appendix 7.2), it is known that the heat flux at the wall surface, F_S, is equal to $a \cdot (T_S - T_{sat})^2$, where T_S is the wall surface temperature and a is only a function of pressure. The heat flux between the mid-wall and the wall surface, F_M, is $b \cdot (T_M - T_S)$, where b is the inverse of the wall heat resistance and T_M is the mid-wall temperature. When F_S is set equal to F_M, a quadratic in $(T_S - T_{sat})$ results,

$$a(T_S - T_{sat})^2 + b(T_S - T_{sat}) - b(T_M - T_{sat}) = 0 \quad (7.3\text{-}51)$$

Thus the wall surface temperature is obtained and then the heat flux at the wall surface, F_S, which is computed at each cell center over the length of the boiling zone. There are thus two functions, F_S and F_D, with values at each cell. In order to obtain the intersection of these two functions and thus the point of boiling crisis, a linear approximation is made to each function proceeding two cells at a time along the length of the steam generator until an intersection of the two lines is reached. The intersection point is tracked exactly and the nucleate boiling and film boiling heat transfer coefficients are prorated in the cell where the intersection occurs. This method gives a smoothly varying, stable calculation of the DNB point.

7.3.3.1.8 Disappearing and Appearing Regions

When the length of a zone is reduced below a certain value, the number of nodes within the zone is reduced from whatever initial number there were in the zone to only one node. However, no matter how long the zone is, no more than the initial number of nodes will be used in the zone. Reducing the number of nodes for small zone lengths greatly enhances numerical stability while reducing computer time and, so long as the criterion for the node reduction is not too large, very little accuracy in the calculation is sacrificed. When the node structure is collapsed to one node, the cell-edge quantities at the inlet and outlet to the zone remain unchanged while the intermediate values are eliminated. The tube wall temperature in the center of the new l-node region is formed as an average of two wall temperatures nearest the center of the old multi-node region. When the zone length increases beyond a certain value and there is only one node in the region then the number of nodes is reset at the original value and the values of parameters at intermediate nodes must be initialized. This is done with simple linear fits (close enough considering the short lengths involved) between the end point values for sodium temperatures, for enthalpies in the subcooled and superheated zones and

for mass flows in the boiling and superheated regions. When the boiling zone has only one node and when it is reinitialized at the original number of nodes, the whole region is assumed to be in the nucleate boiling regime.

When a second length threshold is reached as a region's length is reduced, then the region is eliminated entirely. This only applies to the boiling and superheated zones and they must disappear in order. That is if there is a superheated zone, there must be a boiling zone no matter how small. When the superheated zone disappears, then the boiling zone outlet enthalpy (i.e. void fraction or quality) becomes a free variable rather than fixed at h_g as it is when a superheated zone exists. The criterion for elimination of the superheated zone is a length criterion but the criterion for recreating the superheated zone is that the outlet enthalpy of the boiling zone be somewhat higher than h_g. The mass flow at the outlet of the newly created superheated zone is assumed the same as the outlet flow from the boiling zone. The outlet enthalpy is set to the value of the criterion and the boiling zone outlet enthalpy is set to h_g. The length of the new superheated zone is computed according to the following formula,

$$Z_{SH} = Z_{TP} \cdot \frac{h_{out} - h_g}{h_{out} - h_f} \tag{7.3-52}$$

where Z_{SH} is the new superheated length, Z_{TP} is the old boiling zone length before being reduced by Z_{SH} and h_{out} is the enthalpy calculated at the outlet of the steam generator. Values for the sodium and tube wall temperatures are interpolated according to the new node and zone structure.

The criterion for elimination of the boiling zone is again a length criterion but the criterion for recreating the boiling zone is that the outlet enthalpy of the subcooled zone be somewhat higher than h_f. The mass flow at the outlet of the newly created boiling zone is assumed the same as the outlet flow from the subcooled zone. The outlet enthalpy is set to the value of the criterion and the subcooled zone outlet enthalpy is set to h_f. The length of the new boiling zone is calculated as follows,

$$Z_{TP} = Z_{SC} \cdot \frac{h_{out} - h_f}{h_{out} - h_{in}} \tag{7.3-53}$$

where Z_{TP} is the new boiling length, Z_{SC} is the old subcooled zone length before being reduced by Z_{TP}, h_{out} is the enthalpy calculated at the outlet of the steam generator, and h_{in} is the inlet enthalpy. Values for the sodium and tube wall temperatures are interpolated as for the superheated zone creation above according to the new node and zone structure.

7.3.3.1.9 Miscellaneous Numerical Issues

Nothing has been said so far about the calculation of the time derivative of pressure which appears in the energy Eq. 7.3-15. At each call to the steam generator routine, the balance-of-plant calculation provides the new steam generator pressure at the end of

the time step. It would seem natural to form $\dot{P}$ with the current Δt and P^k and P^{k+1}. This, however, can lead to significant numerical instabilities caused by large temporary spikes in P even when the time-averaged value of $\dot{P}$ is well-behaved and much more gradual than would be predicted by using the stepwise values of P. Therefore, a moving average of $\dot{P}$ is computed over the last 2 m timesteps so that,

$$\dot{P} = \frac{\sum_{i=m+1}^{2m} P_i \Delta t_i - \sum_{i=1}^{m} P_i \Delta t_i}{\frac{1}{2} \cdot \sum_{i=1}^{2m} \Delta t_i} \tag{7.3-54}$$

There is a time step selector currently in the code which chooses a new timestep size for the next step based on information from the current step. However, this selector is preliminary and merely chooses the new step according to fractional changes in a number of parameters over the step. That is, the new time step is computed as follows,

$$\Delta t' = Min\left(X \cdot \left| \frac{\Delta t \cdot Y_i^{k+1}}{Y_i^{k+1} - Y_i^{k}} \right| \right) \tag{7.3-55}$$

where X is an input fractional change in the quantity Y_i, Δt is the current time step, $\Delta t'$ is the new time step and Min indicates that the minimum over all the Y_i values is computed. The various quantities indicated by Y include the sodium side flow, the zone boundaries, the steam generator pressure, the nodal water mass flows, the void fractions in the boiling zone, the enthalpies in the subcooled and superheated zones, the sodium temperatures and the tube wall temperatures. There is also a minimum value criterion for the new step set by the steam generator. There is in effect a maximum value for the time step which is set for the primary loop calculation. However, there is rarely any need for the steam generator to have a larger time step than the primary loop calculation and, almost always, it is the hydrodynamics on the water side of the steam generator which determines the time step.

There are two artificial limitations that are superimposed on the boiling zone calculation that need to be pointed out. The first is that the void fraction solved for in each successive node as the solution proceeds up the zone must be larger than the previous value at the last node. The code simply requires that the new void fraction be at least 0.001 larger than the last. This may seem like a major limitation in the solution method but, in practice, it is rarely used. When it is used, it has very little consequence for the calculation. The only time this fix is used is when there is an extremely flat void fraction profile (which can be caused by a number of things, very low water flow, for example). In the absence of this fix, there is occasionally a tendency for numerical instabilities to form when there is an extremely flat void profile. The other artificial limitation is that the boiling zone length is not allowed to change more than 1% in a time step. This can have some significant implications for the course of a transient.

Without this limitation, there can be a tendency for the boiling zone length to adjust too rapidly to changing conditions, which can cause significant numerical instabilities since a large change in Z_{TP} over a short time produces a large $\dot{Z}_{TP}$ and a large perturbation in the equation set. Since the effect is largely artificial, this limitation within certain bounds is consistent with the physical conditions of the case. However, limiting the change in Z_{TP} means that the void fraction at the top of the zone may not be equal to 1.0 and, if it is too different, then basic assumptions of the model are, of course, being violated. It must be emphasized, however, that this limitation, is not used frequently and, when it is used, the outlet void fraction nearly always remains close to 1.0 while, over a number of time steps, the region length changes to accommodate the changing conditions but avoiding large temporary values of $\dot{Z}_{TP}$ which could drive the calculation unstable.

7.3.3.1.10 Calculation of Pressure Drop for Momentum Equation

Although the balance-of-plant calculation does the actual computation which produces the inlet flow for the steam generator and the pressure boundary conditions at the inlet and outlet plena of the steam generator, the steam generator must provide the pressure drops to the balance-of-plant for this calculation. For the details of the momentum equation solution, it is necessary to refer to the balance-of-plant description (Section 7.2). All that will be done here is to describe the pressure drop calculation itself. For each of the four zones corresponding to each of the four heat transfer regimes *i*, the following is the pressure drop ΔP across the zone,

$$\Delta P_i = -\overline{G}_i^2\left(\frac{1}{\rho_t}-\frac{1}{\rho_b}\right)-Z_i\left[\overline{\rho}_i\,9.8+\dot{\overline{G}}_i+\overline{G}_i^{\,2}\,0.31\cdot FR_i\cdot\left(\frac{\overline{G}_i\,D_H}{\overline{\mu}_i}\right)^{-0.25}\cdot\frac{1}{2}\,\frac{1}{D_H\,\overline{\rho}_i}\,R_i\right] \tag{7.3-56}$$

where $\overline{G}_i$ is an average of the mass flow both spatially over the zone length and temporally over the time step; ρ_t is the density at the top of the zone and ρ_b at the bottom; Z_i is the zone length; $\overline{\rho}_i$ the average density over the zone; $\dot{\overline{G}}_i$ is the average mass flow over the zone length at the end of the time step minus the average mass flow over the zone at the beginning of the time step divided by the time step; FR_i is a calibration factor computed in steady state to provide the proper steady state pressure drop; D_H is the water side hydraulic diameter; and $\overline{\mu}_i$ is the average viscosity for the regime. Equation (7.3-56) is used to compute ΔP_i for the subcooled, the nucleate boiling, the film boiling and superheated zones. The factor R_i is 1.0 for the subcooled and the superheated zones. R_i is computed according to the following formula in the two boiling zones,

$$R_i = 0.95819 - \left(1167.2\, R_i' - 505.\right) \cdot R_i' \tag{7.3-57}$$

$$R_i' = \frac{\overline{\chi}_i}{\left(\frac{P}{1.724 \cdot 10^6}\right)^{2.448} + 16.217} \tag{7.3-58}$$

where P is the steam generator pressure and $\overline{\chi}_i$ is the average quality over each boiling zone. This formula is the Thom correlation [7-2] with constants appropriate for the units used in the code.

Once the ΔP_i's have been calculated, then the ΔP_i's for the boiling zones and the superheated vapor zone are summed and divided by the sum of all four ΔP_i's. This gives the current fraction of the total pressure drop across the steam generator that is above the subcooled zone. The balance-of-plant model uses its current pressures at the inlet and the outlet plena of the steam generator to provide the total pressure drop and estimates the pressure at the top of the subcooled zone with the fractional pressure drop referred to above. The pressure at the top of the subcooled zone provides the balance-of-plant momentum equation with a pressure boundary condition and it can merely include the subcooled liquid zone of the steam generator as the last in a series of incompressible liquid segments bounded by plena which stretches from the feed water inlet to the lower end of the compressible zones in the steam generator (i.e. the subcooled/boiling boundary). Thus the inlet flow (constant throughout the subcooled zone) is determined as part of the solution matrix in the total balance-of-plant momentum equation. Of course, the steam generator must provide the balance-of-plant model with information about the subcooled zone. It needs the average density, the length of the zone, the friction normalization factor FR_1, the average viscosity and the hydraulic diameter. It is clear that, in the case when the subcooled zone extends to the top of the steam generator, the whole steam generator becomes merely one incompressible segment in the balance-of-plant matrix from the feedwater inlet to the turbines.

7.3.3.2 Recirculation-Type Steam Generator

As noted before, the modeling of the evaporator in this node of the steam generator model is done with the same coding as is used for the once-through type steam generator. The difference is that, when it is used as an evaporator, the outlet enthalpy will be less than or equal to h_g. Since this is within the envelope of cases for which the once-through modeling was designed, this has already been described above. The modeling of the steam drum is described elsewhere in detail (See Section 7.4).

There remains only the discussion of the modeling of the superheater. As noted above, it is assumed that incompressible flow is adequate to describe the superheater. The mass flow through the superheater is determined by the balance-of-plant momentum equation. The lower enthalpy boundary condition is h_g. There are no region boundaries to calculate since there is only single phase vapor flow in the

superheater. Since $\dot{\rho}$ = 0 is assumed, the energy Eq. 7.3-15 becomes, for the constant superheater length,

$$\rho_{i+1}\,\dot{h}_{i+1}\,\Delta Z = -G\left(h_{i+1}-h_i\right)+Q_i\;\Delta Z+\dot{P}\Delta Z \tag{7.3-59}$$

The finite difference form of Eq. 7.3-59 is,

$$\rho_{i+1}^{k}\,\Delta Z\,\frac{h_{i+1}^{k+1}-h_{i+1}^{k}}{\Delta t}=-G^{k+1}\left(h_{i+1}^{k+1}-h_i^{k+1}\right)+Q_i^{k}\;\Delta Z+\dot{P}\Delta Z \tag{7.3-60}$$

Equation 7.3-60 is then solved for h_{i+1}^{k+1} resulting in,

$$h_{i+1}^{k+1}=\frac{\rho_{i+1}^{k}\,\dfrac{\Delta Z}{\Delta t}\,h_{i+1}^{k}+G^{k+1}\,h_i^{k+1}+Q_i^{k}\;\Delta Z+\dot{P}\Delta Z}{\rho_{i+1}^{k}\,\dfrac{\Delta Z}{\Delta t}+G^{k+1}} \tag{7.3-61}$$

Equation 7.3-61 is solved for each successive h_{i+1}^{k+1} up to the top of the superheater. ΔZ is, of course, a constant. The lower boundary conditions are h_g and ρ_g. G^{k+1} is provided by the balance-of-plant momentum equation.

The sodium side temperatures are solved according to the same method as used in the once-through steam generator. All the same assumptions concerning incompressible flow and donor-cell differencing are made. The only difference is that the $\dot{Z}$ terms are eliminated and ΔZ becomes a constant because of the constant superheater length. Thus Eq. 7.3-46 becomes,

$$T_i^{k+1}=\frac{T_{i+1}^{k+1}\,G^{k+1}+T_i^{k}\,\dfrac{\Delta Z}{\Delta t}\,\bar{\rho}_i^{k}+\dfrac{\Delta Z}{\bar{c}_{p,i}}\,Q_i^{k}}{\dfrac{\Delta Z}{\Delta t}\,\bar{\rho}_i^{k}+G^{k+1}} \tag{7.3-62}$$

As before, starting at the top of the steam generator, with the new inlet sodium temperature at the end of the time step, the calculation proceeds downward to the bottom of the mesh.

The same considerations apply to the tube wall temperature calculation in the superheater. The solution method is precisely the same as for the once-through steam generator except that the $\dot{Z}$ terms are now eliminated because of the constant superheater length. Thus Eq. 7.3-49 becomes simply,

$$\dot{\bar{T}}_i = \frac{1}{\rho c_p} Q_i^k \tag{7.3-63}$$

Thus there is no difficulty in calculating the ΔT term as there was in Eq. 7.3-49 because it is eliminated.

7.3.3.3 Steady State Solution

7.3.3.3.1 Once-Through Type Steam Generator

7.3.3.3.1.1 Superheated Vapor Region

For a given reactor power, the product of flow rate and enthalpy change across the steam generator must be the same on both the water and sodium sides. In other words, the following holds,

$$RP = G_w A_w \left(h_{w,out} - h_{w,in}\right) = G_s A_w \bar{c}_{p,s} \left(T_{s,in} - T_{s,out}\right) \tag{7.3-64}$$

where RP is the reactor power (or a fraction thereof for multiple steam generators); G_w and G_s are the water and sodium flow rates; A_w and A_s are the water and sodium flow areas; $h_{w,out}$ and $h_{w,in}$ are the outlet steam and inlet water enthalpies; $T_{s,in}$ and $T_{s,out}$ are the inlet and outlet sodium temperatures; and $\bar{c}_{p,s}$ is the average specific heat for sodium over the length of the steam generator. This relationship must determine the above flow rates, water enthalpies, geometry and sodium temperatures. Constraints on any of these parameters must translate into constraints on the other parameters according to the above relationship. For the present purpose, however, geometry, flow rates and inlet and outlet enthalpies are assumed to have been determined elsewhere.

For the steady state, then, $h_{w,out}$ is presumed. If $h_{w,out} > h_g$, then there is a superheated vapor zone. (Of course, in any true steady-state operation for a once-through steam generator, there will be a superheated vapor zone. However, this "steady-state" calculation described here produces starting conditions for a transient calculation of any nature which may be very different than the normal operational conditions.) For the superheated vapor zone, then, the following relation holds,

$$G_w A_w \left(h_{w,out} - h_g\right) = G_s A_s \bar{c}_{p,s} \left(T_{s,in} - T_{s,hg}\right) \tag{7.3-65}$$

where $T_{s,hg}$ is the sodium temperature at the point of saturated vapor enthalpy on the water side and $\bar{c}_{p,s}$ is the average value of the specific heat over the superheated vapor zone. If $\bar{c}_{p,s}$ is known, then Eq. 7.3-65 can be used to determine $T_{s,hg}$. As a practical matter, $c_{p,s}$ varies only 2-3% and quite smoothly over the length of the steam generator. If Eq. 7.3-65 is solved for $T_{s,hg}$ using $c_{p,s}$ calculated with $T_{s,in}$, then the average of $T_{s,in}$ and $T_{s,hg}$ are used to calculate $c_{p,s}$ and if this process is repeated several times, then there is a negligible error in $\bar{c}_{p,s}$ and thus in $T_{s,hg}$.

In order to fully characterize the superheated zone, either the length of the zone must be specified or some calibrating factor on the water side heat transfer coefficient must be specified. This will become clear as the solution description continues. It is also possible to calibrate the sodium side heat transfer coefficient but it is assumed that the water side coefficient involves much more uncertainty. First, the form of the water side heat transfer coefficient is as follows,

$$H_T = \frac{1}{\frac{1}{H_w CF} + WR + FL} \tag{7.3-66}$$

where H_T is the total water coefficient; H_w is the heat transfer coefficient between the tube wall surface and the bulk fluid; *CF* is some calibration factor to be determined; *WR* is the heat resistance of the tube wall; and *FL* is some additional resistance to take into account fouling at the wall surface. H_w is calculated for each heat transfer regime according to correlations given in the Appendix 7.2. The H_w*'s* represent values for experimental conditions and therefore may need to be calibrated for full scale cases. *WR* is calculated from the tube wall geometry and properties. *FL* is specified by the code user in the input.

Before a full nodewise solution is obtained, a rough guess to initialize the iterative process of the final solution is required. The case of specifying the zone length Z_{SH} and computing the calibration factor is considered first. The following equates the average heat transfer in the zone from the bulk sodium to the tube wall with the portion of reactor power known to be derived from the superheated zone,

$$G_s \frac{1}{Z_{SH}} \bar{c}_{p,s} \left(T_{s,in} - T_{s,hg} \right) = H_s \left(\overline{T}_s - \overline{T}_m \right) \frac{2\pi r_s Z_{SH}}{A_s Z_{SH}} \tag{7.3-67}$$

$T_{s,hg}$ is obtained from Eq. 7.3-64. $\overline{T}_s = \frac{1}{2}\left(T_{s,in} + T_{s,hg} \right)$. r_s is the outer tube wall radius. $\overline{T}_m$ averaged over the height of the zone. H_s is the total heat transfer on the sodium side including the wall resistance,

$$H_s = \frac{1}{\frac{1}{H_{Na}} + WRNA} \tag{7.3-68}$$

where H_{Na} is the heat transfer coefficient from the tube surface to the bulk sodium and WRNA is the wall resistance on the sodium side of the tube. The correlation for H_{Na} is given in Appendix 7.2. H_{Na} is a function of G_s, geometry and temperature. The temperature used is $\overline{T}_s$. Eq. 7.3-67 is solved for $\overline{T}_m$ which is inserted into the equation analogous to Eq. 7.3-67 on the water side,

$$G_s \frac{1}{Z_{SH}} \left(h_{w,out} - h_g\right) = \frac{1}{\frac{1}{H_w\, CF} + WR + FL} \left(\overline{T}_m - \overline{T}_w\right) \frac{2\pi r_w Z_{SH}}{A_w Z_{SH}} \tag{7.3-69}$$

where $\overline{T}_w$ is the temperature derived from $\overline{H}_w = \frac{1}{2}\left(h_{w,out} + h_g\right)$, r_w is the inner tube wall radius and H_w is calculated with properties derived from $\overline{h}_w$. Thus Eq. 7.3-69 can be solved for *CF*, the initial guess for the calibration factor on the superheated zone heat transfer coefficient when the zone length is specified. Alternatively, if the calibration factor *CF* is specified, and the zone length is unknown, then Eqs. 7.3-67 and 7.3-69 form a set with two unknowns, $\overline{T}_m$ and Z_{SH}, which can be solved for easily. If there is only one node in the superheated zone, then the steady state solution is finished at this point.

In order to solve the nodal equations, a similar method is used for each node as in the 1-node approximation above. First, there is the nodal energy balance for cell *i* from node *i* to node *i*+1 (the solution proceeds from the bottom to the top of the mesh),

$$G_w A_w \left(h_{w,i+1} - h_{w,i}\right) = G_s A_s\, \bar{c}_{p,s,i} (T_{s,i+1} - T_{s,i}) \tag{7.3-70}$$

where $\overline{c}_{p,s,i}$ is the specific heat corresponding to $\frac{1}{2}\left(T_{s,i+1} + T_{s,i}\right) = \overline{T}_{s,i}$. This equation can be solved for $T_{s,i+1}$ which results in

$$T_{s,i+1} = \left[\frac{G_w\, A_w}{G_s\, A_s\, \overline{c}_{p,s,i}}\right] h_{w,i+1} + \left[T_{s,i} - \frac{G_w\, A_w}{G_s\, A_s\, \overline{c}_{p,s,i}} h_{w,i}\right] \tag{7.3-71}$$

which can be written as,

$$T_{s,i+1} = a\, h_{w,i+1} + b \tag{7.3-72}$$

Next, the sodium side heat transfer is described by the following,

$$G_s \frac{1}{\Delta z} \overline{c}_{p,s,i} \left(T_{s,i+1} - T_{s,i}\right) = H_{s,i} \left[\frac{1}{2}\left(T_{s,i+1} + T_{s,i}\right) - T_{m,i}\right] \frac{2\pi r_s \Delta Z}{A_s \Delta Z} \tag{7.3-73}$$

where $H_{s,i}$ is calculated according to Eq. 7.3-68 with $\overline{T}_{s,i}$ and $T_{m,i}$ is the cell-center value and ΔZ is of course $\frac{1}{n} \cdot Z_{SH}$ with *n* the number of cells in the zone. Eq. 7.3-73 is solved, for $T_{m,i}$, in the following,

$$T_{m,i} = \left[\frac{1}{2} - \frac{G_s\,\bar{c}_{p,s,i}\,A_s}{H_{s,i}\,2\pi r_s\,\Delta Z}\right] T_{s,i+1} + \left[\frac{1}{2} + \frac{G_s\,\bar{c}_{p,s,i}\,A_s}{H_{s,i}\,2\pi r_s\,\Delta Z}\right] T_{s,i} \tag{7.3-74}$$

which can be written as,

$$T_{m,i} = c\,T_{s,i+1} + d \tag{7.3-75}$$

and if Eq. 7.3-72 is substituted into Eq. 7.3-75,

$$T_{m,i} = ac\,h_{w,i+1} + (bc + d) = e h_{w,i+1} + f \tag{7.3-76}$$

Similarly, the water side heat transfer is described by the following,

$$G_w = \frac{1}{\Delta Z}\left(h_{w,i+1} - h_{w,i}\right) = H_{T,i}\left(T_{m,i} - \bar{T}_{w,i}\right)\frac{2\pi r_w\,\Delta Z}{A_w\,\Delta Z} \tag{7.3-77}$$

where $H_{T,i}$ is calculated according to Eq. 7.3-66. Next $\bar{T}_{w,i}$ is replaced by $1/2\left[T_{w,i} + 1 + T_{w,i}\right]$. Then, use is made of the relation,

$$h_{w,i+1} - h_{w,i} = \bar{c}_{p,w,i}\left(T_{w,i+1} - T_{w,i}\right) \tag{7.3-78}$$

Equation 7.3-78 is solved for $T_{w,i+1}$ and then,

$$\bar{T}_{w,i} = T_{w,i} + \frac{1}{2\,\bar{c}_{p,w,i}}\left(h_{w,i+1} - h_{w,i}\right) \tag{7.3-79}$$

Equations 7.3-79 and 7.3-76 are substituted into Eq. 7.3-77, which results in the following,

$$h_{w,i+1} = \frac{G_w\,h_{w,i} - H_{T,i}\,\dfrac{2\pi r_w\,\Delta Z}{A_w}\left[f - T_{w,i} + \dfrac{h_{w,i}}{2\,\bar{c}_{p,w,i}}\right]}{G_w + \dfrac{H_{T,i}\,2\pi r_w\,\Delta Z}{A_w}\left[\dfrac{1}{2\,\bar{c}_{p,w,i}} - e\right]} \tag{7.3-80}$$

When $h_{w,i+1}$ is computed, $T_{m,i}$ and $T_{s,i+1}$ can also be found from Eqs.7.3-76 and 7.3-72.

Now that the basic method of solution of the nodal equation has been described, several points need to be emphasized. First, in the three equation set, Eqs. 7.3-70, -73, and -77, there are the three unknowns $T_{s,i+1}$, $T_{m,i}$ and $h_{w,i+1}$ which are solved for.

However, Eqs. 7.3-70 and 7.3-73 presume that $\bar{c}_{p,s,i}$ is known. Equation 7.3-73 presumes that $H_{s,i}$ is known and this means that an average sodium temperature for the cell must be known. Equation 7.3-77 presumes that $H_{T,i}$ and $\bar{c}_{p,w,i}$ are known and various physical properties are required to compute $H_{T,i}$. All of these quantities are functions of $\bar{T}_{s,i}$ and $\bar{T}_{w,i}$ (or $\bar{h}_{w,i}$) which require $T_{s,i+1}$ and $T_{w,i+1}$ (or $h_{w,i+1}$). Therefore, there is an iterative process required to produce better and better values for the various parameters after starting the whole process with some initial estimate of the $T_{s,i}$'s and the $h_{w,i}$'s. On the very first pass, the nodal values of $T_{s,i}$ and $h_{w,i}$ are simply linear interpolations between the end values but, since there are a number of iterations before the final result is obtained, the effect of this initial assumption is negligible.

Secondly, the main goal of the iterative procedure is to produce either a calibration factor for a specified length or a zone length for a specified calibration factor. The length or calibration factor is simply assumed in the above solution of the nodal equations and when the solution of all the nodal values is complete, then a new length or calibration factor is chosen if the result is not yet acceptable. The nodal solution begins at the point of saturated vapor enthalpy where the $h_{w,i}$ is simply h_g and the $T_{s,i}$ is $T_{s,hg}$, produced from Eq. 7.3-65. It should be mentioned here that Eq. 7.3-65 produces a better and better value of $T_{s,hg}$ on each iteration since the value of $\bar{c}_{p,s}$ used is refined by a recomputation after each iteration by using the new nodal $T_{s,i}$'s calculated in the iteration. The nodal solution proceeds upwards from h_g and $T_{s,hg}$ to the top of the steam generator where values of $h_{w,out}$ the $T_{s,in}$ are calculated. At this point, the criterion for convergence needs to be determined. The new values of $h_{w,out}$ and $T_{s,in}$ can both be compared to the externally calculated values. It was decided to use $T_{s,in}$ as the criterion and thus the length or calibration factor is adjusted until the $T_{s,i+1}$ at the top of the steam generator is as close to $T_{s,in}$ as necessary according to an input criterion. There is only one last point to note. This is that for each outer iteration which uses a new length or calibration factor, there are ten inner iterations for each node in the nodal solution which are necessary to converge on values of the heat transfer coefficients and c_p's for an assumed length or calibration factor. If this inner iteration is not done, the outer iteration will not converge.

7.3.3.3.1.2 Subcooled Liquid Region

Because of the difficulty of obtaining a solution for the boiling zone unless the length of the boiling zone is known, the subcooled zone solution, which may not have its length specified, is completed before the boiling zone. Once the lengths for both the superheated vapor zone and the subcooled liquid zone are determined, the length of the boiling zone is, of course, merely the remainder of the steam generator length. There is a boiling zone, however, only when $h_{w,out} > h_f$.

$$G_w A_w \left(h_{w,t} - h_f\right) = G_s A_s \bar{c}_{p,s} (T_{s,t} - T_{s,hf}) \tag{7.3-81}$$

where $h_{w,t}$ is h_g when there is a superheated vapor zone and $h_{w,out}$ when there isn't; $T_{s,t}$ is $T_{s,hg}$ when there is a superheated vapor zone and $T_{s,in}$ when there isn't; $\bar{c}_{p,s}$ is the

average value of the specific heat over the boiling zone. As is similar to Eq. 7.3-65, $\bar{c}_{p,s}$ is first calculated with $T_{s,t}$ and then with an average of $T_{s,t}$ and $T_{s,hf}$ and this process is repeated several times thus producing better and better values of $T_{s,hf.}$

As was the case with the superheated zone, either the length of the subcooled zone or the calibration factor on its heat transfer coefficient must be specified. The total water side heat transfer coefficient is calculated as in Eq. 7.3-66 with a different correlation for H_w and perhaps a different value for FL.

Again, as with the superheated zone, a one-node initial guess for the subcooled zone length Z_{SC} or calibration factor is obtained starting with an equation analogous to Eq. 7.3-67,

$$G_s \frac{1}{Z_{SC}} \bar{c}_{p,s} \left(T_{s,u} - T_{s,out}\right) = H_s \left(\bar{T}_s - \bar{T}_m\right) \frac{2\pi r_s Z_{SC}}{A_s Z_{SC}} \tag{7.3-82}$$

where $T_{s,u}$ is either $T_{s,in}$ when there is no boiling zone or $T_{s,hf}$ which is obtained from Eq. 7.3-81, $\bar{T}_s = \frac{1}{2}\left(T_{s,u} - T_{s,out}\right), \bar{T}_m$ is the midwall tube temperature averaged over the height of the zone and H_s is defined in Eq. 7.3-68. Again $\bar{T}_m$ is obtained from Eq. 7.3-82 and inserted into the analogous equation to Eq. 7.3-69,

$$G_s \frac{1}{Z_{SC}} \left(h_{w,u} - h_{w,in}\right) = \frac{1}{\frac{1}{H_w CF} + WR + FL} \left(\bar{T}_m - \bar{T}_w\right) \frac{2\pi r_w Z_{SC}}{A_w Z_{SC}} \tag{7.3-83}$$

where $h_{w,u}$ is $h_{w,out}$ when there is no boiling zone and h_f when there is a boiling zone and $\bar{T}_w$ is the temperature derived from $\frac{1}{2}\left(h_{w,u} + h_{w,in}\right)$. Equation 7.3-83 is solved for the initial guess for CF when the zone length is specified. Alternatively, if the calibration factor CF is specified, then the Eqs. 7.3-82 and 7.3-83 form a set with two unknowns, $\bar{T}_m$ and Z_{SC} which are then solved for. If there is only one node in the subcooled zone, the steady state solution is finished here.

In order to solve the nodal equations, the same method is used as was used for the superheated vapor zone except the nodewise solution proceeds from the top of the subcooled zone to the bottom of the steam generator. The nodal energy balance for a cell is exactly the same as Eq. 7.3-70. However, since the direction of solution is from top to bottom, $T_{s,i}$ is solved for,

$$T_{s,i} = \left[\frac{G_w A_w}{G_s A_s \bar{c}_{p,s,i}}\right] h_{w,i} + \left[T_{s,i+1} - \frac{G_w A_w}{G_s A_s \bar{c}_{p,s,i}} h_{w,i+1}\right] \tag{7.3-84}$$

which is written as,

$$T_{s,i} = a\, h_{w,i} + b \tag{7.3-85}$$

As before, the sodium side heat transfer is described by Eq. 7.3-73. As before, Eq. 7.3-73 is solved for $T_{m,i}$ which results in Eq. 7.3-74. However, since $T_{s,i}$ is the unknown now and not $T_{s,i+1}$, Eq. 7.3-74 is written as,

$$T_{m,i} = c\, t_{s,i} + d \tag{7.3-86}$$

and Eq. 7.3-85 is substituted into Eq. 7.3-86,

$$T_{m,i} = ac\, h_{w,i} + \left(bc + d\right) = e\, h_{w,i} + f \tag{7.3-87}$$

The water side heat transfer is described by Eq. 7.3-77 just as for the superheated vapor zone, but Eq. 7.3-78 is solved for $T_{w,i}$ and,

$$\bar{T}_{w,i} = T_{w,i+1} - \frac{1}{2\bar{c}_{p,w,i}}\left(h_{w,i+1} - h_{w,i}\right) \tag{7.3-88}$$

Equations 7.3-88 and 7.3-87 are substituted into Eq. 7.3-77 which results in the following,

$$h_{w,i} = \frac{G_w\, h_{w,i+1} - H_{T,i}\dfrac{2\pi r_w \Delta Z}{A_w}\left[f - T_{w,i+1} + \dfrac{h_{w,i+1}}{2\bar{c}_{p,w,i}}\right]}{G_w + \dfrac{H_{T,i}\, 2\pi r_w \Delta Z}{A_w}\left[e - \dfrac{1}{2\bar{c}_{p,w,i}}\right]} \tag{7.3-89}$$

As before, when $h_{w,i}$ is computed, $T_{m,i}$ and $T_{s,i}$ can also be found from Eqs. 7.3-87 and 7.3-85. The same general considerations apply to the solution of the subcooled zone equation set as applied to the superheated vapor zone equation set. The criterion for convergence is now that $T_{s,i}$ at the bottom of the mesh be arbitrarily close to $T_{s,out}$. The subcooled zone length or the calibration factor *CF* is adjusted until this is achieved.

7.3.3.3.1.3 Boiling Zone

If $h_{w,out} > h_f$, then there is a boiling zone. It has already been shown how the sodium temperatures were determined at each end of the zone, $T_{s,in}$ or $T_{s,hg}$ (depending on whether or not there is a superheated zone) and $T_{s,hf}$. The water enthalpies at the ends of the zone are either $h_{w,out}$ or h_g and h_f. Since the lengths of the superheated vapor and subcooled liquid zones have been determined either by input specification or by the steady state calculation before the boiling zone calculation begins, the length of the boiling zone is also determined and it remains, therefore, to adjust the heat transfer in the boiling zone so that with the known zone length the enthalpy condition at the top of the zone is obtained. That is, either $T_{s,in}$ or $T_{s,hg}$ is obtained on the sodium side and $h_{w,out}$

or h_g on the water side, although the actual criterion used, as in the other zones, is the sodium temperature. There is a complicating factor when trying to adjust the heat transfer in the boiling zone which does not exist in the other two zones, however. This is the fact that there are two heat transfer regimes in the boiling zone separated at the DNB point. Both the calibrating factors on both the heat transfer coefficients cannot be adjusted independently or the solution won't converge. Therefore, the calibrating factor is fixed arbitrarily at a constant value in the nucleate boiling zone while the calibrating factor in the film boiling zone is adjusted to obtain the proper outlet conditions. A related problem is to determine where the DNB point is in the zone. This is done by using the method outlined in the transient section as the solution proceeds up the mesh and when the intersection of the two functions is determined by extrapolation of the two functions, the DNB point is predicted there.

The method of solution, then, is to proceed upwards in the mesh node-by-node in the nucleate boiling zone using the known zone length and the assumed heat transfer coefficient calibration factor and extrapolating ahead to determine the DNB point. When the DNB point is found in a particular cell, then the calculation for that cell is repeated in order to use the properly prorated heat transfer coefficient (apportioned between the nucleate and the film boiling coefficients) for that cell. Then the solution switches to the film boiling zone and then proceeds to the top of the boiling zone and compares the sodium temperature obtained at the top to either $T_{s,hg}$ or $T_{s,in}$. Before the calculation proceeds node-by-node through the film boiling zone on the first iteration, however, an initial guess is made of the calibration factor in the zone is made on a one-node basis just as was done with Eqs. 7.3-67 and 7.3-69 in the superheated vapor zone. The only difference is that the sodium and water ΔT and Δh are now appropriate for the boiling zone and $\overline{T}_w$ becomes T_{sat}. The calibration factor applied to the film boiling heat transfer coefficient is adjusted on each iteration until the sodium temperature at the top of the zone satisfies the criterion. If, as the calculation proceeds upwards in the mesh, no DNB point is predicted before the top of the boiling zone is reached, then it is assumed there is no film boiling zone and the calibration factor in the nucleate boiling zone, otherwise constant, is searched upon until the criterion at the top of the zone is satisfied.

In order to solve the nodal equations, a method similar to that used in the superheated vapor zone is used. First a nodal energy balance equation exactly the same as Eq. 7.3-70 is solved for $T_{s,i+1}$ as in Eq. 7.3-71 and rewritten as in Eq. 7.3-72. Again, $T_{m,i}$ is solved for from the sodium side heat transfer Eq. 7.30-73 resulting in Eq. 7.3-74, rewritten as Eq. 7.3-75 and then 7.3-76. The water side heat transfer equation is slightly simpler than in the superheated zone because the water temperature is known at each node to be T_{sat}. Equation 7.30-77 becomes,

$$G_w \frac{1}{\Delta Z}\left(h_{w,i+1} - h_{w,i}\right) = H_{T,i}\left(T_{m,i} - T_{sat}\right)\frac{2\pi r_w \Delta Z}{A_w \Delta Z} \tag{7.3-90}$$

Equation 7.3-90 is solved for $h_{w,i+1}$ after $T_{m,i}$ is replaced with $e\ h_{w,i+1} + f$ from Eq. 7.3-76. The result is the following,

$$h_{w,i+1} = \frac{G_w h_{w,i} + H_{T,i} \frac{2\pi r_w \Delta Z}{A_w} \left(f - T_{sat} \right)}{G_w - h_{w,i} \frac{2\pi r_w \Delta Z}{A_w} e} \tag{7.3-91}$$

As before, when $h_{w,i+1}$ is computed, $T_{m,i}$ is found from Eq. 7.3-76 and $T_{s,i+1}$ from Eq. 7.3-72. The same considerations concerning the calculation of properties and heat transfer coefficients during the iterative process and concerning the inner and outer iterations apply to the boiling zone as apply to the superheated zone.

7.3.3.3.1.4 Friction Factors for Momentum Equation

As mentioned before in the section concerning the calculation of the pressure drops in the steam generator, the factor FR_i for each heat transfer regime in Eq. 7.3-56 needs to be defined for steady state conditions. If the "steady state" calculation does not include all heat transfer regimes, then the FR_i for the missing zones is arbitrarily set to 1.0. First an unnormalized pressure drop ΔP_i^u is calculated for heat transfer regime i,

$$\Delta P_i^u = -G_w^2 \left(\frac{1}{\rho_t} - \frac{1}{\rho_b} \right) - Z_i \left[\bar{\rho}_i 9.8 + G_w^2 0.31 \left(\frac{G_w D_h}{\bar{\mu}_i} \right)^{-0.25} \cdot \frac{1}{2} \frac{1}{D_\mu \bar{\rho}_i} R_i \right] \tag{7.3-92}$$

where all parameters except G_w are defined as in Eq. 7.3-56. Next, a normalized pressure drop ΔP_i^n is calculated,

$$\Delta P_i^n = \Delta P_i^u \frac{\Delta P_{SG}}{\sum_i \Delta P_i^u} \tag{7.3-93}$$

where ΔP_{SG} is the specified pressure drop across the entire steam generator length. The FR_i's are calculated as follows,

$$FR_i = \frac{\frac{\Delta P_i^n}{Z_i} + 9.8 \bar{\rho}_i + \frac{G_w^2}{Z_i} \left(\frac{1}{\rho_t} - \frac{1}{\rho_b} \right) 2 D_H \bar{\rho}_i}{0.31 G_w^2 \left(\frac{G_w D_H}{\bar{\mu}_i} \right)^{-0.25} R_i} \tag{7.3-94}$$

7.3.3.3.2 Recirculation-Type Steam Generator

Only the superheater steady-state condition needs to be described here since, as was explained above, the evaporator steady-state is described in the once-through steam generator section which can account for the situation with $h_{w,out} \leq h_g$. The steady state solution for the superheater is identical with the steady-state solution for the

superheated vapor zone covered in the once-through steam generator section. Obviously the option of the fixed length with the search on the calibration factor is the relevant option for the superheater. The water side outlet enthalpy is specified and the inlet water enthalpy is h_g. The sodium inlet temperature, as before, is externally determined and the sodium temperature at the outlet of the superheater must be determined just as it is in Eq. 7.3-65. The solution proceeds upwards to the top of the superheater and the sodium temperature calculated at the top is compared to $T_{s,in}$ and the calibration factor is adjusted until they are sufficiently close.

7.4 Component Models

Models of power plant heat transfer components, turbine, and relief valve have been implemented in the SASSYS-1 balance-of-plant network model. These models extend the scope of the existing balance-of-plant model in the SASSYS-1 LMFBR systems analysis code to handle nonadiabatic conditions and two-phase conditions along flow paths, and to account for work done across the boundaries of compressible volumes. Simple conservation balances and extensive component data in the form of correlations constitute the basis of the various types of components reported here.

This work is part of a continuing effort in plant network simulation based on general mathematical models. The models described in this section are integrated into the existing solution scheme of the balance-of-plant coding. While the mass and momentum equations remain the same as in Section 7.2 (except for the nozzle, which has different momentum equations), the energy equation now contains a heat source term due to energy transfer across the flow boundary or to work done through a shaft. The heat source term is treated fully explicitly. To handle two-phase conditions, the equation of state is expressed differently in terms of the quality and separate intensive properties of each phase.

Table 7.4-1 lists the various types of component models reported. The models are simple enough to run quickly, yet include sufficient detail of dominant plant component characteristics to provide reasonable results. All heater models have been tested as standalone models except the steam drum, which has been tested as part of a recirculation loop. Also an integrated plant test problem simulating an entire LMR plant was carried out with some of the heater models incorporated, and then the turbine model and the relief valve model were included and tested in similar but separate integrated test problems.

7.4.1 General Assumptions

For the simplicity of the models and for the convenience of modeling the components, certain common assumptions are made in all of the heater models. Additional assumptions necessary for each heater model will be described wherever appropriate. Assumptions for the turbine and relief valve models are given in the sections containing the discussions of these models.

The following assumptions are made in all eight heater models. Flow is incompressible on both shell and tube sides. Any two-phase fluid entering on the shell side instantaneously separates into liquid and vapor, and a new thermal equilibrium is

reached immediately. The two-phase interface on the shell side serves as the reference point for the saturation pressure of the heater. The two phases are at a common saturation temperature, and each phase is assumed to be at a uniform enthalpy. The momentum equation governing flow entering and exiting the shell side accounts for elevation pressure differences as gravity heads. Nevertheless, intensive properties such as specific volume and thermophysical properties such as viscosity are taken to be uniform for each phase, neglecting elevation effects, when considering heat transfer coefficients.

Table 7.4-1. Component Models

Heaters:

Deaerator, steam drum, condenser, reheater, flashed heater, drain cooler, desuperheating heater, desuperheater/drain cooler.

Rotating Machinery:

Turbine (including nozzle).

Valve:

Relief Valve.

Additional assumptions are made for the heaters containing tube bundles. Phase change does not occur within the tube bundle irrespective of the fluid temperature on the shell side. Although two-phase fluid may flow through pipes between two volumes, it is not allowed to be present inside the tube bundle which is the tube side of a heater. In general, the tube bundle is modeled as a single tube. Mass flux and pressure drop in the single tube of the model are the same as in the actual tube bundle, and the mass of the metal tubing is also conserved. These constraints do not allow tube length or surface area to be conserved, and so the tube surface heat transfer area is corrected to simulate the bundle heat transfer area through the use of calibration factors which provide an effective thermal resistance for conduction heat transfer.

Details of each heater will now be described, beginning with the simplest model, the deaerator, and progressing to the more complex models. The turbine and relief valve models then follow to yield a total of ten models discussed in this section.

7.4.2 Deaerator

There are two categories of heaters: open heaters and closed heaters. A deaerator is an open heater which refers to the fact that there is no distinction between tube and shell sides, so that hot fluid and cold fluid entering the heater mix together. Actually, a deaerator consists of a closed volume containing liquid and vapor at saturation conditions and is used to remove dissolved gases from an incoming fluid.

7.4.2.1 Model Description

As shown in Fig. 7.4-1, a deaerator is a right circular cylinder standing on end. Due to the existence of the two-phase interface, an appropriate response has to be implemented if the interface rises to the level of a pipe through which fluid enters or

exits the heater. In the situation when fluid enters the heater, the calculation will be stopped when the interface rises to the flow opening if the incoming fluid is other than either saturated or subcooled liquid. On the other hand, if fluid flows out of the heater through the pipe, a special treatment is required as follows. Normally, each flow opening is located entirely within either the liquid or the vapor region, with outgoing fluid quality equal to 0 or 1, respectively. However, the two-phase interface may also intersect an opening, causing two-phase fluid to flow out of the heater. Under these circumstances, the model assumes a slip ratio of one for the two-phase fluid and uses area weighting to compute the quality of the exiting fluid.

Consider the shaded area in Fig. 7.4-2 as the area occupied by vapor exiting the pipe. Then the ratio of this shaded area to the entire opening is simply the void fraction of the exiting flow, i.e., $\alpha \equiv A_g/A$.

Slip ratio is defined as

$$\frac{u_g}{u_f} = \left(\frac{\beta}{1-\beta}\right)\left(\frac{1-\alpha}{\alpha}\right),$$

which reduces to $\alpha = \beta$ when $u_g = u_f$ (slip ratio = 1).

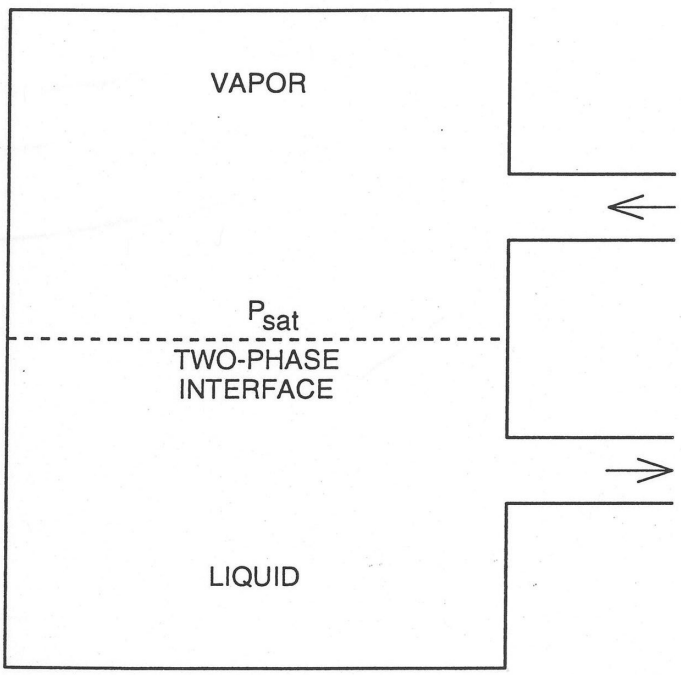

Figure 7.4-1. Deaerator

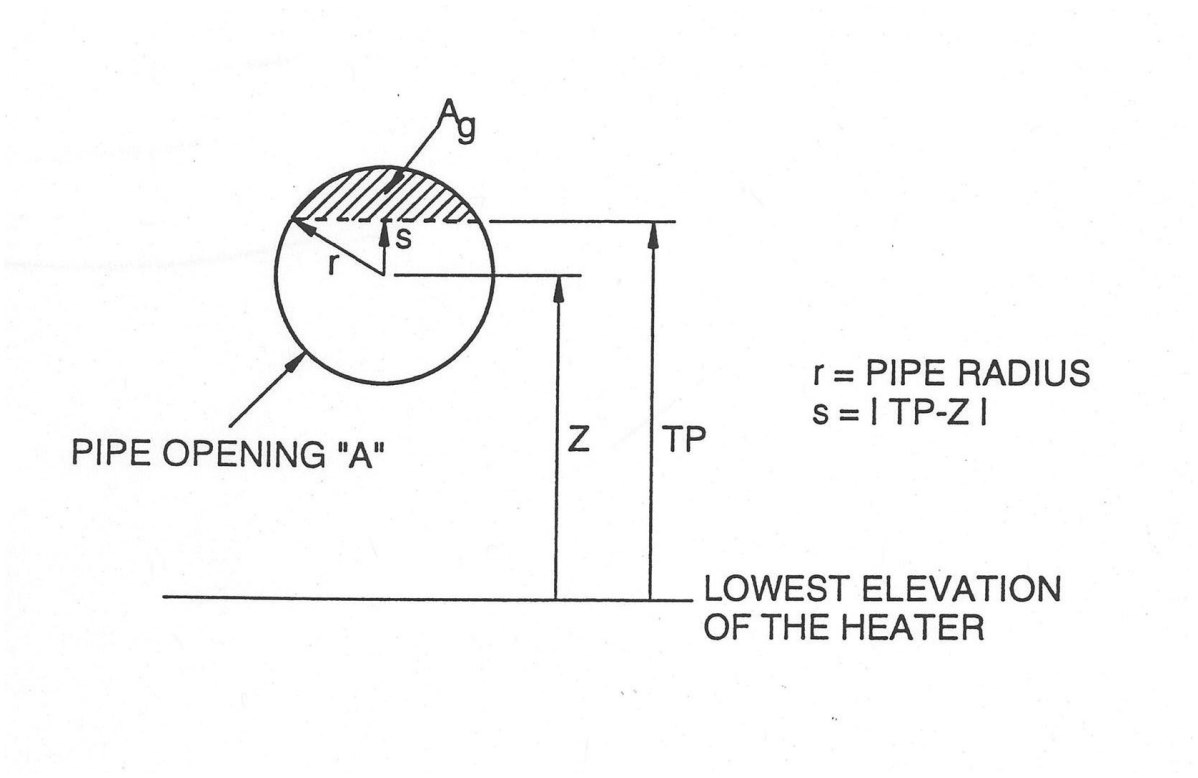

Figure 7.4-2. Area-Weighted Two-Phase Outflow Quality

Since β is defined as

$$\beta = \frac{1}{1+\left(\frac{(1-x)\nu_f}{x\nu_g}\right)}, \tag{7.4-1}$$

the quality can be expressed in terms of density and void fraction by rearranging Eq. 7.4-1 and using the fact that $\alpha = \beta$,

$$x = \frac{\nu_f \alpha}{\left(\nu_g(1-\alpha)+\nu_f \alpha\right)} = \frac{\rho_g \alpha}{\rho}, \tag{7.4-2}$$

where

$$\alpha = \left(r^2 \cos^{-1}\frac{s}{r} - s\left(r^2 - s^2\right)^{1/2}\right) / \pi r^2 \tag{7.4-3}$$

if the two-phase interface is higher than the center of the pipe but lower than the top of the opening, or

$$\alpha = 1 - \left(r^2 \cos^{-1} \frac{s}{r} - s\left(r^2 - s^2\right)^{1/2} \right) / \pi r^2 \tag{7.4-4}$$

if the two-phase interface is lower than the center of the pipe but higher than the bottom of the opening. The above area-weighted quality evaluation method also applies to all of the other heaters for treating two-phase outlet flow.

The two-phase interface of the heater has to be known before deciding the need to evaluate the area-weighted outlet flow quality. To determine the two-phase interface, the shell-side quality, x_S, of the heater has to be found first, which is calculated according to the enthalpy of the heater since the heater is at the saturation pressure, i.e., both the saturation enthalpies of the liquid and the vapor can be obtained from the known saturation pressure. Then, the two-phase interface *TP* is simply

$$TP = \frac{M\left(1 - x_s\right)v_f}{A_s} = \frac{\rho_s A_s H_s \left(1 - x_s\right)v_f}{A_s} = \rho_s H_s \left(1 - x_s\right)v_f, \tag{7.4-5}$$

where M is the heater total mass, A_s is the heater cross section, ρ_s is the heater density, and H_s is the heater height.

The deaerator must cope with small imbalances between incoming and outgoing energies in the steady state. These imbalances are caused by minor inconsistencies between user-specified thermodynamic conditions and the SASSYS-1 correlations for the thermodynamic properties. This problem is solved by the introduction of a pseudo-heat conduction energy transfer term. The temperature gradient between the heater and the ambient conditions serves as the driving force, and the code computes a pseudo-heat transfer coefficient which will give a steady-state energy balance. The coefficient is positive if energy is accumulating and negative if energy is draining. This coefficient is then kept constant throughout the transient. In formula form, the pseudo-coefficient can be expressed as

$$U_{pseu} = \frac{\sum (wh)_{in} - \sum (wh)_{out}}{T_s - T_\infty} \tag{7.4-6}$$

where T_s is the saturation temperature of the heater and T_∞ is the ambient temperature. The other heater models deal with the imbalances this same way.

The thermal-hydraulic effects of noncondensible gas on the model are neglected and the heat conductor term is not applied.

7.4.2.2 Analytical Equations

The applicable mass and energy equations for the deaerator are the same as those used in Section 7.2, so they will not be reiterated here. However, it should be noted that, unlike the volumes described in Section 7.2, there is strict separation of liquid and vapor in the deaerator, and so outgoing flow enthalpies are affected by the elevation of

the flow outlet. Calculations of outgoing flow enthalpies must take into account whether the outgoing flow is strictly liquid, strictly vapor, or a two-phase mixture if the outlet intersects the two-phase interface.

The separation of the phases affects the following equation, relating the change in compressible volume pressure to the changes in the flows in each of the segments attached to the volume, which is simply Eq. 7.2-47 in Section 7.2,

$$\Delta P_l = -\Delta t \left\{ Q_\ell^n + \sum_j w_j^n \left[h_j^n - h_\ell^n + v_\ell^n \left(DHDN(\ell) \right) \right] \mathrm{sgn}(j,\ell) + \sum_j \Delta w_j \left[h_j^n - h_\ell^n + v_\ell^n \left(DHDN(\ell) \right) \right] \mathrm{sgn}(j,\ell) \right\} / DENOM(\ell). \quad (7.4\text{-}7)$$

The superscript n, which denotes the time step, will be omitted for simplicity in the following discussion. Previously, in a volume with perfectly mixed two-phase fluid, the term h_j, which is the enthalpy of segment j attached to volume l, has the same enthalpy as volume l if segment j leads flow out of volume l; h_j is the enthalpy transported along segment j from the volume preceding segment j if fluid flows through segment j into volume l. Now, for the current heater volume, perfect mixing of two-phase fluid no longer exists and immediate separation of liquid from vapor is assumed to take place, so the value of h_j will be different from the mixture enthalpy of volume l due to the existence of the two-phase interface. That is, depending on the relative positions of segment j (pipe) and the two-phase interface, segment j may contain pure vapor, pure liquid, or two-phase fluid with an area-weighted quality determined by the scheme described in Section 7.4.2.1. Therefore, if segment j is an outlet segment, h_j can be $h_{\ell,g}$, the vapor enthalpy of volume l when the opening of segment j is higher than the two-phase interface; or$h_{l,f}$, the liquid enthalpy of volume l when the opening of segment j is lower than the two-phase interface; or else $h_{l,f} + x(h_{l,g} - h_{l,f})$, where x is the area-weighted quality when the two-phase interface lies within the segment opening. On the other hand, if segment j is an inlet segment, h_j will have to be determined according to which of the three possible situations exists in the volume at the inlet to segment j rather than in volume l. It is also possible that h_j may just be the transported enthalpy of the preceding volume if the preceding volume is not a heated volume but a volume with fluid of perfect mixing.

For two-phase flow in the pipe, the momentum equation is again basically the same as for single-phase flow except that a two-phase multiplier, which is a function of both quality and pressure, has to be included wherever a two-phase flow is present in the segment (e.g., pipe) to adjust the friction factor for modeling pressure drop. See Section 7.2 for the discussion of this empirically-determined multiplier. One more thing to mention regarding the energy equation is that the source term Q_ℓ in Eq. 7.4-7 is computed explicitly as $(T_s - T_\infty)U_{pseu}$, where U_{pseu} is determined in the steady state by Eq. 7.4-6. T_s is the saturation temperature of the heater in the previous time step and T_∞ is the constant ambient temperature specified by the user in the steady state.

7.4.3 Steam Drum

A steam drum is mainly used to separate two-phase fluid from the recirculation loop and then provide saturated steam to the superheater. Like the deaerator, a steam drum is categorized as an open heater.

7.4.3.1 Model Description

The physical configuration of a steam drum is similar to that of a deaerator except that it is a cylinder now lying on the side, as depicted in Fig. 7.4-3. The call for an appropriate response when the two-phase interface falls within the pipe opening as well as the need for coping with small imbalances between incoming and outgoing energies are handled the same way as previously described in the deaerator model.

Predicting the level of the two-phase interface in transients is a difficult problem in a heater of this configuration because the cross-sectional area parallel to the cylinder axis varies in the vertical direction (remember, the cylinder is lying on the side), and so the two-phase interface must be found from a transcendental equation. Since the steam drum is a right circular cylinder, it is obvious from the end view in Fig. 7.4-3 that the ratio of A_g to A_g plus A_f is the void fraction α_s, i.e.,

$$\alpha_s = \frac{A_g}{A_g + A_f},$$

where A_g is the projected area occupied by the vapor and A_f is the area by liquid. By taking a similar approach to that carried out in Section 7.4.2.1 and bearing in mind that the cross-sectional area of the entire cylinder is now under consideration, rather than just the opening of a pipe which is attached to the heater as depicted in Fig. 7.4-2, equations of the same form as Eqs. 7.4-3 and 7.4-4 are obtained,

$$\alpha_s = \left[r_s^2 \cos^{-1}\frac{L}{r_s} - L\left(r_s^2 - L^2\right)^{1/2} \right] / \pi r_s^2 \ , \ CV \le TP < CV + r_s \ , \tag{7.4-8}$$

and

$$\alpha_s = 1 - \left[r_s^2 \cos^{-1}\frac{L}{r_s} - L\left(r_s^2 - L^2\right)^{1/2} \right] / \pi r_s^2 \ , \ CV - r_s \le TP < CV \ , \tag{7.4-9}$$

where $L = |TP - CV|$.

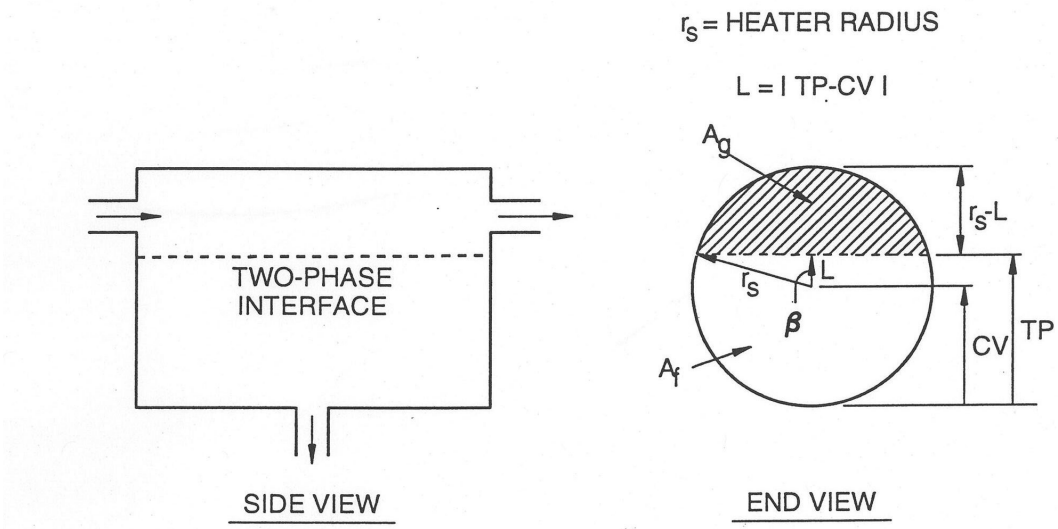

Figure 7.4-3. Steam Drum

The difference between Eqs. 7.4.3 and 7.4-8 (or Eqs. 7.4-4 and 7.4-9) is that *s* on the right-hand side of Eq. 7.4-3 is a known quantity and α is to be found, which in turn yields the pseudo-quality *x* for the outgoing flow, whereas in the current situation, *L* in Eq. 7.4-8 is an unknown and α_s is already known from the corresponding quality x_s by the relation $\alpha_s = x_s v_g / v$. The quality x_s is simply calculated from the updated heater pressure and enthalpy. Thus, Eq. 7.4-8 or Eq. 7.4-9 becomes a transcendental equation to be solved for the two-phase interface, *TP*.

A noniterative scheme has been developed to solve this equation. See Appendix 7.3 for a description of this scheme.

7.4.3.2 Analytical Equations

As is obvious from the similarity in the configurations of the deaerator and the steam drum, what is described in Section 7.4.2.2 about the analytical equations for the deaerator is also applicable to the steam drum model.

7.4.4 Condenser

Beginning with this section, a total of six closed heaters including condenser, reheater, flashed heater, drain cooler, desuperheating heater, and desuperheater/drain cooler will be described. The term "closed heater" indicates that hot and cold fluids are separated between a shell side and a tube side. Heat transfer occurs across the tube without contact between hot and cold fluids. Closed heaters consist of a closed volume, or shell side, and a tube bundle, or tube side. Flow is carried into and out of the tube bundle by pipes which lie outside the heater boundary. The condenser is the simplest

one among these closed heaters, and it is used to convert steam from the turbine to liquid.

7.4.4.1 Model Description

As diagramed in Fig. 7.4-4, a condenser is a box with a tube bundle passing horizontally through it; this is essentially a deaerator with a tube bundle running through the vapor region. The tube bundle may have bends in it. The fluid on the tube side is assumed to be single phase. The tube bundle is assumed to be contained entirely in the vapor region, so a condensation heat transfer coefficient is used on the shell side under the normal conditions when the temperature on the tube side, in which river water or cooling fluid flows, is lower than the shell-side vapor temperature. The model also includes the contingency to use a shell-side heat transfer coefficient computed from the Dittus-Boelter equation (Ref. 7-4),

$$h = 0.023 \frac{k}{D_h} \mathrm{Re}^{0.8} \mathrm{Pr}^{0.4}, \tag{7.4-10}$$

in case the tube-side temperature is higher than that on the shell side, as in an accident or any unfavorable transients. In either case, the heat transfer coefficient must be adjusted in the steady state so that the tube-side temperature distribution is consistent with the temperatures in the remainder of the plant, i.e., the temperatures at the tube inlet and outlet coincide with the user-specified temperatures.

The heat transfer coefficient on the tube side is calculated using the Dittus-Boelter equation. Heat transfer between the tube side and the shell side is assumed to take place through the mechanism of radial conduction only; axial conduction is neglected. This radial conduction assumption for the tube bundle is made for all of the closed heater models.

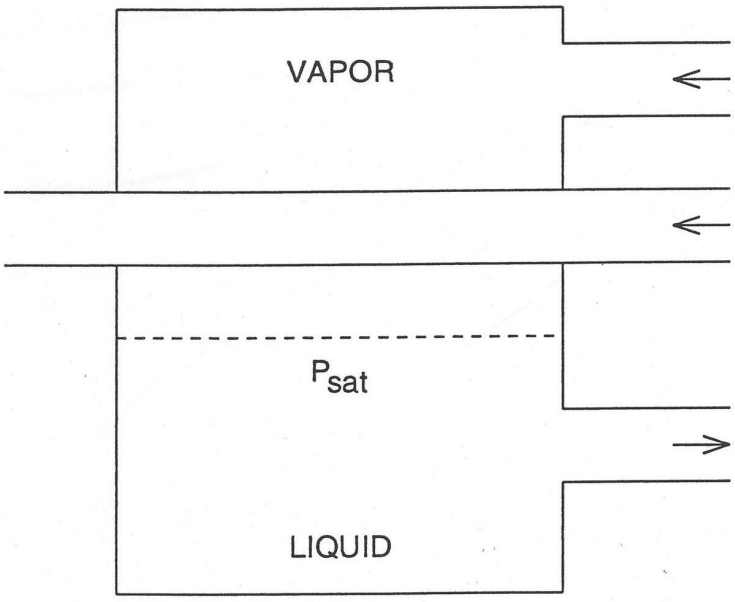

Figure 7.4-4. Condenser

7.4.4.2 Analytical Equations

The mass and energy equations for the shell side of the condenser are the same as those used in the open heaters, and these equations are also valid for the shell side in all the closed heaters. Also, the same momentum equation used in Section 7.2 is again applicable to the tube side (the heated section of the flow segment) of the condenser and other closed heaters. Naturally, the two-phase friction multipliers should be included whenever an inlet or outlet pipe contains other than single-phase fluid. In addition, a simplified energy equation based on the first law of thermodynamics is needed for the heated tube element, i.e., the tube side fluid and the metal tube itself.

For the tube side fluid, the energy equation can be expressed as

$$m_t \frac{dh_t}{dt} = Q_t + w(h_{in} - h_{out}) \tag{7.4-11}$$

if the kinetic energy and potential energy are negligible.

For the metal tube, the energy balance has the form,

$$m_m c_m \frac{dT_m}{dt} = Q_m . \tag{7.4-12}$$

7.4.4.3 Discretized Equations

The tube side is discretized as shown in Fig. 7.4-5, and the temperature distribution on the tube side is determined using the differenced form of the first law of thermodynamics,

$$m_{it} \frac{\Delta h_{it}}{\Delta t} = Q_{it} + w\left(h_{i-1,t} - h_{it}\right), \tag{7.4-13}$$

where

$$Q_{it} = \left(T_{im} - T_{it}\right) \Big/ \left(\frac{1}{2\pi \Delta z r h_t} + \frac{\ln\left(1+\frac{\delta}{2r}\right)}{2\pi \Delta z k_m} \right) \equiv \frac{\left(T_{im} - T_{it}\right)}{R_t}. \tag{7.4-14}$$

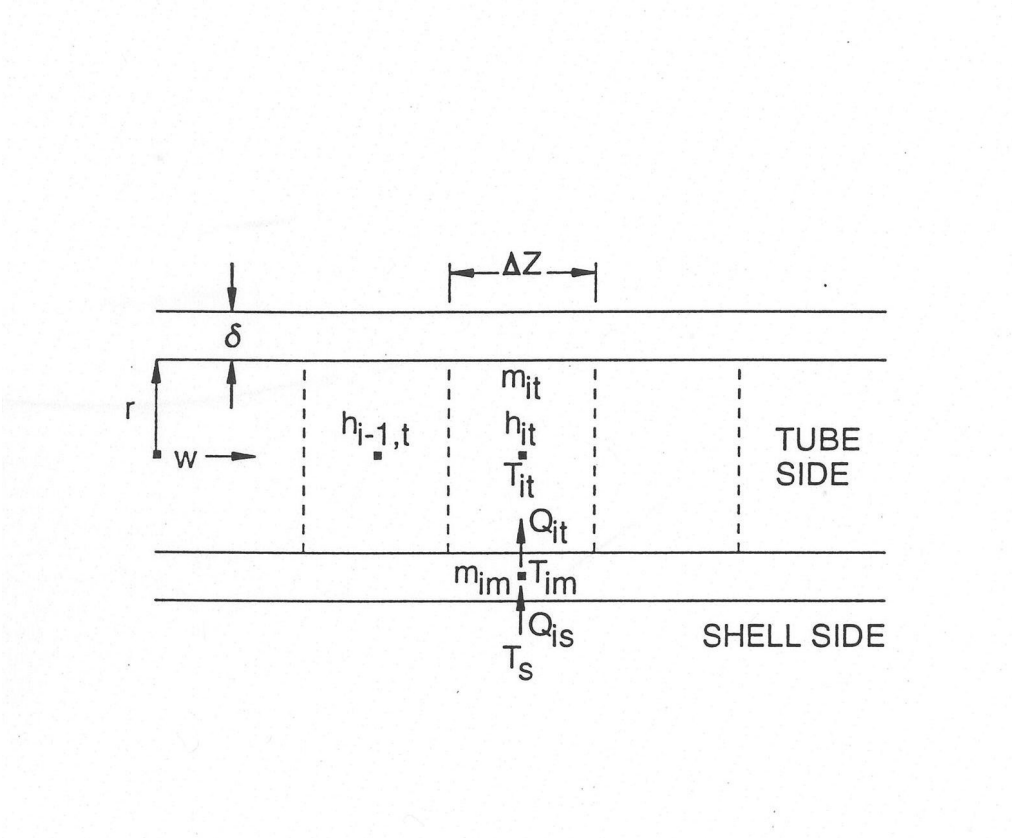

Figure 7.4-5. Tube-side Nodalization

The metal tube temperatures T_{im} are computed from a similar set of equations,

$$m_{im} C_m \frac{\Delta T_{im}}{\Delta t} = Q_{is} - Q_{it}, \tag{7.4-15}$$

and

$$Q_{is} = \left(T_s - T_{im}\right) \Big/ \left(\frac{\left(\ln \frac{r+\delta}{r+\delta/2} \right)}{2\pi \Delta z k_m} + \frac{1}{2\pi \Delta z \left(r+\delta\right) h_{is}} \right) \equiv \frac{\left(T_s - T_{im}\right)}{R_{is}}. \tag{7.4-16}$$

Note that T_s, the shell-side temperature, is considered to be uniform throughout the entire heater volume, whether in the steam region or in the liquid region, and that the specific heat and the thermal conductivity of the metal tube are assumed to be constant within the temperature range under consideration. The thermal resistance on the tube side, R_t, is the same at each node along the tube side but on the shell side, R_{is}, may vary node to node along the shell side if the tube is partially submerged in the liquid region. When the shell side is hotter than the tube side, it is assumed that no local boiling

occurs on the tube side and that the condensate does not form a wetted perimeter along the tube outer periphery.

The updated fluid enthalpy at each node is calculated explicitly using quantities at the previous time step, so from Eq. 7.4-13 it can be expressed

$$h_{it}^{n+1} = h_{it}^{n} + \frac{\Delta t^{n}}{m_{it}^{n}}\left(Q_{it}^{n} + w^{n}\left(h_{i-1,t}^{n} - h_{it}^{n}\right)\right), \tag{7.4-17}$$

where

$$Q_{it}^{n} = \frac{\left(T_{im}^{n} - T_{it}^{n}\right)}{R_{t}^{n}}. \tag{7.4-18}$$

Similarly, Eq. 7.4-15 can be rewritten in explicit form for updating the metal tube temperatures at each node,

$$T_{im}^{n+1} = T_{im}^{n} + \frac{\Delta t^{n}}{m_{im}\, C_{m}}\left(Q_{is}^{n} - Q_{it}^{n}\right), \tag{7.4-19}$$

where

$$Q_{is}^{n} = \frac{\left(T_{s}^{n} - T_{im}^{n}\right)}{R_{is}^{n}}. \tag{7.4-20}$$

The superscript n in R_t^n denotes that the tube side heat transfer coefficient h_t is a function of time, i.e., h_t^n, whereas the metal thermal conductivity k_m is assumed to be constant throughout the transient. This is also true for h_{is} and k_m in R_{is}.

The tube-side fluid temperature T_{it}^{n} in Eq. 7.4-18 is readily computed according to the equation of state from the fluid enthalpy and pressure at each node, and T_s^n is just the saturation temperature of the shell side fluid in the heater.

All of the terms on the right-hand side of Eq. 7.4-17 are known from the previous time step, so h_{it}^{n+1} can be updated, which will then yield T_{it}^{n+1} for use in Eq. 7.4-18 in the next time step. T_{im}^{n+1} on the other hand is determined independently from Eq. 7.4-19, with Q_{is}^{n} and Q_{it}^{n} given respectively by Eqs. 7.4-18 and 7.4-20. The link between the condenser model and the rest of the balance-of-plant models is made through the heat source terms, i.e., Q_ℓ^n in Eq. 7.4-7 and Q_ℓ^n in Eq. 7.4-20. The summation of Q_{is}^{n} at each node along the shell side is in fact the negative of the heat source term Q_ℓ^n for the heater in Eq. 7.4-7. The sign change reflects the fact that Q_{is} should be a heat sink term for the heater when the shell side temperature is higher than the tube side temperature.

7.4.5 Reheater

A reheater is used to improve turbine performance by reheating the moist steam to the superheated phase as it passes between stages of the turbine.

7.4.5.1 Model Description

The basic features of a reheater are depicted in Fig. 7.4-6, for illustrative purposes it is a right circular cylinder standing on end. The shell side is assumed to be at a lower temperature than the tube side. In this type of heater, the shell side is all vapor, and the reheater appears to be little more than the vapor section of a condenser with a vertically bent tube bundle. However, there is one important difference: the fluid on the tube side changes phase from steam to two-phase as it passes through the reheater. Modeling this phase transition requires use of the energy equation; however, the energy equation in the balance-of-plant formulation is solved at flow junctions (such as the shell side of a heater), not along flow paths (such as the tube side). Therefore, the reheater is modeled in the configuration shown in Fig. 7.4-7. The shell side of Fig. 7.4-6 becomes the tube side in Fig. 7.4-7, with steam which is being heated flowing within the tube, and the tube side of Fig. 7.4-6 becomes the shell side in Fig. 7.4-7. The shell side of Fig. 7.4-7 then easily models the phase transition which occurs in the tube side of the reheater.

The reconfiguration of the reheater to Fig. 7.4-7 is done so as to conserve volume on both sides of the heater. The height, H, of the cylinder in Fig. 7.4-7 is now taken as the difference between the elevations of the highest tube and the lowest tube in the tube bundle of the original configuration in Fig. 7.4-6. Therefore the cross sectional area A_s on the shell side in Fig. 7.4-7 is determined as

$$A_s = \frac{V_t}{H}$$

where V_t is the internal volume of all tubes in the tube bundle in Fig. 7.4-6. Furthermore, the mass of the metal tube, m_{im}, in each node in Fig. 7.4-7 is obtained by dividing the total metal mass of all original tubes, M_m, by H and then multiplying by the node length Δz,

$$m_{im} = \frac{M_m}{H}\Delta z \tag{7.4-21}$$

Similarly, the internal tube surface area in each node is computed based on the total internal heat transfer surface of all tubes, A_t, in Fig. 7.4-6 to be $(A_t/H)\ \Delta z$. Both the inside radius and the outside radius of the tube in Fig. 7.4-7 are also needed for use in equations like Eqs. 7.4-14 and 7.4-16 in order to compute heat transfer across the tube boundaries. The inside radius is readily calculated using the internal tube surface area in each node just described above. From the relationship, $2\pi r\Delta z = (A_t/H)\ \Delta z$, the inside radius r_i is computed as

$$\mathrm{r_i} = \frac{\mathrm{A_t}}{2\pi \mathrm{H}},$$

and the outside radius can then be deduced by making use of Eq. 7.4-21 to be

$$r_o = \left(r_i^2 + \frac{M_m}{H\rho\pi} \right)^{1/2} ,$$

where ρ is the metal density which is assumed to remain the same throughout the reconfiguration.

The model of Fig. 4-7 is very similar to a condenser except that the tube side is vertical instead of horizontal. This means that the tube passes through both liquid and vapor. Since the tube side vapor is heated by the shell side fluid, the heat transfer coefficient on the shell side h_{is} is computed from the Dittus-Boelter correlation in the liquid region and a condensation coefficient in the vapor region. Usually, the two-phase interface will fall within one of the nodes which discretizes the tube side; in this case, the heat transfer coefficient within the node is an area-weighted combination of the condensation coefficient and the Dittus-Boelter coefficient.

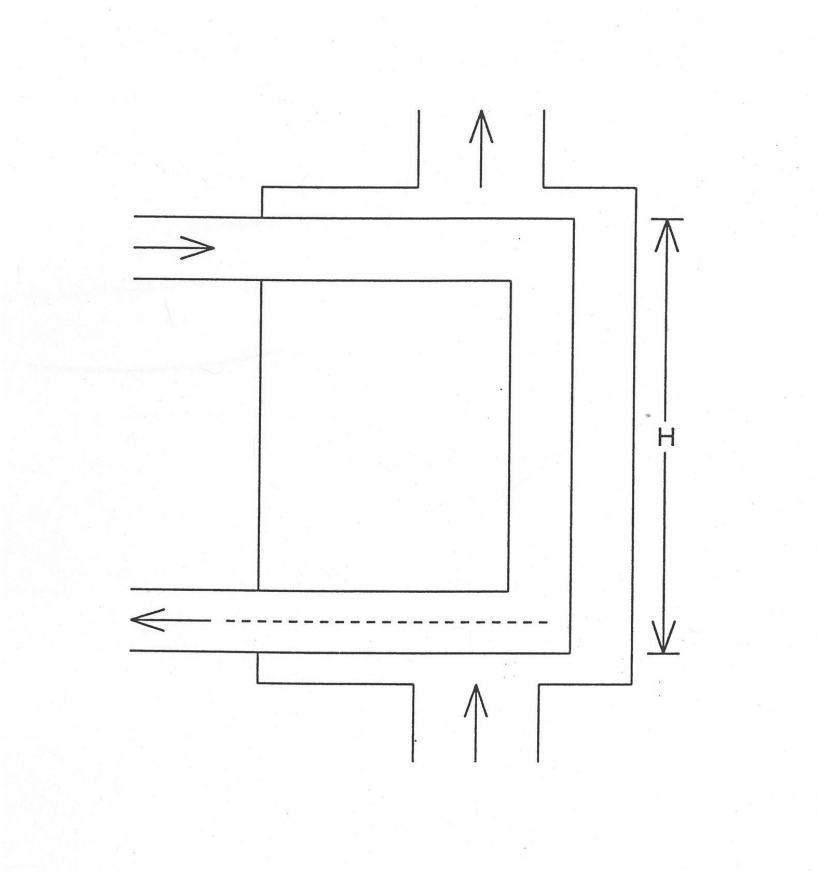

Figure 7.4-6. Reheater

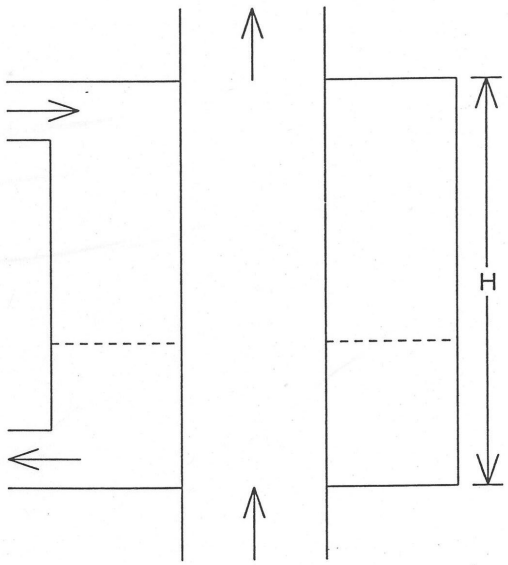

Figure 7.4-7. Reconfiguration of the Reheater

7.4.5.2 Analytical Equations and Discretized Equations

The equations discussed in Sections 7.4.4.2 and 7.4.4.3 for the condenser model also apply to the reheater model and to the remaining closed heater models. The only difference between the energy equations for the condenser and reheater models is in the calculation of the shell-side heat transfer coefficient, as described in Section 7.4.5.1.

7.4.6 Flashed Heater

A flashed heater is needed when liquid upstream of the heater shell side is above the shell side saturation point. The flashed heater allows the liquid to flash safely upon entering the heater.

7.4.6.1 Model Description

The geometry of the flashed heater is given in Fig. 7.4-8. This is a right circular cylinder lying on the side, with a U-shaped tube bundle that is partially submerged in liquid and partially surrounded by vapor. The bundle enters and leaves the shell side through one end of the cylinder, with the entrance and exit at two different elevations. The tube-side fluid is assumed single phase, and fluid can enter at either the lower or the upper elevation. These assumptions are also made in the drain cooler, desuperheating heater, and desuperheater/drain cooler models to be described in subsequent sections. Therefore, there are two bends in the tube, and the tube is considered to consist of three sections: two horizontal ones of equal length and a vertical one of length equal to the distance between the elevations of the tube entrance and exit.

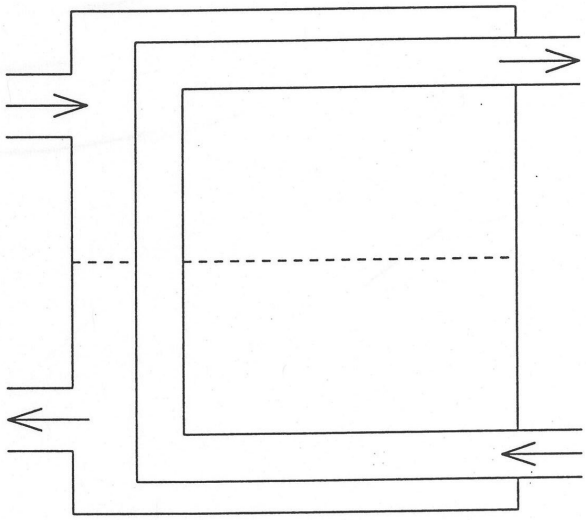

Figure 7.4-8. Flashed Heater

7.4.6.2 Analytical Equations and Discretized Equations

As discussed in Section 7.4.5.2 for the reheater model, the equations of Sections 7.4.4.2 and 7.4.4.3 also apply to the flashed heater model. However, some details specific to the flashed heater need further explanation. The determination of the heat transfer coefficient on the shell side becomes more complicated due to the bending of the tube. The two-phase interface will not only fall within one of the nodes as before in the reheater, but also might fall within many of the nodes when it reaches either of the two horizontal sections of the tube.

In the latter situation, the scheme of area-weighted heat transfer coefficients is again used. In either of the situations, provision is made to handle the case when the tube side temperature is higher than the shell side temperature, an additional possibility likely to occur during transients. If the tube side is cooler than the shell side, the heat transfer coefficients along the tube surface are computed as for the reheater. If the tube side is hotter than the shell side, the coefficient within the vapor region is calculated from the Dittus-Boelter correlation, and in the liquid region, a boiling heat transfer coefficient from the nucleate boiling regimes (Ref. 7-9)

$$h = \left(e^{P/(8.7\times10^{6})}/22.65\right)q^{0.5} \tag{7.4-22}$$

is used. The tube side heat transfer coefficient is always calculated from the Dittus-Boelter correlation no matter if the tube side is cooler or hotter than the shell side, i.e., assuming no phase change on the tube side in any case.

Predicting the level of the two-phase interface is a complicated problem in a heater of this configuration for two reasons. First, as in the steam drum, the cross-sectional area parallel to the cylinder axis varies in the vertical direction, and so the two-phase interface must be found from a transcendental equation. See Appendix 7.3 for the noniterative scheme to solve this equation. Second, the volume taken up by the tube bundle must be considered when determining the two-phase interface. In order to simplify the calculations, the void fraction is taken to be the ratio of the vapor volume divided by the vapor volume plus the liquid volume (rather than dividing by the total volume, which is the sum of the volumes of vapor, liquid, and tube bundle) when the interface falls between the bundle inlet and outlet, i.e.,

$$\alpha = \frac{x v_g}{x v_g + (1 - x) v_f} \tag{7.4-23}$$

where x is known once the new volume pressure and enthalpy are updated. Equation 7.4-8 (or Eq. 7.4-9) can then be combined with Eq. 7.4-23 to solve for the two-phase interface.

7.4.7 Drain Cooler

When the shell side outlet liquid from a heater must be sufficiently subcooled so as to remain liquid at the lower pressure of a downstream component, a drain cooler is needed.

7.4.7.1 Model Description

As shown in Fig. 7.4-9, the drain cooler configuration is identical to that of the flashed heater with the addition of a drain built into a lower corner of the cylinder. The top of the drain extends horizontally across the cylinder perpendicular to the cylinder axis (see end view in the same figure). The drain is separated from the remainder of the shell side except for a flow inlet which brings saturated liquid from the heater into the drain. This flow inlet is assumed to be always submerged in the saturated liquid, and calculation will be stopped whenever the two-phase interface drops below the inlet and uncovers it, since this might cause the subcooled fluid to flow out of the drain and into the shell side of the heater. There is also a flow outlet which carries liquid out of the drain and away from the heater. Liquid within the drain is always assumed to be subcooled at the saturation pressure of the shell side of the heater. Inlet and outlet flows are assumed to be nearly equal during a transient, for no phase-change is allowed in the drain and thus flow may be assumed incompressible. One end of the tube bundle passes through the drain, as seen in Fig. 7.4-9. The tube-side fluid can enter at either the lower or the upper elevation.

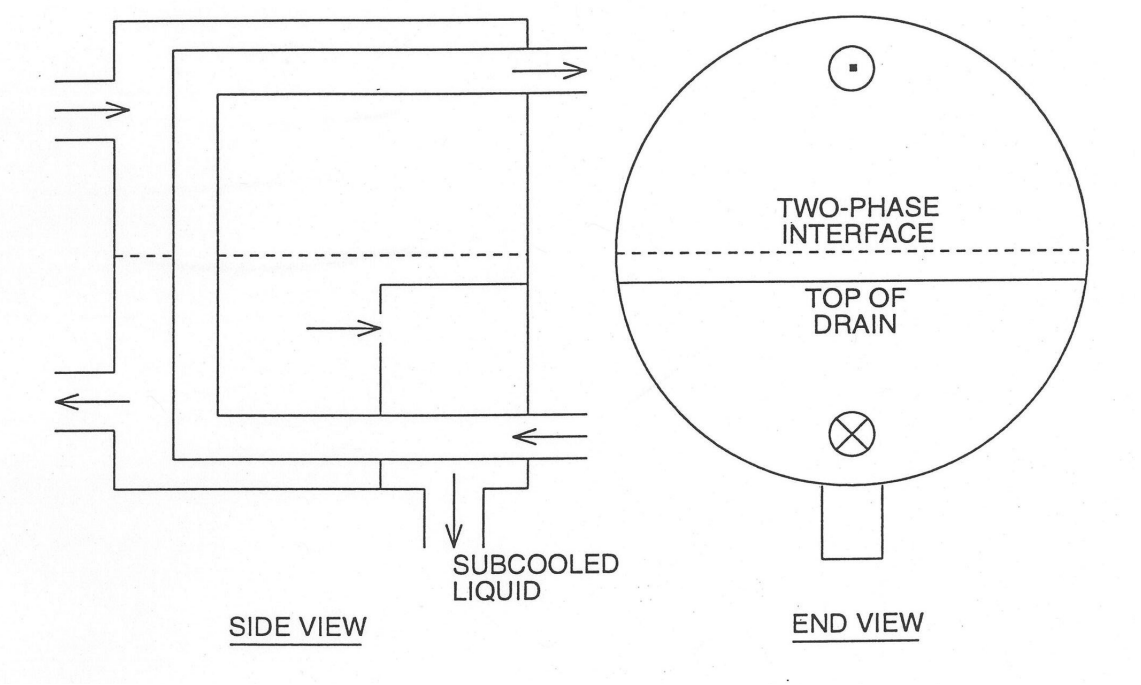

Figure 7.4-9. Drain Cooler

7.4.7.2 Analytical Equations and Discretized Equations

For the part of the drain cooler outside the drain, the discussion in Section 7.4.6.2 about the flashed heater is applicable to the drain cooler model. Nevertheless, there are two further points to be noted. First, although the fluid flowing out of the drain through the pipe which is attached to the drain has the same enthalpy as that of the subcooled liquid in the drain, the energy being lost from the shell side of the heater is actually the saturation enthalpy of the shell side liquid. Therefore, the term h_j^n in Eq. 7.4-7 has to be equal to the saturated liquid enthalpy. When j corresponds to the outlet flow segment from the drain in order for this equation to compute the shell-side pressure change correctly. On the other hand, the fluid enthalpy being transported from the drain to the next component must be set to the subcooled liquid enthalpy of the drain. Second, the heat source term Q_l in Eq. 7.4-7 will now have contributions only from the heat transfer through the boundaries of the tube bundle outside the drain. The energy heat transfer occurring across the tube boundaries within the drain will be considered as Q_D of the drain to be used in Eq. 7.4-24 below.

A one-node energy equation,

$$m_D \frac{dh_D}{dt} = Q_D + W_D(h_{in} - h_{out}) \tag{7.4-24}$$

is currently used on the shell side along the tube within the drain. Plans are to add a multi-node energy equation on the shell side to improve the treatment of the energy balance within the drain, which is especially important in the counterflow situation. On the tube side, the multi-node treatment is retained.

In discretized form, Eq. 7.4-24 is rewritten as,

$$h_D^{n+1} = h_D^n + \frac{\Delta t^n}{m_D^n}\left(Q_D^n + w_D^n\left(h_{in}^n - h_{out}^n\right)\right), \tag{7.4-25}$$

where h_{in}^n is the saturated liquid enthalpy and h_{out}^n in the current one-node treatment, is actually h_D^n. Q_D^n is the summation of the contributions from all the nodes within the drain, i.e.,

$$Q_D^n = \sum_i Q_{iD}^n . \tag{7.4-26}$$

with

$$Q_{iD}^n = \frac{T_{iD}^n - T_{im}^n}{R_{iD}^n}, \tag{7.4-27}$$

where

$$R_{iD}^n = \frac{\ln\left(\dfrac{r+\delta}{r+\delta/2}\right)}{2\pi\,\Delta z\,k_m} + \frac{1}{2\pi\,\Delta z\left(r+\delta\right)h_{iD}^n} . \tag{7.4-28}$$

Note that R_{iD}^n is simply R_D^n and T_{iD}^n merely T_D^n in the current one-node treatment on the shell side within the drain, which means h_{iD}^n is equal to h_D^n. Q_D^n is calculated explicitly.

For the tube side within the drain, Eqs. 7.4-17 and 7.4-18 are used, and Eq. 7.4-19 is applied to the metal tube within the drain, with Q_{is}^n in Eq. 7.4-15 replaced by Q_{iD}^n from Eq. 7.4-27.

Within the drain, a heat transfer coefficient h_D^n is computed from the Dittus-Boelter equation on the shell side of the tube surface, regardless of whether the tube side is hotter or colder than the shell side.

Adjustments are made separately to the drain and to the remainder of the shell side in order to achieve a steady-state energy balance which is consistent with conditions in the remainder of the plant. First, the code computes a calibration factor to adjust the tube surface heat transfer area within the drain. Then, energy is balanced in the remainder of the heater by computing a separate factor plus a pseudo-heat transfer coefficient as described previously.

7.4.8 Desuperheating Heater

A desuperheating heater is needed when the steam entering the heater shell side is highly superheated. The entering steam is initially contained in a desuperheating region, where it transfers heat to the tube side fluid rather than dissipating heat to the shell side saturated steam. Steam moving from the desuperheating region to the main section of the shell side is near saturation. The desuperheating region also protects the remainder of the heater from being damaged by highly superheated steam.

7.4.8.1 Model Description

The desuperheating heater is diagrammed in Fig. 7.4-10; it can be summed up as a drain cooler turned upside down. Instead of a drain at the bottom, it has a desuperheating region built into an upper corner. The desuperheating region is filled with superheated vapor at the saturation pressure of the heater two-phase interface. Normally, the tube side is filled with a single-phase fluid which is cooler than the vapor in the desuperheating region; the model also allows the tube side temperature to be higher than the shell side temperature, within or outside the desuperheating region. The desuperheating heater model does not handle the situation when the two-phase interface reaches the outlet of the desuperheating region, which might cause the desuperheating region to be partially filled with liquid. If the two-phase interface reaches this point, the calculation is stopped. All other aspects of the drain cooler model, such as inlet and outlet flows of the drain are nearly equal and the tube-side fluid can enter at either of the tube ends, apply to the desuperheating heater.

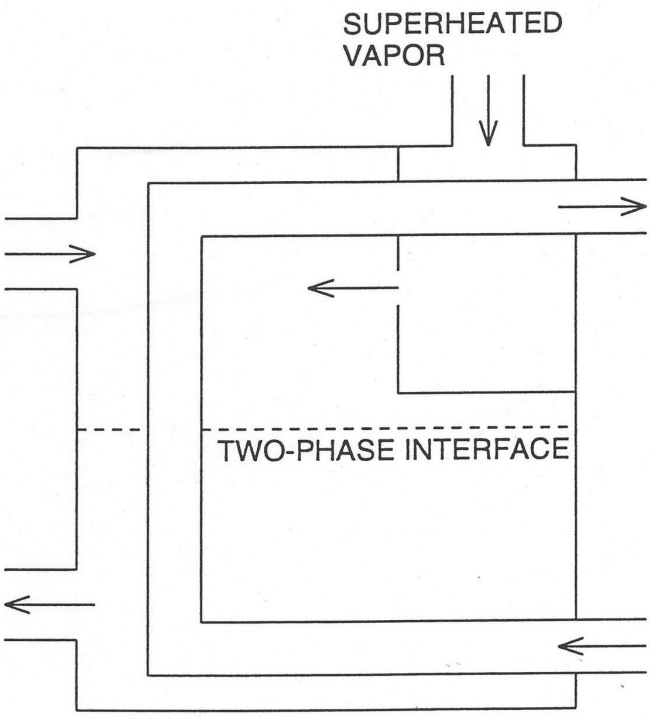

Figure 7.4-10. Desuperheating Heater

7.4.8.2 Analytical Equations and Discretized Equations

All the aspects described in Section 7.4.7 for the drain cooler model are applicable to the desuperheating heater and, wherever necessary, the subscript D for the drain should be replaced by DS for the desuperheating region, such as in Eqs. 7.4-24 to 7.4-28. However, it should be noted that the term h_j^n in Eq. 7.4-7 now is the superheated steam enthalpy of the desuperheating region when j corresponds to the inlet flow segment into the desuperheating region.

7.4.9 Desuperheater/Drain Cooler

7.4.9.1 Model Description

This heater is pictured in Fig. 7.4-11 and is a combination of the drain cooler and the desuperheating heater. All details discussed in Sections 7.4.7.1 and 7.4.8.1 for these two models apply also to the desuperheater/drain cooler.

7.4.9.2 Analytical Equations and Discretized Equations

All aspects described in Sections 7.4.7.2 and 7.4.8.2 for the drain cooler and the desuperheating heater are applicable to the desuperheater/drain cooler. Three additional points to note are that 1) the mass flow rate entering the desuperheating region can differ from that entering the drain, 2) separate calibration factors are used in the desuperheating section and in the drain for adjusting the tube surface heat transfer area to conserve energy, and 3) the heat source term Q_l in Eq. 7.4-7 will now have contributions only from the energy transferred across the boundaries of the tube bundle outside the desuperheating region and the drain.

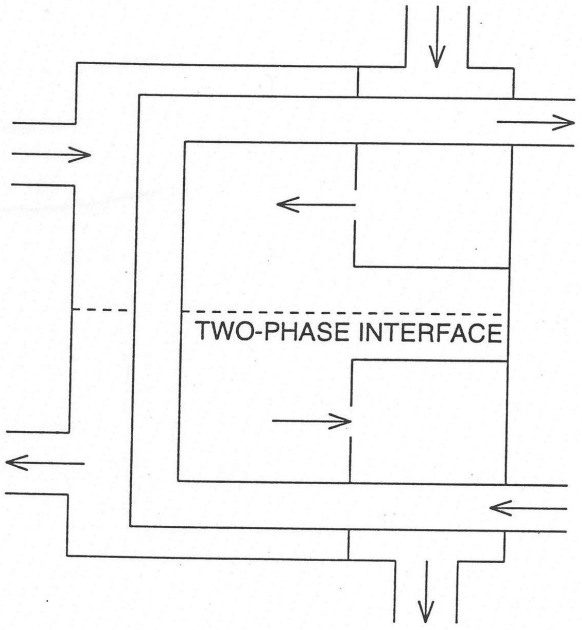

Figure 7.4-11. Desuperheating/Drain Cooler

7.4.10 Turbine

A turbine is a device in which energy is removed from the fluid as a result of work performed by the flow; it actually is composed of many stages driving one rotor which extracts work from the flow. The stages are connected by nozzles which permit both non-choked and choked flow. Compressible flow is now very important in describing the flow behavior in the nozzles.

7.4.10.1 Model Description

The basic features of a turbine are depicted in Fig. 7.4-12. This schematic shows two of the stages connected by nozzles driving one common rotor which in turn drives a generator. Also shown in the figure are the extraction steam ports, in which the steam is treated as incompressible flow. A series of volumes is used to model the various stages in the turbine, and each individual stage is represented by a compressible volume. There is no limit on the number of turbine stages so long as it does not exceed the maximum number of compressible volumes allowed in the code. Nozzles are modeled by special segments using a different form of the momentum equation from that discussed in Section 7.2 in order to account for the characteristics of the compressible flow. Separate expressions based on thermodynamic conditions at the inlet alone, when the flow is choked, or at the outlet as well, when the flow is nonchoked, are used to compute the nozzle flow. These correlations will be discussed in detail in Section 7.4.10.2.

Turbine efficiency is based on losses to isentropic expansion, and shaft work is then calculated using quasi-empirical correlations for stage efficiency. Stage efficiency is affected by many loss factors, such as rotation loss, moisture loss, nozzle-end loss, etc., but only rotation loss and moisture loss are included in the current model because they are significant losses and their functional formulations are known. More loss factors will be included in future model improvements.

7.4.10.2 Analytical Equations

The assumption that the liquid and vapor are strictly separated in the heater models reported above does not apply to the turbine model. Instead, perfect mixing within the compressible volumes which model the turbine stages is now adopted due to the movement of the rotating blades; this is the same assumption made for the energy equation governing the compressible volumes discussed in Section 7.2. Both the mass and the energy equations used in the turbine model are the same as those used in the heater models and in Section 7.2 except that the energy equation used in the turbine model has an additional term included accounting for the energy loss through the work done by the turbine.

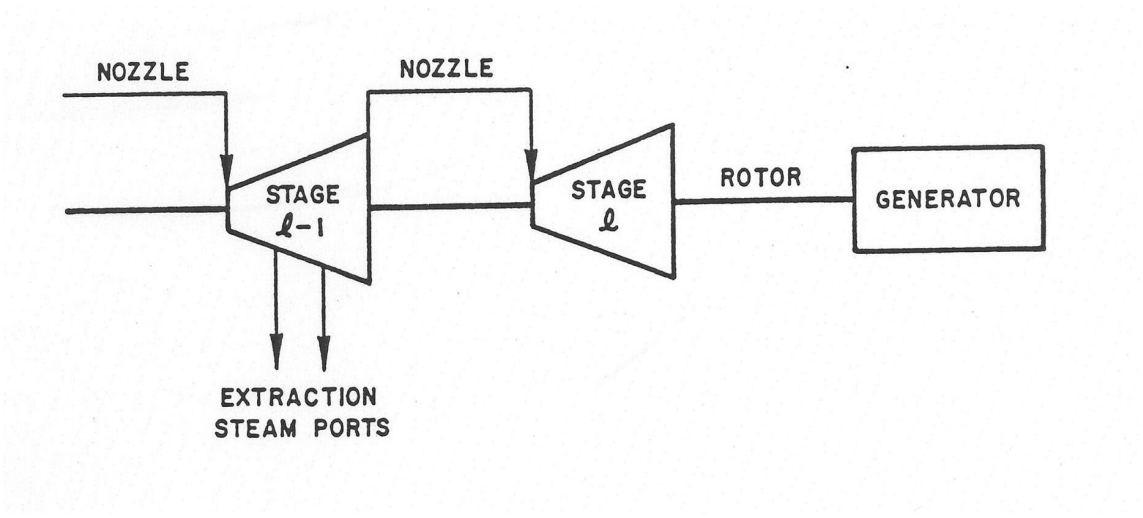

Figure 7.4-12. Turbine

For simplicity, look first at the energy equation used in the heater models,

$$\frac{\partial \rho h}{\partial t} = -\frac{\partial \rho h u}{\partial z} - \frac{\partial q}{\partial z} + \frac{\partial P}{\partial t}\ , \tag{7.4-29}$$

which is simply the same equation as Eq. 7.2-6. Then by integrating this equation over the entire volume V_l for each volume ℓ and writing a separate energy equation for each volume with the work term added, Eq. 7.4-29 becomes

$$\frac{d\left(m_\ell\, h_\ell\right)}{dt} = \sum_j h_j\, w_j\, \mathrm{sgn}\left(j,\ell\right) + Q_\ell + V_\ell \frac{dP_\ell}{dt} - H_\ell\ , \tag{7.4-30}$$

when the work term H_l is in terms of turbine efficiency based on losses to isentropic expansion and is expressed as

$$H_l = \eta_l w_{in} \Delta \bar{h}_l \tag{7.4-31}$$

where η_ℓ is the stage efficiency, w_{in} is the flow rate at the inlet nozzle, and $\Delta \bar{h}_l$ is the loss due to isentropic expansion, defined as

$$\Delta \bar{h}_\ell = h_{\ell-1}\left(P_{\ell-1}, s_{\ell-1}\right) - \bar{h}_\ell\left(P_\ell, S_{\ell-1}\right). \tag{7.4-32}$$

Note that $\bar{h}_\ell$ is evaluated at $P = P_\ell$ and $s = s_{l-1}$, which is the entropy at the previous stage $l - 1$.

Fundamentals of the turbine thermodynamics are given in many standard books and Salisbury (Ref. 7-10) discusses the subject comprehensively.

The stage efficiency η_ℓ is just the blade efficiency $\eta_{\ell,B}$ minus loss factors from rotation $\left(R_{\ell,R}\right)$ and moisture $\left(R_{\ell,M}\right)$,

$$\eta_\ell = \eta_{\ell,B} - R_{\ell,R} - R_{\ell,M} - R_{misc} \ , \tag{7.4-33}$$

where R_{misc} represents all other minor losses currently not considered. In addition, an exhaust loss term has to be included in the right-hand side of Eq. 7.4-33 if the turbine stage is the last stage of the turbine. The exhaust loss is expressed as

$$R_E = K_E V_{exit} \ ,$$

where V_{exit} is the velocity leaving the last stage and K_E is the exhaust loss constant.

The blade efficiency is defined as the ratio of the energy transfer to the blades to the theoretically available energy at the nozzle. From the velocity vector diagram shown in Fig. 7.4-13 (the variables in the figure are explained in the context), the rate of energy transfer from the steam to the blades is obtained as the product of the blade velocity V_B and the force F exerted by the steam on the blades. The available energy (rate) at the nozzle is simply the kinetic energy in the isentropic expansion of the steam. Therefore,

$$\eta_{\ell,B} = \frac{F V_B}{w_{in} \dfrac{V_o^2}{2}} \ , \tag{7.4-34}$$

where w_{in} is the same as in Eq. 7.4-31 and V_o is the theoretical nozzle (steam) velocity in the isentropic expansion. By the principle of impulse and momentum, the force on the blades is equal to the steam flow rate w_{in} multiplied by the total change in steam velocity, relative to the blades, i.e.,

$$F = w\left(V_a + V_b\right), \tag{7.4-35}$$

where V_a and V_b are the steam velocity relative to the blade and parallel to the motion of the blade at the blade entrance and exit, respectively, as indicated in Fig. 7.4-13. The plus sign in Eq. 7.4-35 indicates, as a result of the vector operation, that V_a and V_b are in opposite directions. Substituting Eq. 7.4-35 into 7.4-34 thus gives the blade efficiency as

$$\eta_{\ell,B} = \frac{w_{in}\left(V_a + V_b\right) V_B}{w_{in} \dfrac{V_o^2}{2}} = \frac{2\left(V_a + V_b\right) V_B}{V_o^2}, \tag{7.4-36}$$

The actual velocity V_1 of steam leaving the nozzle is slightly less than V_o and becomes even smaller when the effect of reaction, i.e., energy released in the bucket (Ref. 7-10), is considered. Thus,

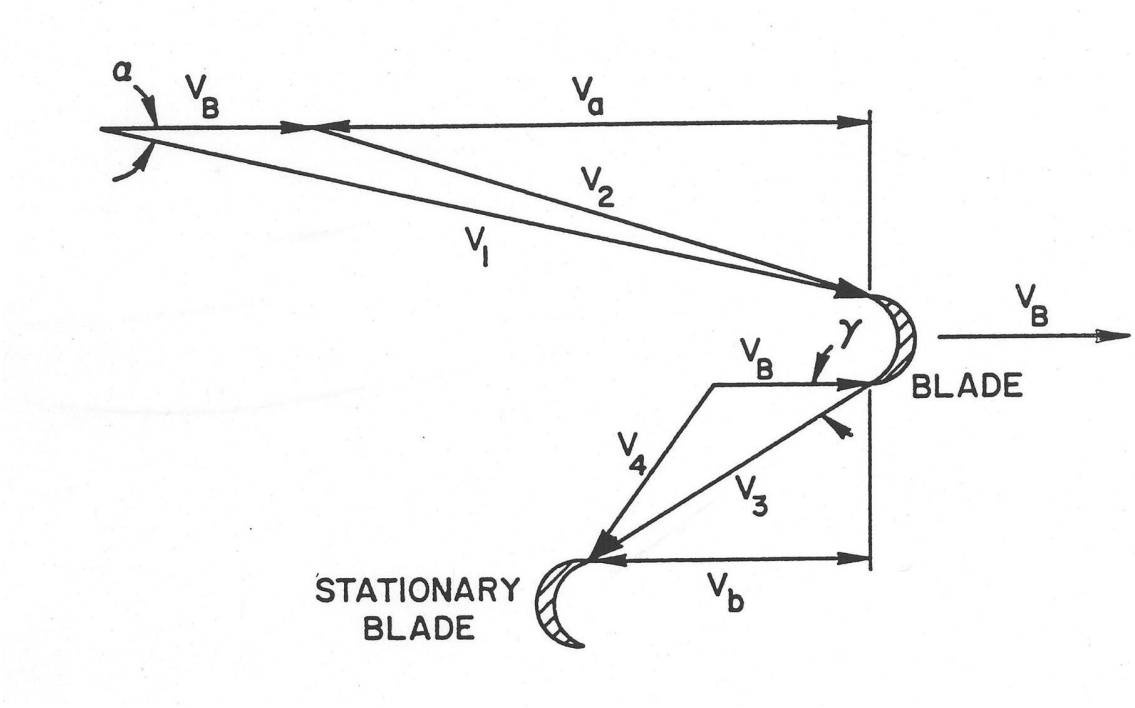

Figure 7.4-13. Velocity Vector Diagram for Single Row of Moving Blades

$$V_1 = V_o C_n a \,, \tag{7.4-37}$$

with $a \equiv (1-x)^{1/2}$, C_n the nozzle velocity coefficient, and x the fraction of stage energy released in the bucket system.

In an actual turbine system, it is impossible for the entrance angle of the steam to the blades system to be horizontal or in the plane of the wheel; otherwise, there would be mechanical interference between the rotating blades and the nozzle. Therefore, the steam has to leave the nozzle at a nozzle angle α, as shown in Fig. 7.4-13. Furthermore, it is impossible for the steam to exit the blades at an angle of zero with respect to the plane of rotation of the blades; otherwise, there would be no way for the flow of steam to progress axially through the turbine. Thus, the blade exit angle γ in Fig. 7.4-13 provides an axial leaving velocity component perpendicular to the plane of rotation of the blades for the exit velocity V_3.

Two additional loss factors must also be considered in a real turbine system: the fraction of the kinetic energy entering the blades which is realized at the blade exit C_b^2 and the fraction of the stage energy released in the blades which is finally realized at the bucket exit, C_r^2. The exit velocity can then be represented (Ref. 7-10) by

$$V_3 = \left(C_b^2 V_2^2 + C_r^2 x V_o^2\right)^{1/2} \tag{7.4-38}$$

in a single row of moving blades. For simplicity, C_b will be called the bucket coefficient, C_r the reaction coefficient, and x the reaction fraction. V_3 is in fact the steam velocity at the blade exit, relative to the blade, while V_2 is the steam velocity at the blade entrance, relative to the blade, and, by the law of cosines, is written as,

$$V_2 = (V_1^2 + V_B^2 - 2V_1V_B cos\alpha)^{1/2} \tag{7.4-39}$$

The absolute steam velocity at the blade exit, V_4, is then

$$V_4 = (V_3^2 + V_B^2 - 2V_3V_B cos\gamma)^{1/2} \tag{7.4-40}$$

In summary, by using the fact that

$$V_a = V_1 \cos\alpha - V_B \ ,$$

and

$$V_B = V_3 cos\gamma,$$

the blade efficiency in Eq. (7.4-36) can be rewritten explicitly, along with Eqs. 7.4-37 to 7.4-39, as

$$\eta_{\ell,B} = \frac{2V_B}{V_o}\left\{ a\, C_n \cos\alpha - \frac{V_B}{V_o} + \cos\gamma\left[C_r^2\, x + C_b^2\, C_n^2\, a^2 \cdot \left(1 + \left(\frac{V_B}{V_o}\right)^2 \frac{1}{C_n^2 a^2} - 2\frac{V_B}{V_o}\frac{1}{C_n a}\cos\alpha \right) \right]^{1/2} \right\}. \tag{7.4-41}$$

Salisbury recommends the following expressions for the rotation loss and moisture loss:

$$R_{\ell,R} = K_{\ell,R} \frac{\left(V_h / V_o\right)^3}{A_{\ell,n}} \ ,$$

and

$$R_{\ell,M} = K_{\ell,M}\left(1 - x_{\ell-1}\right),$$

where $K_{\ell,R}$ is the rotation loss constant, $K_{\ell,M}$ is the moisture loss constant, $A_{\ell,n}$ is the nozzle area, and $x_{\ell-1}$ is the fluid quality at the previous stage $\ell - 1$. All the quantities used in Eq. 7.4-41 are volume dependent.

Since the work of the turbine is done through the rotors, which are aligned along a shaft to drive the generator, a relation has to be established between the turbine work and the rotor angular velocity ω. The turbine work is a summation of the work by

individual turbine stages, and the turbine work is related to the rotor angular velocity as,

$$\sum_{\ell} H_{\ell} = \omega \tau_T \ , \tag{7.4-42}$$

where τ_T is the turbine torque. The rotor angular velocity is changing during a transient according to the relative magnitudes of the turbine torque and the generator torque as follows,

$$I \frac{d\omega}{dt} = \tau_T - \tau_G \ , \tag{7.4-43}$$

where I is the turbine/generator rotor moment of inertia and τ_G is the generator torque.

As mentioned in Section 7.4.10.1, the momentum equation used in the nozzle model is completely different from the one used in the heater models and in Section 7.2 because of the compressible flow considered for the nozzle. For nonchoked flow, the nozzle velocity is based on thermodynamic conditions at the inlet and at the outlet and is calculated from

$$V_{nz} = V_o C_n = \sqrt{2}\, C_n \, \Delta \bar{h}_{\ell}^{1/2} \ , \tag{7.4-44}$$

where C_n is just the nozzle coefficient and $\Delta \bar{h}_{\ell}$ is defined in Eq. 7.4-32, and the mass flux G is given by

$$G = V_{nz} \, \bar{\rho}_{\ell} \ , \tag{7.4-45}$$

where $\bar{\rho}_{\ell}$ is the density evaluated at P_{ℓ} and $\bar{h}_{\ell}$, i.e., $\bar{\rho}_{\ell} = \bar{\rho}_{\ell}\left(P_{\ell}, \bar{h}_{\ell}\right)$. For choked flow, the nozzle velocity is based on thermodynamic conditions at the inlet only and is determined (Refs. 7-11, 7-12) separately for steam flow and for two-phase flow as:

for steam:

$$V_{nz} = V_o C_n = -.6611 C_n \left[\frac{P_{\ell-1}}{\rho_{\ell-1}}\right]^{1/2} \ , \tag{7.4-46}$$

when the criterion $0.545 \ P_{\ell-1} \geq P_{\ell}$ is satisfied,

for two-phase flow:

$$V_{nz} = V_o C_n = \sqrt{2}\, C_n \left[\frac{P_{\ell-1} - P^*}{\rho_{\ell-1}} \right]^{1/2}, \tag{7.4-47}$$

where

$$P^* = 0.284\, P_{sat}\left(T_{\ell-1}\right)\left(\frac{-0.284\, f\left(T_{\ell-1}\right)}{f\left(T_r\right)} + 1 \right). \tag{7.4-48}$$

$$f(T) = 113.368 - 0.14T\ .$$

and

$$T_r = 467.37K$$

when the criterion $P^* \geq P_l$ is satisfied. For both steam flow and two-phase flow, the mass flux G is calculated by

$$G = V_{nz}\, \rho_{\ell-1}\ , \tag{7.4-49}$$

Where ρ_{l-1} is the density at the previous stage.

In the steady state, each of the user-specified nozzle flow rates is compared to the calculated nozzle flow rate, which is the nozzle velocity, computed (according to the steady-state pressure conditions) from one of the equations in Eqs. 7.4-44, 7.4-46, and 7.4-47, multiplied by the user-specified nozzle area. If the calculated nozzle flow rate differs from the user-specified nozzle flow rate, the computed nozzle velocity together with the user-specified nozzle flow rate is used to adjust the user-specified nozzle area, so that the two nozzle flow rates (computed and user-input) will then be consistent. The adjusted nozzle area in the steady state is used for calculations throughout the transient. This flow area calibration algorithm is also used in the relief valve model, discussed in Section 7.4.11, to modify the user-input relief valve flow area based on the user-input relief valve capacity.

7.4.10.3 Discretized Equations

The energy equation for the turbine stage, Eq. 7.4-30, contains only an additional term, $-H_\ell$, compared with the energy equations for the heater models or for non-heater compressible volumes Eq. 7.2-26. The work term H_ℓ is written separately to emphasize the energy loss of the steam during isentropic expansion while driving the blades in the turbine stages; alternatively, H_l can be absorbed into the heat source term Q_ℓ in Eq. 7.4-30, since it is only an energy term to be subtracted from the energy equation. Equation 7.4-30 can then be rewritten as,

$$\frac{d(m_\ell h_\ell)}{dt} = \sum_j h_j w_j \,\mathrm{sgn}(j,\ell) + Q_\ell + V_\ell \frac{dP_\ell}{dt}, \tag{7.4-50}$$

where Q_ℓ now includes implicitly an energy loss due to the stage work. Equation 7.4-50 has the same form as Eq. 7.2-26, and so Eq. 7.4-50 can be discretized in exactly the same way as Eq. 7.2-26; see Section 7.2 for details of the discretization.

The discretization of the momentum equation for nozzles is a complicated process, since the momentum equation now is entirely different from the one used in the previous models. In the existing solution scheme of the balance-of-plant coding, the momentum equation Eq. 7.2-5 is rewritten, after discretization, such that the change in mass flow rate in each segment is expressed in terms of the changes in volume pressures at the segment inlet and outlet as,

$$\Delta w = \left\{a_1 + \left[a_2 + \Delta t \cdot \left(\Delta P_{in} - \Delta P_{out}\right)\right]\right\} / \left(a_o - a_3\right). \tag{7.4-51}$$

Then an LxL matrix equation is created by combining Eq. 7.4-51 and the discretized energy equation to solve for all L volume pressure changes simultaneously. In order to integrate the momentum equations for nozzles into the established matrix equation solution scheme, Eqs. 7.4-44 to 7.4-49 have to be discretized to a form, similar to Eq. 7.4-51, relating flow changes to pressure changes in the volumes at the segment ends.

The derivation will begin with the momentum equation for nonchoked flow and proceed to choked flow, for which two separate treatments are needed for single-phase (steam) and two-phase flow.

Consider the flow rate w_{in} at the inlet nozzle to stage ℓ as shown in Fig. 7.4-12. By definition, the flow rate for nonchoked flow is the mass flux (or mass velocity) G in Eq. 7.4-45 multiplied by the nozzle area A_n; for brevity, w_{in} will be designated as w, V_{nz} as V, and A_n as A in the derivation. Thus,

$$w = \bar{\rho}_\ell V A\,. \tag{7.4-52}$$

Equation 7.4-52 can be written in a differential form as,

$$dw = A\bar{\rho}_\ell\, dV + AV d\bar{\rho}_\ell\,, \tag{7.4-53}$$

where dV can be obtained from Eq. 7.4-44,

$$dV = \frac{\sqrt{2}}{2} C_n \Delta\bar{h}_\ell^{-1/2} \left(dh_{\ell-1} - d\bar{h}_\ell\right) = \frac{V}{2\Delta\bar{h}_\ell}\left(dh_{\ell-1} - d\bar{h}_\ell\right), \tag{7.4-54}$$

and $d\bar{\rho}_\ell$ can be expressed as

$$d\bar{\rho}_\ell = -\bar{\rho}_\ell^2\, d\bar{v}_\ell \ , \tag{7.4-55}$$

with $1/\bar{\rho}_\ell = \bar{v}_\ell\left(P_\ell, \bar{h}_\ell\right)$ which follows the definition of $\bar{\rho}_\ell$ in Eq. 7.5-45. Substituting Eqs. 7.4-54 and 7.4-55 into Eq. 7.4-53 yields, after rearranging,

$$dw = \frac{w}{2\Delta\bar{h}_\ell}\left(dh_{\ell-1} - d\bar{h}_\ell\right) - w\bar{\rho}_\ell\, d\bar{v}_\ell \ . \tag{7.4-56}$$

Both $d\bar{h}_\ell$ and $d\bar{v}_\ell$ in Eq. 7.4-56 are related to the pressure of stage ℓ as, respectively,

$$d\bar{h}_\ell = \left.\frac{\partial\bar{h}_\ell}{\partial P}\right|_{s_{\ell-1}} dP_\ell + \left.\frac{\partial\bar{h}_\ell}{\partial s}\right|_{P_\ell} ds_{\ell-1} \ , \tag{7.4-57}$$

(remember, $\bar{h}_\ell \equiv \bar{h}_\ell\left(P_\ell, s_{\ell-1}\right)$ as seen in Eq. 7.4-32, and

$$d\bar{v}_\ell = \left.\frac{\partial\bar{v}_\ell}{\partial P}\right|_{\bar{h}_\ell} dP_\ell + \left.\frac{\partial\bar{v}_\ell}{\partial h}\right|_{P_l} d\bar{h}_\ell \ . \tag{7.4-58}$$

By combining Eqs. 7.4-56, 7.4-57, and 7.4-58, the finite change in flow rate can be rewritten as

$$\begin{aligned}\Delta w = {} & \frac{w}{2\Delta\bar{h}_\ell}\left(\Delta h_{\ell-1} - \left.\frac{\partial\bar{h}_\ell}{\partial P}\right|_{s_{\ell-1}}\Delta P_\ell - \left.\frac{\partial\bar{h}_\ell}{\partial s}\right|_{P_\ell}\Delta s_{\ell-1}\right) \\ & - w\bar{\rho}_\ell\left[\left.\frac{\partial\bar{v}_\ell}{\partial P}\right|_{\bar{h}_l}\Delta P_\ell + \left.\frac{\partial\bar{v}}{\partial h}\right|_{P_\ell}\left(\left.\frac{\partial\bar{h}_\ell}{\partial P}\right|_{s_{\ell-1}}\Delta P_\ell + \left.\frac{\partial\bar{h}_\ell}{\partial s}\right|_{P_\ell}\Delta s_{\ell-1}\right)\right].\end{aligned} \tag{7.4-59}$$

At this point, it is assumed that the change in enthalpy in the previous stage $\Delta h_{\ell-1}$ can be expressed explicitly as a function of the change in pressure in stage $\ell-1$ and the current time flows in the attached segments, without introducing unacceptable errors; that is, Eq. 7.2-33 can be simplified for the turbine stages (compressible volumes) by neglecting Δw_j, giving

$$\begin{aligned}\Delta h_\ell = {} & \frac{v_\ell}{V_\ell}\Delta t\left\{-h_\ell\sum_j w_j\,\mathrm{sgn}(j,\ell) + \sum_j h_j\, w_j\,\mathrm{sgn}(j,\ell) + Q_\ell\right\} + v_\ell\,\Delta P_\ell \\ \equiv {} & \{\ell, j\} + v_\ell\,\Delta P_\ell\end{aligned} \tag{7.4-60}$$

Treating the stage enthalpy implicitly would result in a discretization form which is tediously complicated and cumbersome; however, this might be included in future model improvements.

The final discretization form is arrived at by replacing the subscript ℓ with $\ell-1$ in Eq. 7.4-60 and then using Eq. 7.4-60 in Eq. 7.4-59 to give

$$\Delta w = \frac{w}{2\Delta\bar{h}_\ell} v_{\ell-1}\,\Delta P_{\ell-1} - w\left[\left(\frac{1}{2\Delta\bar{h}_\ell} + \bar{\rho}_\ell\,\frac{\partial\bar{v}_\ell}{\partial h}\Big|_{P_\ell}\right)\frac{\partial h_\ell}{\partial P}\Big|_{s_{\ell-1}} + \bar{\rho}_\ell\,\frac{\partial\bar{v}_\ell}{\partial P}\Big|_{\bar{h}_\ell}\right]\Delta P_\ell$$
$$+ w\left[\frac{1}{2\Delta\bar{h}_\ell}\{\ell-1, j\} - \left(\frac{1}{2\Delta\bar{h}_\ell} + \bar{\rho}_\ell\,\frac{\partial\bar{v}_\ell}{\partial h}\Big|_{P_\ell}\right)\frac{\partial\bar{h}_\ell}{\partial s}\Big|_{P_\ell}\Delta s_{\ell-1}\right]. \tag{7.4-61}$$

The two discretized momentum equations, Eqs. 7.4-51 and 7.4-61 have analogous forms, as can be seen by comparing terms; for instance, $\Delta t/[a_o\text{-}a_3]$ in Eq. 7.4-51 corresponds to $wv_{\ell-1}/\left(2\Delta\bar{h}_\ell\right)$ in Eq. 7.4-61, and so on. Thus, when considering the volume pressure change due to the contribution of a nozzle segment, Eq. 7.4-61 becomes the counterpart of Eq. 7.4-51. Equation 7.4-61 can be combined with the discretized energy equation Eq. 7.2-47 to render Eq. 7.2-55, which is expressed entirely in terms of changes in compressible volume pressures and is used to form the LxL matrix equation system.

Since a functional form expressing enthalpy as a function of pressure and entropy is not available, the known expression for entropy as a function of pressure and enthalpy is used to compute the derivative terms $\left(\partial\bar{h}_\ell/\partial P\right)$ and $\left(\partial\bar{h}_\ell/\partial s\right)$ in Eq. 7.4-61. In the case of $\left(\partial\bar{h}_\ell/\partial P\right)$ at $s=s_{\ell-1}$, the derivative is calculated by using the known values of $\bar{h}_\ell$ and P_ℓ as the starting points and then iteratively searching for the other enthalpy value at pressure P_ℓ plus a small increment and at entropy $s_{\ell-1}$. The derivative $\left(\partial\bar{h}_\ell/\partial s\right)_{P_\ell}$ is easier to obtain from

$$\frac{\partial\bar{h}_\ell}{\partial s}\Big|_{P_\ell} = 1\Big/\frac{\partial\bar{s}_{\ell-1}}{\partial h}\Big|_{P_\ell}, \tag{7.4-62}$$

since entropy is a known function of pressure and enthalpy. In addition, the change in the entropy $\Delta s_{\ell-1}$ is also computed explicitly.

An alternative to calculating $\Delta h_{\ell-1}$ in Eq. (7.4-59) is to express $\Delta h_{\ell-1}$ in terms of the pressure and the entropy, i.e.,

$$\Delta h_{\ell-1} = \frac{\partial h_{\ell-1}}{\partial P}\Big|_{s_{\ell-1}}\Delta P_{\ell-1} + \frac{\partial h_{\ell-1}}{\partial s}\Big|_{P_{\ell-1}}\Delta s_{\ell-1}, \tag{7.4-63}$$

Since $h_{\ell-1} = h_{\ell-1}\left(P_{\ell-1}, s_{\ell-1}\right)$. Then, the discretization of the momentum equation becomes

$$\Delta w = \frac{w}{2\Delta\bar{h}_\ell}\frac{\partial h_{\ell-1}}{\partial P}\Big|_{s_{\ell-1}}\Delta P_{\ell-1} - w\left[\left(\frac{1}{2\Delta\bar{h}_\ell} + \bar{\rho}_\ell\,\frac{\partial\bar{v}_\ell}{\partial h}\Big|_{P_\ell}\right)\frac{\partial\bar{h}_\ell}{\partial h}\Big|_{s_{\ell-1}} + \bar{\rho}_\ell\,\frac{\partial\bar{v}_\ell}{\partial P}\Big|_{\bar{h}_\ell}\right]\Delta P_\ell$$
$$+ w\left[\frac{1}{2\Delta\bar{h}_\ell}\,\frac{\partial h_{\ell-1}}{\partial s}\Big|_{P_{\ell-1}} - \left(\frac{1}{2\Delta\bar{h}_\ell} + \bar{\rho}_\ell\,\frac{\partial\bar{v}_\ell}{\partial h}\Big|_{P_\ell}\right)\frac{\partial\bar{h}_\ell}{\partial s}\Big|_{P_\ell}\right]\Delta s_{\ell-1}\,. \tag{7.4-64}$$

The calculation of $\left(\partial h_{\ell-1}/\partial s\right)$ at $P = P_{\ell-1}$ (using an expression of the same form as Eq. 7.4-62) in Eq. 7.4-64 and the calculation of the term $\left\{\ell-1, j\right\}$ in Eq. 7.4-61 probably take about the same amount of time. However, Eq. 7.4-64 is more time-consuming to solve than Eq. 7.4-61 because of the need, to use the equation of entropy as a function of pressure and enthalpy, to evaluate $\left(\partial h_{\ell-1}/\partial P\right)$ at $s = s_{\ell-1}$ by iteration. In addition, Eq. 7.4-61 can be improved by expressing $\left\{\ell-1, j\right\}$ in an implicit form, whereas the additional $\Delta s_{\ell-1}$ term makes Eq. 7.4-64 more explicit (note the difference in the $\Delta s_{\ell-1}$ terms between the two equations). Currently, Eq. 7.4-61 is used in the turbine model.

For choked flow of steam, the flow rate at the inlet nozzle to stage ℓ is obtained by multiplying Eq. 7.4-49 by the nozzle area,

$$w = \rho_{\ell-1} V A\,, \tag{7.4-65}$$

where the nozzle velocity V is given in Eq. 7.4-46. In the following derivations for choked flow of steam, the subscript $\ell = 1$ is omitted for convenience, since the nozzle velocity is based on thermodynamic conditions at the inlet stage only. Differentiating Eq. 7.4-65 and rearranging gives,

$$dw = \frac{w}{2}\left(\frac{dP}{P} + \frac{d\rho}{\rho}\right), \tag{7.4-66}$$

where, from Eqs. 7.4-55 and 7.4-58,

$$d\rho = -\rho^2\left(\frac{\partial v}{\partial P}\Big|_h dP + \frac{\partial v}{\partial h}\Big|_P dh\right). \tag{7.4-67}$$

Now, introducing Eq. 7.4-67 into Eq. 7.4-66 and rewriting the differential change in flow in a finite change form yields,

$$\Delta w = \frac{w}{2}\left[\frac{\Delta P}{P} - \rho\left(\left.\frac{\partial v}{\partial P}\right|_h \Delta P + \left.\frac{\partial v}{\partial h}\right|_P \Delta h\right)\right], \tag{7.4-68}$$

where Δh is again given by Eq. 7.4-60 except that the subscript ℓ should now be $\ell = 1$. Thus the discretization of the momentum equation results in, after inserting Eq. 7.4-60 into Eq. 7.4-68 and rearranging,

$$\Delta w = \frac{w}{2}\left[\frac{1}{P} - \rho\left(\left.\frac{\partial v}{\partial P}\right|_h - \left.\frac{\partial v}{\partial h}\right|_P\right)\Delta P - \rho \left.\frac{\partial v}{\partial h}\right|_P \{\ell - 1, j\}\right]. \tag{7.4-69}$$

Similarly, Δh in Eq. 7.4-68 can also be expressed in an implicit form as described in Eq. 7.4-64. It is not surprising that ΔP_ℓ does not appear in Eq. 7.4-69, since the flow rate is affected by the volume pressure only at the previous stage as long as the flow is choked.

As can be seen in Eqs. 7.4-47 to 7.4-49, the two-phase choked flow between stages $\ell = 1$ and ℓ is also dependent on thermodynamic conditions at the inlet turbine stage $\ell = 1$ only. For simplicity, the subscript $\ell = 1$ is not shown in the derivation of the equation for change in mass flow rate. It facilitates the derivation if Eq. 7.4-48 is rewritten in a simplified form, by carrying out the algebra in the equation, as,

$$P^* = P_{sat}(T)(a + bT) = P(a + bT). \tag{7.4-70}$$

where a = 9.325 x 10^{-2} and b = 2.356 x 10^{-4}. The flow rate in the nozzle now is just $w = \rho VA$ with V given by Eq. 7.4-47. From the analogy between Eqs. 7.4-46 and 7.4-47, the differential change in the two-phase choked flow can be deduced readily from Eq. 7.4-66, which is for choked flow for steam, to be,

$$dw = \frac{w}{2}\left(\frac{dP - dP^*}{P - P^*} + \frac{d\rho}{\rho}\right). \tag{7.4-71}$$

From Eq. 7.4-70, it is obvious that

$$dP^* = (a + bT)dP + bPdT \tag{7.4-72}$$

where, since the saturation temperature is determined solely by the saturation pressure, dT can be rewritten as,

$$dT = \frac{dT}{dP}dP. \tag{7.4-73}$$

Combining Eqs. 7.4-71, 7.4-72, and 7.4-73 and rearranging results in,

$$dw = \frac{w}{2}\left[\left(\frac{1}{P} + c\frac{dT}{dP}\right)dP - \rho dv\right] , \tag{7.4-74}$$

where

$$c = \frac{-b}{1-a-bT} .$$

Since the specific volume in a two-phase fluid is a function of pressure and quality, *dv* in Eq. 7.4.74 should be expressed as,

$$\begin{aligned} dv &= \left[\frac{dv_f}{dP} + x\frac{dv_{fg}}{dP} - \left(\frac{dh_f}{dP} + x\frac{dh_{fg}}{dP}\right)\frac{v_{fg}}{h_{fg}}\right]dP + \frac{f_{fg}}{h_{fg}}dh \\ &\equiv \left[v,h\right]dP + \frac{v_{fg}}{h_{fg}}dh . \end{aligned} \tag{7.4-75}$$

Substituting Eq. 7.4-75 into Eq. 7.4-74 gives the finite change in the nozzle flow

$$\Delta w = \frac{w}{2}\left[\left(\frac{1}{P} + c\frac{dT}{dP} - \rho\left[v,h\right]\right)\Delta P - \rho\frac{v_{fg}}{h_{fg}}\Delta h\right] . \tag{7.4-76}$$

Finally, the discretized equation for two-phase choked flow is reached by applying Eq. 7.4-60 to Eq. 7.4-76,

$$\Delta w = \frac{w}{2}\left[\left(\frac{1}{P} + c\frac{dT}{dP} - \rho\left[v,h\right] - \frac{v_{fg}}{h_{fg}}\right)\Delta P - \rho\frac{v_{fg}}{h_{fg}}\left\{\ell - 1, j\right\}\right] . \tag{7.4-77}$$

dT/dP in Eq. 7.4-77 is computed by introducing perturbations in the pressure in the following equation (Ref. 7-13),

$$T = c_1 + \frac{c_2}{\ln P + c_3} , \tag{7.4-78}$$

where c_1 = 0.426776x10^2, c_2 = -0.389270x10^4 and c_3 = -0.948654x10^1 if 0.000611 ≤ *P* < 12.33 *MPa*, or c_1 = -0.387592x10^3, c_2 = -0.125875x10^5, and c_3 = -0.152578x10^2 if 12.33 ≤ *P* < 22.1 *MPa*. Equation 7.4-77 does not contain ΔP_ℓ as in the discretized equation for choked flow for steam, Eq. 7.4-69.

7.4.11 Relief Valve

A relief valve is part of the System Pressure Relief System used to relieve overpressure transients occurring during plant isolations and load rejections. The relief valves open rapidly (self-actuated) during plant transients to discharge fluids to the environment or relief tanks and close following the transients so that normal operation can be resumed. Normally the relief valves are located on the main steam line piping, and each valve is piped through its own uniform diameter discharge line.

7.4.11.1 Model Description

Relief valves, like the other types of valves used in the balance of plant, are modeled as flow elements, since a relief valve primarily affects mass flow rate and pressure drop along a flow path and thus is best described through the momentum equation. The details of the relief valve model are dictated by the behavior of this type of valve. A relief valve is normally closed, opening very quickly when the pressure drop across the valve reaches a specified set pressure. The fractional valve opening area is related to the pressure drop across the valve by a hysteresis curve; the one used in the current model is shown in Fig. 7.4-14. Valve flow area varies linearly from fully open at or above the accumulated pressure to partially closed to the fraction A(1) at the set pressure. The flow area then remains constant until the valve pressure drop is below the blowdown pressure, at which point the valve closes fully. The relief valve, therefore, behaves in many respects like a check valve. However, flow through the relief valve is normally choked and so must be modeled using a momentum equation such as the ones described in Section 7.4.10 for choked flow in the nozzle model. The relief valve is therefore modeled as a nozzle which can open and shut in much the same way as the check valve does.

In order to avoid the numerical instabilities which might be caused by the step changes in flow area shown at the blowdown and set pressures in Fig. 7.4-14, the step changes are modified to linear changes of flow area as a function of pressure within a response time. This alteration of the ideal hysteresis curve of Fig. 7.4-14 actually makes the model more realistic, since an actual relief valve exhibits a response time which is the maximum valve opening time (for example, 0.2 second). This response time is to be specified by the user as part of the valve input data.

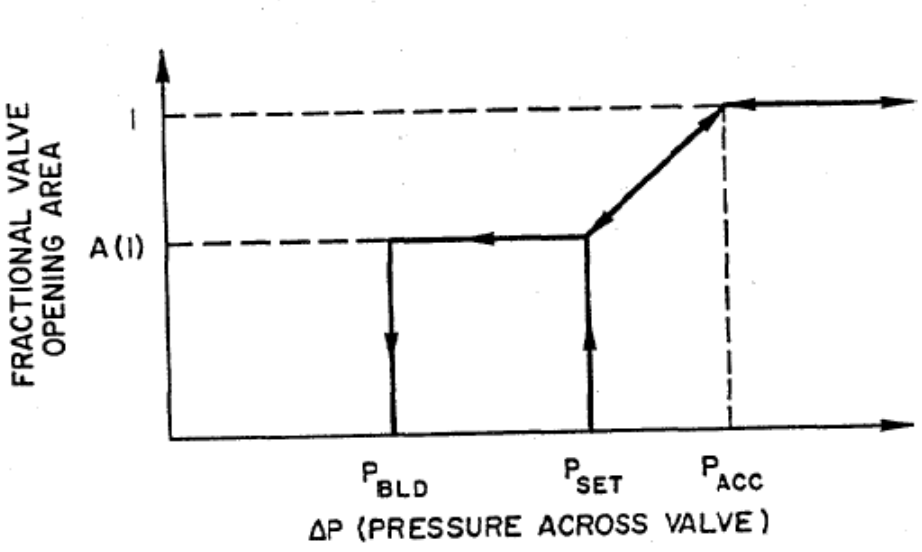

Figure 7.4-14. Simple Relief Valve Hysteresis Curve

In summary, the relief valve model consists of a modified check valve model and a modified nozzle model. The modified check valve model determines the fractional valve opening area, according to the hysteresis curve and the pressure difference across the relief valve, and then the modified nozzle model uses this flow area in calculating the flow rate through the relief valve.

The difference between the check valve model and the modified check valve model is that the check valve changes state (close or open) by adjusting the orifice coefficient in the incompressible flow momentum equation according to a user-input table of orifice coefficients versus time, whereas the modified check valve model changes state by adjusting the fractional valve opening area to a user-input value, in accordance with the hysteresis curve, within a user-input response time. In fact, the orifice coefficient functions like an inverse fractional opening area, since the orifice coefficient is inversely proportional to the square of the flow rate through the check valve under a fixed pressure drop across the valve (Eq. 7.2-24). The modified nozzle model differs from the nozzle model in that there is sometimes no flow through the nozzle (the relief valve) if the fractional valve opening area generated by the modified check valve model is zero, whereas the nozzle model always has a flow, either choked or nonchoked, between two stages.

7.4.11.2 Analytical Equations and Discretized Equations

All aspects discussed in Sections 7.4.10.2 and 7.4.10.3 about the momentum equations for the nozzle model apply to the relief valve model. Two additional points to note are that 1) the work term H_ℓ in Eqs. 7.4-30 and 7.4-50 (included in Q_ℓ) is removed when these two energy equations are used for the volume following the relief valve, since there is no work done by the flow through the valve and 2) when there is no flow through the valve, the pressure change in the volumes at either end of the relief

valve will have no contributions from the momentum equation of the relief valve (as is easily seen in Eqs. 7.4-61, 7.4-69, and 7.4-77 when $w = 0$).

7.4.12 Steady-State Initialization

The steady-state initialization process takes the input data entered by the user and from the data computes the steady-state parameters which characterize each component. The elements of the initialization process for the models discussed in this report can be separated into three groups: those for heater models, those for the turbine model, and those for the relief valve model. These three groups of calculations will now be discussed separately.

7.4.12.1 Steady-State Initialization for the Heater Models

Some steady-state parameters must be calculated for all heater models, both open and closed. These include:

(1) compute the heater temperature from the equation of state,

(2) determine the quality of the heater if the user inputs the two-phase interface and vice versa, by Eq. 7.4-5 or Eq. 7.4-8,

(3) check the mass conservation from all of the inlet and outlet flows,

(4) calculate the heat source term steady-state value from the net energy entering the volume through the inlet and outlet flows,

(5) introduce the pseudo heat conduction coefficient, to account for the minor energy imbalance resulting from inconsistencies between user-specified thermodynamic conditions and the SASSYS-1 correlations for the thermodynamic properties, and

(6) calculate the area-weighted quality for the outlet flow, if the two-phase interface intersects any of the outlet openings, from Eq. 7.4-2.

In addition, there are some calculations required only for the initialization of closed heaters. These include:

(7) initialize the heat transfer coefficients, both on the tube side and on the shell side,

(8) determine the calibration factor for the tube surface heat transfer area,

(9) initialize the fluid enthalpy at each node on the tube side,

(10) find the temperature distributions of the tube side fluid and the metal tube, and

(11) include the heat transfer energy between the shell side fluid and the metal tube in the heat source term steady-state value (item (4) above).

Furthermore, for those heaters which contain a drain and/or a desuperheating region, the following initialization is also performed for the shell side of the drain and/or the desuperheating region:

(12) calculate the enthalpy from the equation of state,

(13) initialize the heat transfer coefficient, from Eq. (7.4-10),

(14) compute the heat source term steady-state value from the net energy gain through the inlet and outlet flows, and

(15) determine the calibration factor, separate from the one used for the shell side of the heater, for the tube surface heat transfer area to obtain a balance between the energy transfer through the tube boundary and the heat source term steady-state value from item (14).

7.4.12.2 Steady-State Initialization for the Turbine Model

The turbine model requires initialization of parameters both for each turbine stage and for each nozzle between stages. The job of the turbine stage steady-state initializer is the following:

(1) check the mass conservation from all of the in]et and outlet flows,

(2) compute the steady-state stage work, from Eq. 7.4-31,

(3) calculate the turbine torque and set the generator torque equal to the turbine torque,

(4) check the energy conservation (work balanced with the net energy in through flows), and

(5) introduce a pseudo-heat conduction coefficient to account for any minor energy imbalance within the stage.

The steady-state nozzle initializer performs the following:

(1) calibrate the nozzle area according to the user-specified flow rate, using the mass flux calculated from Eqs. 7.4-45 or 7.4-49, and

(2) compute the isentropic enthalpyh $\bar{h}_l(P_l, s_{l-1})$ and density $\bar{\rho}_l(P_l, \bar{h}_l)$.

7.4.12.3 Steady-State Initialization for the Relief Valve Model

The steady-state relief valve initializer does the following:

(1) calibrate the valve flow area when the valve is fully open, according to the user-specified relief valve capacity (since the relief valve is normally closed in the steady state), using the same equations for calculating the mass flux as are used in the nozzle model, and

(2) set the flag to reflect the state of the relief valve as being on the upper section of the hysteresis curve in Fig. 7.4-14, or on the lower section of the hysteresis curve.

7.4.13 Code Implementation and Operation

7.4.13.1 The Transient Solution Algorithm

This section describes the incorporation of the component models discussed in this section into the transient solution algorithm discussed in Section 7.2.6.2.

Perhaps the easiest way to document the revised transient solution algorithm is to start with the algorithm of Section 7.2.6.2. The original algorithm is broken up into eleven steps; some of these steps are affected by the addition of the heater, turbine, and relief valve models, and some steps are not. The modifications to the algorithm which are necessary to incorporate the additional models are as follows:

Steps 1 and 2: These involve only the steam generator and superheater models and thus are not affected by the additional models.

Step 3: The calculation of the matrix coefficients and source terms performed in this step must properly account for the enthalpy of fluid leaving any of the heater volumes, as discussed in Sections 7.4.2.2, 7.4.7.2, and 7.4.8.2 of this report. Also, the heat source term Q_ℓ^n should include the stage work term H_ℓ^n for each stage of a turbine.

Step 4: The incompressible flow momentum equation for which the coefficients are computed in this step must be replaced by Eq. 7.4-61, 7.4-69, or 7.4-77 (the choice of equation being dependent upon flow conditions, as discussed in Section 7.4.10.3) in the case of a nozzle or relief valve.

Steps 5 and 6: These involve the mechanics of assembling and solving the matrix equation and so are not affected by the additional models.

Step 7: In addition to updating the volume pressures and the flows in incompressible flow segments, the flows in any nozzles or relief valves must be updated.

Step 8: In this step, the heat source terms for any of the heater models discussed in this report are updated. The temperature profiles of the tube side fluid and the metal tube are updated for any closed heaters, and the heater shell side temperature is also updated. In addition, the temperature, enthalpy, and heat source are updated in any drains or desuperheating regions. For any turbine stages, the work term, the turbine torque, and the rotor angular velocity are updated.

Step 9: Volume-averaged densities and enthalpies are computed here, and this calculation does not change for the new models.

Step 10: In non-heated flow segments, enthalpy transport is applied at this point to update the enthalpy distribution along each segment. In the heated elements within closed heaters, the fluid enthalpy at each node along the element is updated according to the energy equations discussed earlier. Flow segments which involve a combination of heated and non-heated elements use enthalpy transport in all non-heated elements and compute energy transfer within heated elements.

Step 11: Pump parameters and gravity heads are computed in this final step, and so this step is not affected by the additional models.

7.4.13.2 Code Operation

The calculation procedures described in Sections 7.4.12 and 7.4.13.1 are implemented by the set of subroutines and functions listed in Table 7.2-1. Most subroutines with names beginning with SS (Steady State) are called from the steady-state balance-of-plant driver SSBOP (the exception is subroutine SSRVW, which is called from subroutine RENUM, the balance-of-plant input data and nodalization routine). Subroutines with names beginning with TS (Transient State) are called from the driver subroutine WTRDRV.

The structure of the balance-of-plant coding, including the subroutines of Table 7.2-1, is shown in Fig. 7.2-1 for the steady-state coding and in Fig. 7.2-2 for the transient coding.

As seen in Fig. 7.2-1, the balance-of-plant operation starts with subroutine RENUM, which is called from the SASSYS PRIMAR-4 subroutine SSPRM4. SSPPM4 is an initialization subroutine which has been modified to call the balance-of-plant initialization subroutines also. Subroutine SSRVW is called by RENUM to calibrate the relief valve flow areas once the input data for each relief valve have been entered through RENUM. After the work is completed in RENUM, SSPRM4 calls SSBOP to execute the remainder of the steady-state balance-of-plant initialization. All the calculations necessary to complete the steady-state initialization of the balance-of-plant components are done in SSBOP or in subroutines called by SSBOP. First, SSBOP calls the nozzle initializer, SSNZZL, to compute the isentropic enthalpies and the fluid densities following the isentropic expansion, and to adjust the nozzle areas. Next, SSBOP calls SSTRBN, the turbine initializer, to calculate the steady-state turbine stage work, check mass and energy conservation, and initialize the turbine and generator torques. SSBOP then calls SSHTRW, the heater initializer, to compute the shell-side temperatures and/or the tube-side temperature profile (along with the heat transfer area calibration factor), calculate the heat source terms (including heat source terms in the drain and/or the desuperheating region, if such regions are present), check mass and energy conservation, and find the pseudo-heat conduction coefficient. SSBOP then goes on to call other initialization subroutines.

With the steady-state initialization completed, the balance-of-plant transient calculation starts with subroutine TSBOP by a call from the PRIMAR-4 subroutine STEPTM (see Fig. 7.2-2). TSBOP is the driver for the entire waterside transient calculation, including the steam generator and superheater models. TSBOP is called once each PRIMAR-4 timestep. After updating the balance-of-plant standard valves (which operate on the PRIMAR-4 timestep), TSBOP enters a loop that operates on the balance-of-plant timestep, which is generally smaller than the PRIMAR-4 timestep and is never larger than the PRIMAR-4 timestep. For each balance-of-plant timestep, TSBOP first calls the steam generator (and superheater, if any are present in the system) subroutines, then it calls WTRDRV, the driver subroutine for the remainder of the balance of plant. WTRDRV assembles the matrix equation for the compressible volume

pressure changes, solves for the pressure changes, and updates the flow rates and the remaining balance-of-plant parameters. In the process of assembling the matrix equation, WTRDRV must compute, for each flow segment, the contribution of each component in the segment (e.g., pipes, valves, pumps, etc.) to the segment momentum equation. These contributions are calculated, for the different component types, by the six subroutines grouped together in Fig. 7.2-2, beginning with SGMOM and ending with TSRVW. The first four subroutines are discussed in Section 7.2; the remaining two are TSNZZL, which calculates the contribution for nozzles, and TSRVW, which calculates the contribution for relief valves. Once the matrix equation has been solved for the compressible volume pressure changes, TSNZZL and TSRVW are called again to update nozzle flow rates and relief valve flow rates, respectively. Since relief valves are normally closed, TSRVW checks to find out first if the relief valve is open, to decide whether to proceed with the generation of the momentum equation coefficients or simply to bypass the calculation if the valve is closed. In updating the relief valve flow, subroutine TSRVW calls REVLW to obtain the new valve flow area and then calculates the new valve flow rate; again, TSRVW will skip the computation of the new flow rate and set the new flow rate to zero if the new valve flow area is found to be zero.

WTRDRV moves on to call TSTRBN, which updates the turbine stage work and the turbine torque. Next, WTRDRV calls TSHTRW, which executes most calculations related to heaters, other than those simulated by the simple heater model in Section 7.2. Subroutine TSHTRW updates the shell-side temperature and/or the tube-side temperature profile and also the heat source terms (including the heat source terms in the drain and/or desuperheating regions, if such regions are present). After these calls, the enthalpy transport calculation along unheated flow elements is performed by a call to TRNSPT, which will also account for enthalpy transport in flow paths following heated elements within heaters. Subroutine ARF is then called, as necessary, to determine the new two-phase interface in heaters configured as cylinders lying on the side.

Once WTRDRV has returned control to TSBOP, the balance-of-plant timestep is updated and TSBOP performs another series of calls to the steam generator and superheater subroutines and to WTRDRV, until the end of the PRIMAR-4 timestep is reached. TSBOP then goes on to perform I/O tasks, then returns control to STEPTM.

REFERENCES

NOTICE

Several references in this document refer to unpublished information. For a list of available open-literature citations, please contact the authors.

APPENDIX 7.1:
LISTING OF BALANCE-OF-PLANT VARIABLES

Many of the variables used in the balance-of-plant subroutines are listed below in alphabetical order, together with a short definition of each variable. All input variables are included in the list and are preceded by an asterisk. In the case of a variable which has a counterpart in the sodium loop coding (e.g, the segment flow), the counterpart variable name is listed in parentheses after the variable definition.

* ALFANZ(NSEG) --	nozzle angle.
* APMWHD(20,NPUMPW) --	pump head coefficients and torque coefficients (APMPHD).
* APRMHT(NHTR) --	the heat transfer area between the primary and secondary sides of a heater.
* AREAW(NELEW) --	cross-sectional area of an element (AREAEL).
* ARNAS --	the superheater sodium flow area per tube.
* AXPMHT(NHTR) --	the flow area on the primary side of a heater.
* BENDW(NELEW) --	the number of bends in a flow element (BENDNM).
* CBBKCF(NSEG) --	nozzle bucket coefficient.
* CHCALB(NCVLVW) --	calibration constant for a check valve.
CHDELT(2,NCVLVW) --	CHDELT(1) is the closure time for a check valve.
	CHDELT(2) is the opening time for a check valve.
* CHEPS1(NCVLVW) --	the value of the pressure drop across a check valve or the value of the mass flow rate through the check valve at which the valve begins to close.
* CHEPS2(NCVLVW) --	the value of the pressure drop across a check valve or the value of the mass flow rate through the check valve at which the valve begins to open.
* CHPHIW(NCVLVW) --	absolute valve characteristic value for a check valve which is fully open.
CHTIME(NCVLVW) --	the time since initiation of closure or of opening of a check valve.
* CNNZCF(NSEG) --	nozzle velocity coefficient.
* CONSKl(NSEG) --	nozzle rotation loss coefficient.
* CONSK2(NSEG) --	nozzle moisture loss coefficient.
* CONSK3 --	turbine exhaust loss coefficient.
* CRRXCF(NSEG) --	nozzle reactor coefficient.

* CSAREA(NCVW) -- the effective cross-sectional area of a heater.
* CSARLW(NCVW) -- the effective cross-sectional area of the drain in a heater containing a drain.
* CSARUP(NCVW) -- the effective cross-sectional area of the desuperheating region in a heater containing a desuperheating region.
* CVMLTW(2,NSEGW) -- the multiplicity factors at the entrance (1) and exit (2) of a flow segment (CVLMLT).
* CVPHIC(10,NCVLVW) -- normalized valve characteristic for a closing check valve as a function of time since the start of valve closure.
* CVPHIO(10,NCVLVW) -- normalized valve characteristic for an opening check valve as a function of the time since the start of valve opening.
* CVTIMC(10,NCVLVW) -- time table for CVPHIC.
* CVTIMO(10,NCVLVW) -- time table for CVPHIO.
* DEWI -- the evaporator booster tube outer diameter.
* DEWIS -- the superheater booster tube outer diameter.
* DEWOS -- the superheater steam tube inner diameter.
* DHLWW(NCVW) -- the hydraulic diameter of the drain in a heater containing a drain.
* DHNAS -- the superheater sodium hydraulic diameter per tube.
* DHPMHT(NHTR) -- the hydraulic diameter of the primary side of a heater.
* DHSHW(NCVW) -- the hydraulic diameter of the shell side of a heater.
* DHUPW(NCVW) -- the hydraulic diameter of the desuperheating region in a heater containing a desuperheating region.
* DHW(NELEW) -- hydraulic diameter of an element (DHELEM).
* DNSW(NCVW) -- compressible volume density.
* DOUTS -- the superheater steam tube outer diameter.
* DPACC(NRVLVW) -- the accumulated pressure drop for a relief valve.
* DPBLD(NRVLVW) -- the blowdown pressure drop for a relief valve.
  DPELW(NELEW) -- pressure drop across an element (DPRSEL).
* DPSET(NRVLVW) -- the set pressure drop for a relief valve.
  DTSUBO -- previous timestep.
* FLOWLS -- the relief valve capacity at the accumulated pressure drop.

* FLOWSS(NSEGW) --	steady state flow in each segment (FLOSSL).
FLOW4(NSEGW) --	segment flow at the end of the current PRIMAR time subinterval. At the beginning of the subinterval, flow is given by FLOW3, and at the end of the PRIMAR timestep, it is given by FLOW2 (FLOSL2 FLOSL3, FLOSL4)
* GAMABL(NSEG) --	turbine blade exit angle.
GRAVW(NELEW) --	gravity head in an element (GRAVHD).
* G2PW(NELEW) --	the orifice coefficient in the momentum equation (G2PRDR).
* HCVI --	the initial upstream enthalpy for a relief valve.
HCVW(NCVW) --	specific enthalpy of the compressible volumes.
* HEADWR(NPUMPW) --	rated pump head (HEADR).
HEADW2(NPUMPW) --	pump head at end of PRIMAR timestep (HEADP2).
HEADW3(NPUMPW) --	pump head at beginning of timestep (HEADP3).
HEADW4(NPUMPW) --	pump head at end of timestep (HEADP4).
HELEW(NELEW) --	enthalpy at an element outlet.
* HIGHLW(NCVW) --	the height of the drain in a heater containing a drain.
* HIGHUP(NCVW) --	the height of the desuperheating region in a heater containing a desuperheating region.
* HTOTO(NHTR) --	the initial value of the total heat transfer coefficient between the primary and secondary sides of a heater.
* HTRELV(NCVW) --	the elevation of the lowest point of a heater.
* HTRRAD(NCVW) --	the radius of a heater.
* IBOPRT --	the number of PRIMAR timesteps between full balance-of-plant prints.
* ICHVLK(2,NCHVLV) --	a flag for the criteria which trigger a check valve to open and to close. ICHVLK(1,IVLV) flags whether an open check valve will start to close based on a pressure criterion (ICHVLK = 1) or on a flow criterion (ICHVLK = 2). ICHVLK(2,IVLV) does the same for the opening criteria of a closed valve.
* ICVLEW(NCVLVW) --	the element number of a check valve (initially entered as the user's number for the element, then changed to the code's number).
* ICVSGN(M,NSGN) --	for M=1, ICVSGN is the user's number of the compressible volume of a steam generator inlet plenum; for M=2, it is the volume number of the outlet plenum.

* IELPW(NPUMPW) -- element number of waterside pump (IELPMP).

* IELVLW(NVLVW) -- element number of a valve (ordered by the code-generated valve number).

* IEMPW(NPUMPW) -- type of waterside pump (IEMPMP\).

* IFBWCL(NCVW) -- flags whether a flow boundary condition is controlled by a table or by the control system, with IFBWCL = 0 if the boundary condition is controlled by a table, = 1 if the boundary condition is controlled by the control system.

* IHTLW(NSEGW) -- the user's number of the volume containing the drain to which the segment is attached.

* IHTUP(NSEGW) -- the user's number of the volume containing the de-superheating section to which the segment is attached.

* IHTSEG(NSEGW) -- the user's number of the heater volume (if any) through which the segment passes.

ILEGW(NLEGS) -- the number of compressible volumes in each leg of the water side.

* ILRPW(NPUMPW) -- flag for locked rotor (ILRPMP).

* IPMWCL(NPUMPW) -- control system flag for waterside pumps (IPMPCL).

* IRVLVW(NRVLVW) -- the user's number for the element assigned to a check valve.

ISEGCV(NCVW,6) -- segment numbers of segments attached to each compressible volume (maximum of 6 segments currently allowed).

* ISGIN -- entries (1-10), user number of first segment in leg,

entries (11-20), code-generated number of first flow boundary condition pseudo-segment in leg,

entries (21-30), code-generated number of first steam generator inlet pseudo-segment in leg.

ISGNCV(-NCVW,6) -- for each compressible volume, ISGNCV identi£ies the flow from each segment attached to the volume as flowing into or out of the volume at steady state. ISGNCV = 1 indicates flow into the volume, while YSGNCV = -1 indicates flow out of the volume.

* ISGOUT -- entries (1-10), user number of last segment in leg,

entries (11-20), code-generated number of last flow boundary condition pseudo-segment in leg,

entries (21-30), code-generated number of last steam

generator inlet pseudo-segment in leg.

* ITYPW(NELEW) -- element type for each element (ITYPEL).

* IVBWCL(NCVW) -- flags whether a volume boundary condition is controlled by a table or by the control system, with IVBWCL = 0 if the boundary condition is controlled by a table, = 1 if the boundary condition is controlled by the control system.

IVLELW(NVLVW) -- code-generated element number of a valve (ordered by the code-generated valve number).

* IVLWCL(NVLVW) -- control system flag for waterside valves (IVLVCL).

IVLWCL = 0 if the control system does not control the valve,

IVLWCL = 1 if the control system controls the valve driving function, and

IVLWCL = 2 if the control system controls the valve stem position directly.

* JCVW(M,NSEGW) -- compressible volume numbers at each end of a segment (M=1 at the flow inlet, M=2 at the flow outlet) (JCVL).

* JCVlFG(NSEGW) -- indicates where a segment attached to a heater volume is attached to the volume, with

JCVlFG = -1 if the segment is attached to the bottom of the volume,

= 0 if the segment is attached in between the top and the bottom of the volume,

= 1 if the segment is attached to the top of the volume.

* JFSEW(NSEGW) -- first element in a segment (JFSELL).

* JLSEW(NSEGW) -- last element in a segment.

* JPRINT (17) -- an array of flags through which the user selects which parameters to include in the full balance-of-plant print.

LEGBCK(NLEGS) -- the translator array from the user's numbering of the legs on the balance of-plant side to the code's internal numbering of the legs.

* LEGORD(NLEGS) -- lists the order in which the legs into which the balance--of-plant is divided should be ordered in the output listing.

* LMPDOT -- the number of steam generator timesteps averaged to compute the time derivative of pressure in the steam

generator.

* NBCCVF(NBCFLO) -- the number of the compressible volume to which the flow boundary condition pseudo-segment is attached (input as the user's c.v. number, then changed to the code's number).

* NBCCVP(NBCPRS) -- the number of the compressible volume which serves as a boundary condition (input as the user's c.v. number, then changed to the code's number).

NBCFLO -- number of flow boundary condition tables.

* NBCINF(NBCFLO) -- table number for the time-dependent data for the flow boundary conditions.

* NBCINP(NBCPRS) -- table number for the time-dependent data for the compressible volume boundary conditions.

NBCINT -- number of interior volumes (volumes which are not boundary condition volumes).

* NBCSEG(NBCFLO) -- code-generated pseudo-segment number for each flow boundary condition.

NBCPRS -- number of volume boundary condition tables.

* NBOREL(M,NELEW) -- neighboring element numbers for each element (M=1 for the upstream neighbor, M=2 for the downstream neighbor). NBOREL(1,I) = 0 for the first element in a segment and NBOREL(2,I) = -1 for the last element in a segment.

* NCHVST(NCVLVW) -- flags the state or each check valve as follows:

= 1, valve is fully open and will begin to close if the pressure drop across the valve is less than the user-input value CHEPS1.

= 2, valve is fully open and will begin to close if the flow through the valve is less than CHEPSl.

= 3, valve is in the process of closing.

= 4, valve is fully closed but leaking slightly and will begin to open if the pressure drop across the valve becomes greater than the user-input value CHEPS2.

= 5, valve is fully closed but leaking slightly and will begin to open if the flow through the valve becomes greater than CHEPS2.

= 6, valve is in the process of opening.

* NCVBCW -- identifies compressible volumes as boundary condition,

steam generator plenum, etc., with NCVBCW

= 0 for a standard interior volume,

= 1 for a volume boundary condition volume,

= 2 for an inlet flow boundary condition volume,

= 3 for an outlet flow boundary condition volume,

= 4 for a steam generator inlet plenum,

= 5 for a steam generator outlet plenum,

= 6 for a heater volume,

= 7 for a turbine.

NCVIN(NLEGS) -- user number of first compressible volume in loop.

NCVLBK(NCVLVW) -- array which maps the user's number for a check valve to the code's number for that check valve.

NCVLTR(NCVLVW) -- array which maps the code's number for a check valve to the user's number for the same check valve.

NCVLVW -- number of check valves in the balance-of-plant loop.

NCVOUT(NLEGS) -- user number of last compressible volume in loop.

NCVQ(NHTR) -- code-generated compressible volume number of a heater (by code-generated heater number).

NCVW -- number of compressible volumes (NCVT).

NELEW -- number-of elements (NELEMT).

* NELSGW(NELEW) -- user's number of the segment in which an element lies.

* NELSUH -- the user's element number for a superheater.

* NENTRF(NCVW) -- flag for the type of floating-point input data entered for a volume, with NENTRF

= 1 for single-phase volumes, pressure and temperature entered,

= 2 for single-phase volumes, pressure and enthalpy entered,

= 3 for two-phase volumes, pressure and quality entered,

= 4 for two-phase volumes, temperature and quality entered,

= 5 for two-phase heater volumes, pressure, two-phase level and ambient temperature entered,

= 6 for two-phase heater volumes, temperature,

two-phase level, and ambient temperature entered.

* NFLSEG(NCVW) -- flags the type of floating point data entered for an inflow boundary condition, with NFLSEG

= 0 if enthalpy is entered,

= 1 if temperature and pressure are entered for a subcooled liquid boundary condition,

= 2 if temperature and pressure are entered for a superheated steam boundary condition,

= 3 if quality and pressure are entered for a two-phase boundary condition,

= 4 if quality and temperature are entered for a two-phase boundary condition.

NHTR -- number of heaters in the balance-of-plant.

NLEGS -- number of legs (a leg is a section of the balance of plant for which all flows and volume pressures are solved simultaneously. For example, the volumes and segments from the inlet to the steam generator might be one leg (a liquid leg), and those from the steam generator to the outlet might be another leg (a vapor leg).

* NLGCVW(NCVW) -- the number of the leg of the loop to which a volume belongs.

NLVOL -- number of liquid compressible volumes.

* NODMAX(NSEGW) -- the maximum number of enthalpy transport nodes into which a segment may be divided.

* NODSC -- the number of nodes in the evaporator subcooled zone.

* NODSH -- the number of nodes in the evaporator superheated zone.

* NODTP -- the number of nodes in the evaporator two-phase zone.

* NODSHT -- the number of nodes in the superheater.

* NOSGW(NSGN) -- user's number for the segment which is at the outlet of the vapor leg which is fed by the steam generator (used for saving plot data only).

NPUMPW -- number of pumps in the balance-of-plant.

* NPUTRN(NPUMPW) -- user's number of pump.

* NQFLG(NCVW) -- user-assigned heater number for a compressible volume which is a heater.

NSEGCV(NCVW) -- number of segments attached to each compressible

volume.

NSEGT -- the number of flow segments entered by the user (NSEGLT).

NSEGW -- total number of segments, including pseudo-segments generated by flow boundary conditions and steam generator interfaces.

* NSSIN(NSSEG) -- the compressible volume number at a supersegment inlet.

* NSSOUT(NSSEG) -- the compressible volume number at a supersegment outlet.

* NSUPSG(NCVW) -- the number of the supersegment in which a vapor volume is contained.

* NTABVL(NBCPRS) -- flags the types of parameters entered in the floating point volume boundary condition table, with NTABVL

= 1 for pressure and enthalpy entered for a liquid volume

= 2 for pressure and temperature entered for a liquid volume,

= 3 for pressure and enthalpy entered for a vapor volume,

= 4 for pressure and temperature entered for a vapor volume,

= 5 for pressure and quality entered for a two-phase volume,

= 6 for temperature and quality entered £or a two-phase volume.

* NTPCVW(NCVW) -- compressible volume type, with NTPCVW

= 1 for a subcooled liquid volume,

= 2 for a superheated vapor volume,

= 3 for a two-phase volume,

= 4 for a pseudo-volume at the liquid/two-phase interface in an evaporator.

NTPELW(NELEW) -- state of an element, with NTPELW

= 1 for a subcooled liquid element,

= 2 for a superheated vapor element,

= 3 for a two-phase element.

* NTRNPT --	flags whether or not enthalpy transport is used in the vapor leg, with NTRNPT = 0 if enthalpy transport is used, = 1 if enthalpy transport is not used.
NVLBCK(NVLVW) --	array which takes the number assigned to a valve by the user and gives the number assigned to the valve by the code.
NVLTRN(NVLVW) --	array which takes the code-generated number assigned to a valve and gives the number assigned to the valve by the user.
NVLVW --	number of valves in the balance-of-plant (NVALVE).
* OMEGAR --	turbine rotor angular velocity.
* ORIFLW(NCVW) --	the elevation of the drain orifice in a heater which contains a drain.
* ORIFUP(NCVW) --	the elevation of the desuperheating region orifice in a heater which contains a desuperheating region.
* PCVI --	the initial upstream pressure for a relief valve.
* PCVO --	the initial downstream pressure for a relief valve.
* PELEW(NELEW) --	pressure at an element outlet.
* PMPFWR(NPUMPW) --	rated pump flow (PMPFLR).
PMPHDW --	coefficients in centrifugal pump option 2 (PMPHD).
* PMPSWR(NPUMPW) --	rated pump speed (PMPSPR).
PMPTQW --	torque coefficients in cent. pump option 2 (PMPTQ).
* PMWEFR(NPLPMPW) --	pump efficiency (PMPEFR).
* PMWINR(NPUMPW) --	moment of inertia, pump and motor (PMPINR).
PMWTQR(NPUMPW) --	steady state pump torque (PMPTQR).
* PRESW4(NCVW) --	pressure in each compressible volume at the end of the current PRIMAR time subinterval (PRESL4). Pressure at the beginning of the subinterval is PRESW3, and the pressure at the end of the PRYMAR timestep is PRESW2.
PSPDW2(NPUMPW) --	pump speed at start of PRIMAR timestep (PSPED2).
PSPDW3(NPUMPW) --	pump speed at start of timestep (PSPED3).
PSPDW4(NPUMPW) --	pump speed at end of timestep (PSPED4).
* QRATIO(NCVW) --	the percentage of incoming energy to a heater lost due to imperfect insulation.

* ROUGHW(NELEW) -- the roughness of an element wall (ROUGHL).
* RROTOR(NCVW) -- the radius of a turbine rotor.
* RVA(NRVLVW) -- the fractional valve area to which a relief valve opens when the set pressure drop is reached.
* RVFRAC(NRVLVW) -- the fractional relief valve opening area.

SEGLW(NSEGW) -- length of a segment.

* SHHTCC(NCVW) -- the shell side condensation coefficient for a heater.
* TABSEG(10,3,NBCFLO) -- table for flow boundary condition input data. TABSEG(x,1,y) contains time, TABSEG(x,2,y) contains absolute flows, and TABSEG(x,3,y) contains enthalpies.
* TABVOL(10,4,NBCPRS) -- table for compressible volume boundary condition input data. TABVOL(x,1,y) contains time, TABVOL(x,2,y) contains pressures, TABVOL(x,3,y) contains enthalpies, and TABVOL(x,4,y).contains qualities.
* TAMBNT(NCVW) -- the ambient temperature for a heater volume.
* TBCP(NELEW) -- the specific heat of the tube in an element representing a heater tube bundle.
* TBKPMO(NELEW) -- the thermal conductivity of the tube in an element representing a heater tube bundle.
* TBLNLW(NELEW) -- the length of the section of the element within the drain for an element representing a tube bundle in a drain cooler or desuperheater/drain cooler.
* TBLNUP(NELEW) -- the length of the section of the element within the desuperheating section for an element representing a tube bundle in a desuperheating heater or a desuperheater/drain cooler.
* TBNDLW(NELEW) -- the number of nodes for the section of the element within the drain for an element representing a tube bundle in a drain cooler or desuperheater/drain cooler.
* TBNDUP(NELEW) -- the number of nodes for the section of the element within the superheating section for an element representing a tube bundle in a desuperheating heater or desuperheater/drain cooler.
* TBNMBR(NELEW) -- the total number of tubes in a heater tube bundle.
* TBNODE(NELEW) -- the number of nodes for the heat transfer calculation in an element representing a heater tube bundle.
* TBPODS -- the superheater bundle pitch-to-diameter ratio.

* TBRHO(NELEW) -- the tube material density in an element representing a heater tube bundle
* TBTHIK(NELEW) -- the tube thickness in an element representing a heater tube bundle.
* TCVW(NCVW) -- compressible volume temperature (TLQCV2).
* TEMPLW(NCVW) -- the temperature of the drain in a heater containing a drain.
* TEMPUP(NCVW) -- the temperature in the desuperheating region in a heater containing a desuperheating region.
* TIMERV(NRVLVW) -- the relief valve delay time for opening or closing.
* TPFACE(NCVW) -- the two-phase level in a volume in which liquid and vapor are separated.

  TQMBW3(NPUMPW) -- motor torque at start of timestep (TQMB3).

  TQMBW4(NPUMPW) -- motor torque at end of timestep (TQMB4).

  TQPBW3(NPUMPW) -- pump torque at start of timestep (TQPB3).

  TQWSAV(NPUMPW) -- torque from PUMPFL (TQBSAV).
* TRGRMI -- turbine/generator rotor moment of inertia.
* TRKLSW(NPUMPW) -- windage (TRKLSC).

  TRQMSW(NPUMPW) -- initial steady state speed (TRQMSS).
* TSECHT(NHTR) -- the temperature of the secondary fluid in a heater.
* TUBNOS -- the number of superheater tubes.

  VCALBW(NVLVW) -- calibration constant for a standard valve.
* VCONSW(NVLVW) -- the proportionality constant between the stem position and the valve characteristic for a standard valve.
* VDAMPW(NVLVW) -- damping coefficient for the valve stem position equation.

  VDRIVW(NVLVW) -- driving function for the valve stem position equation.
* VLVMSW(NVLVW) -- valve mass.
* VPHINW(NVLVW) -- valve characteristic at the current PRIMAR subinterval.

  VPHIW(10,NVLVW) -- valve characteristic curve for a standard valve.
* VPOSW(10,NVLVW) -- valve stem position for points in VPHIW.
* VSPRGW(NVLVW) -- spring constant for the valve stem position equation.
* VSTEMW(NVLVW) -- valve stem position.

  VSTMWl(NVLVW) -- valve stem position from the previous timestep.

* VTABDW(10,NVLVW) -- table of driving function vs. time for a standard valve (this array is used to vary driving function with time if the control system is not used to control the valve).
* VTIMW(10,NVLVW) -- values of time for VTABDW.
* VOLCVW(NCVW) -- volume of each compressible volume (VOLLGC).
* VOLLW(NCVW) -- the volume of the drain in a heater containing a drain.
* VOLUP(NCVW) -- the volume of the desuperheating region in a heater containin desuperheating region.
* WMOTTK(20,NPUMPW) -- motor torque table and times (AMOTTK).
* XCVW(NCVW) -- compressible volume quality.
* XKTUBE -- the evaporator tube thermal conductivity.
* XLENLW(NCVW) -- the length of the drain in a heater containing a drain.
* XLENUP(NCVW) -- the length of the desuperheating region in a heater containing a desuperheating region.
* XLENW(NELEW) -- length of an element (XLENEL).
* XRXFR(NSEG) -- nozzle reaction fraction.
* ZCVW(NCVW) -- compressible volume midpoint elevation (ZCVL).
* ZINW(NSEGW) -- elevation of the segment inlet (ZINL).
* ZLOWST(NELEW) -- the lowest elevation of the element within the heater for an element representing a heater tube bundle.
* ZONLE(3) -- the zone lengths in the evaporator. ZONLE(1) is the subcooled zone length, and ZONLE(3) is the superheated zone length; these are both input, with ZONLE(2) (the two-phase zone length) calculated from EL, ZONLE(1), and ZONLE(3) (ELEV).
* ZOUTLW(NELEW) -- elevation of the element outlet (ZOUTEL).

APPENDIX 7.2:
STEAM GENERATOR WATER-SIDE HEAT TRANSFER CORRELATIONS

Subcooled Water

The Dittus-Boelter correlation [7-4] is used.

$$N = 0.023\,\mathrm{Re}^{0.8}\,\mathrm{Pr}^{0.4} = \frac{h_w D_H}{k}$$

Bulk liquid properties are used to calculate Re, Pr and k; h_w is the heat transfer coefficient between the wall surface and the bulk water.

Nucleate Boiling Water

A correlation developed by Thom, et al. [7-5] is used.

$$h_w = 3.1968\left(e^{P/8.65\cdot 10^6}\right)\frac{1}{0.072}(q)^{0.5}$$

h_w is the heat transfer coefficient between the wall surface and the bulk water; q = $H_T(\mathrm{T_m} - T_{sat})$ where H_T is defined as in Eq. 7.3-66; T_m is the average wall temperature; P is the steam generator pressure.

Film Boiling Water

A correlation of A. A. Bishop et al. [7-6] is the following

$$N = 0.0193\,\mathrm{Re}^{0.8}\,\mathrm{Pr}^{1.23}\left[x + (1-x)\frac{\rho_g}{\rho_f}\right]^{0.68}\left(\frac{\rho_g}{\rho_f}\right)^{0.068} = \frac{h_w D_H}{k}$$

A modification of the original formulation is used. The original formulation specified that properties appropriate for the wall film temperature be used to calculate Re and Pr. All temperature-dependent properties are calculated with T_{sat}. The wall film temperature is only crudely approximated and the relevant properties are very insensitive to temperature when above T_{sat}. h_w is the heat transfer coefficient between the wall surface and the bulk water and x is the local nodal quality. The mass flux used in the Reynold's number is the local value.

Superheated Steam

A correlation developed by A. A. Bishop [7-7] is used.

$$N = 0.0073\,\mathrm{Re}^{0.886}\,\mathrm{Pr}^{0.61} = \frac{h_w D_H}{k}$$

Although the original correlation specified that the film temperature be used to evaluate the relevant properties, the bulk temperature is instead used since these properties are very insensitive to temperature above T_{sat}. h_w is the heat transfer coefficient between the wall surface and the bulk steam.

Liquid Sodium Heat Transfer

A variation of the Maresca-Dwyer correlation is used [7-8]. The heat transfer coefficient between the outside wall and the bulk sodium is the following.

$$H_{Na} = N\, c_p\, \mu/(PrD_H)$$

where c_p, μ and D_H are the specific heat, viscosity and hydraulic diameter respectively. The Prandtl number is computed according to the following,

$$Pr = 0.00212 + 2.329/(1.8T - 410.92)$$

Nusselt numbers are computed for both turbulent flow and molecular conduction. The greater of the two is used. For turbulent flow,

$$Nu = 6.66 + 3.126POD + 1.184POD^2 + 0.0155(PrReS)^{0.86}$$

where POD is the tube pitch-to-diameter ratio. S is calculated according to the following,

$$S = 1.0 - 1.82/(PrE)$$

and E is given by,

$$E = 0.000175\ \mathrm{Re}^{1.32}/\mathrm{POD}^{1.5}$$

The Nusselt number for molecular conduction is given by the following,

$$Nu = 6.4353 + 3.97\mathrm{POD} + 1.025\mathrm{POD}^2 - 29494./(\mathrm{Re} + 20363)$$

APPENDIX 7.3:
TWO-PHASE INTERFACE SOLUTION SCHEME FOR HEATER CYLINDERS LYING ON THE SIDE

The solution scheme described below is used to solve for the two-phase interface, for heater cylinders lying on the side, form the transcendental equations given in Eqs. 7.4-8 and 7.4-9. Since the problem is symmetric with respect to the center point of the cylinder, as is obvious by looking at Fig. 7.4-3, only Eq. 7.4-8 is used to demonstrate the solution scheme.

By defining the angle between the vertical section L and the radius r_s as β in Fig. 7.4-3, Eq. 7.4-8 can be rewritten as,

$$\alpha_s = \left[\beta - \frac{\sin(2\beta)}{2}\right]/\pi \ , \qquad \text{(A7.3-1)}$$

for $0 \le \alpha_s \le 1/2$ and $0 \le \beta \le \pi/2$. The height of the vapor region A_g corresponding to α_s in Fig. 7.4-3 is r_s - L, which can be normalized to the cylinder radius r_s as

$$\omega \equiv \frac{r_s - L}{r_s} = 1 - cos\beta \qquad \text{(A7.3-2)}$$

The aim now is to obtain an expression for β as a function of α_s, in order to avoid using an iterative solution to find β. The most straight-forward way would be to generate a polynomial expression in α_s for β. However, a study of the curvature of the β vs. α_s curve indicates that the slope is very steep at β close to zero, changes dramatically as β increases, and levels off as β approaches $\pi/2$. A single polynomial of high order to approximate the curve is difficult to obtain without unacceptable errors in some part of the curve, and the computation of the polynomial may be time-consuming. Thus, an alternative method is used and is described as follows.

The range of α_s on the β vs. α_s curve is divided into three regions based on the slopes along the curve, i.e., $0 \le \alpha_s < \alpha_1$, $\alpha_1 \le \alpha_s < \alpha_2$, and $\alpha_2 \le \alpha_s \le 1/2$, where α_1 and α_2 are chosen to be at the suitable values 0.015 and 0.225, respectively. Also, the polynomials of β for each region are given the forms,

$$\beta = C_1 (1.5\alpha_s)^{1/3} \ , \ 0 \le \alpha_s < \alpha_1 \ , \qquad \text{(A7.3-3)}$$

$$\beta = \frac{\beta_1 + C_2 X_1 + C_3 X_1^2}{1 + C_4 X_1 + C_5 X_1^2} \ , \ \alpha_1 \le \alpha_s < \alpha_2 \ , \qquad \text{(A7.3-4)}$$

$$\beta = \frac{\beta_2 + C_6 X_2 + C_7 X_2^2}{1 + C_8 X_2 + C_9 X_2^2} \text{ , } \alpha_2 \le \alpha_s < 1/2 \text{ ,} \qquad \text{(A7.3-5)}$$

where β_1 and β_2 are values of β corresponding to α_1 and α_2, respectively, X_1 and X_2 are defined as

$$X_1 = (\alpha_s - \alpha_1) \text{ ,}$$

and

$$X_2 = (\alpha_s - \alpha_2) \text{ ,}$$

and the coefficients C_1 through C_9 are determined using a least squares fit separately on each region. The coefficient values are as follows:

C_1 =1.00377, C_2 =1.41595 x 10^1,

C_3 =6.98089 x 10^1, C_4 =2.76847 x 10^1,

C_5 =4.47906 x 10^1, C_6 =2.37819,

C_7 =6.38891 x 10^{-1}, C_8 =1.72658,

C_9 =4.94197 x 10^2.

More significant digits for C_1 through C_9 are used in the coding. The polynomials A7.3-3 through A7.3-5 are chosen such that continuity conditions are satisfied at α_s equal to α_1 and α_2.

Once β is calculated from one of Eqs. A7.3-3, A7.3-4, and A7.3-5 for a given α_s, the two-phase interface can be computed as

$$TP = (1-\omega) r + CV \text{ ,}$$

where ω is given in Eq. A7.3-2.

The maximum error, defined as the difference between ω, as calculated from Eq. A7.3-2 with β obtained by Eqs. A7.3-3, A7.3-4, or A7.3-5, and the actual ω, is within ±4.53 x 10^{-4}. If more accuracy is needed, a better value for ω can be obtained by introducing the Newton iteration method and using the calculated ω as an initial base value. With one iteration, the maximum error could be reduced to ±2.67 x 10^{-7}, and with two iterations, to ±9.17 x 10^{-13}.

APPENDIX 7.4:
DICTIONARY OF STEAM GENERATOR MODEL VARIABLES

Variables in COMMON

Note: Variables in block SGEN1, SGEN2, and SGEN3 apply to the once-through steam generator or to the evaporator in the recirculation type steam generator. Variables in blocks SGENS1, SGENS2, and SGENS3 apply to the superheater only.

Name	Block	Units	Explanation
ARM	SGEN2	m^2	Cross-sectional area of tube wall
ARMS	SGENS2	m^2	Cross-sectional area of tube wall
ARNA	SGEN2	m^2	Flow area of sodium
ARNAS	SGENS2	m^2	Flow area of sodium
ARW	SGEN2	m^2	Flow area of water
ARWS	SGENS2	m^2	Flow area of water
AWB(100)	SGEN1	-	Void fraction at each node in boiling zone at beginning of time step
AWE(100)	SGEN1	-	Void fraction at each node in boiling zone at end of time step
CNAFRS	SGENS2	-	Constant used in sodium heat transfer coefficient calculation; equal to 6.66 + (1.184TBPODS + 3.126) TBPODS
CNAFR1	SGEN2	-	Constant used in sodium heat transfer coefficient calculation; equal to 6.66 + (1.184TUBPOD + 3.126)TUBPOD
DDW	SGEN2	m	Hydraulic diameter on water side
DDWS	SGENS2	m	Hydraulic diameter on water side
DELP24	SGEN2	-	Fraction of total pressure drop in subcooled zone
DEWI	SGEN2	m	Booster tube outer diameter on water side
DEWIS	SGENS2	m	Booster tube outer diameter on water

			side
DEWO	SGEN2	m	Tube wall inner diameter
DEWOS	SGENS2	m	Tube wall inner diameter
DOUT	SGEN2	m	Tube wall outer diameter
DOUTS	SGENS2	m	Tube wall outer diameter
DHNA	SGEN2	m	Hydraulic diameter on sodium side
DHNAS	SGENS2	m	Hydraulic diameter on sodium side
DZONE(2)	SGEN2	m/s	Velocity of subcooled and superheat zone boundaries
FACT1	SGEN2	-	Not currently used
FACT1S	SGENS2	-	Not currently used
FACT2	SGEN2	-	$1.04*10^4*TUBPOD^{1.5}$; used in sodium heat transfer coefficient calculation
FACT2S	SGENS2	-	$1.04*10^4*TBPODS^{1.5}$; used in sodium heat transfer coefficient calculation
FACT3	SGEN2	m^{-1}	π * DEWO/ARW
FACT3S	SGENS2	m^{-1}	π * DEWOS/ARWS
FACT4	SGEN2	m^{-1}	π * DOUT/ARNA
FACT4S	SGENS2	m^{-1}	π * DOUTS/ARNAS
FACT5	SGEN2	-	ARNA/ARM
FACT5S	SGENS2	-	ARNAS/ARMS
FACT6	SGEN2	-	ARW/ARM
FACT6S	SGENS2	-	ARWS/ARMS
FACT7	SGEN2	K	Constant used in viscosity function
FACT8	SGEN2	kg/m^3	Constant used in viscosity function
FACT9	SGEN2	J/m^3-K	Density x specific heat for tube wall
FACT10	SGEN2	-	$0.023 * DDW^{-0.2}$; used in subcooled heat transfer coefficient

FACT11	SGEN2	-	0.0193 * $DDW^{-0.2}$; used in film boiling heat transfer coefficient
FACT12	SGEN2	-	0.0073 * $DDW^{-0.114}$; used in superheat zone heat transfer coefficient
FACTSP	SGENS2	-	0.0073 * $DDWS^{-0.114}$; used in superheater heat transfer coefficient
FOULR(4)	SGEN2	m^2-K/w	Tube wall heat resistance on the water side plus any fouling heat resistance on water side for each heat transfer regime
FOULRS	SGENS2	m^2-K/w	Tube wall heat resistance on the water side plus any fouling heat resistance on water side
FRIC1(4)	SGEN2	-	Normalizing friction factor in Eqs. 7.3-56 and 7.3-94 for each heat transfer regime
FRIC1S	SGENS2	-	Normalizing fraction factor in superheater
GNA	SGEN2	kg/m^2-s	Sodium side mass flow
GNAS	SGENS2	kg/m^2-s	Sodium side mass flow
GWB(100)	SGEN1	kg/m^2-s	Water side mass flow at each node at beginning of time step
GWE(100)	SGEN1	kg/m^2-s	Water side mass flow at each node at end of time step
GWS	SGENS2	kg/m^2-s	Sodium side mass flow
HD	SGEN2	(J/kg)/(BTU/lb)	Conversion factor for enthalpies since functions are in BTU/lb
HDNB	SGEN2	-	Fraction of cell where DNB point lies which is in the nucleate boiling regime
HFG	SGEN2	J/kg	h_{fg}
HFSAT	SGEN2	J/kg	h_f
HFSATP	SGEN2	BTU/lb	h_f/HD

HGSAT	SGEN2	J/kg	h_g
HGSATP	SGEN2	BTU/lb	h_g/HD
HN(520)	SGEN2	s	Array which stores all potential time steps from which is selected the minimum
HSTEP	SGEN2	s	Primary loop time step
HTF(4)	SGEN2	-	Calibration factor for heat transfer coefficients for each regime
HTFS	SGENS2	-	Calibration factor for heat transfer coefficient in superheater
HTW(100)	SGEN2	w/m^2-K	Heat transfer coefficient between the tube wall surface and the bulk water by cell center
HTWS	SGENS2	w/m^2-K	Heat transfer coefficient between the tube wall surface and the bulk water by cell center in superheater
HUNIT	SGEN2	s	Current steam generator time step
HUNITN	SGEN2	s	Newly selected steam generator time step for next step
HUNITS	SGENS2	s	Current superheater time step
HWB(100)	SGEN1	J/kg	Enthalpy by node at beginning of step
HWBS(100)	SGENS1	J/kg	Enthalpy by node at beginning of step
HWE(100)	SGEN1	J/kg	Enthalpy by node at the end of step
HWES(100)	SGENS1	J/kg	Enthalpy by node at the end of step
H1MIN	SGENS2	w/m^2-K	Minimum value allowed for HTW in subcooled zone
H2MIN	SGEN2	w/m^2-k	Minimum value allowed for HTW in nucleate boiling zone
H3MIN	SGEN2	w/m^2-k	Minimum value allowed for HTW in film boiling zone
H4MIN	SGEN2	w/m^2-k	Minimum value allowed for HTW in superheated zone or for HTWS in

			superheater
IDNB	SGEN3	-	Cell number when DNB point occurs
IDNBL	SGEN3	-	Value of IDNB during previous time step
ISTEPW	SGEN3	-	Number of current primary loop time step
LAR	SGEN3	-	Array size limit for nodal arrays
LIM	SGEN3	-	Length of SGEN1 COMMON block
NCOUNT	SGEN3	-	Number of steam generator time substeps within primary loop step
NODSC	SGEN3	-	Number of cells within subcooled zone
NODSCO	SGEN3	-	Initial value of NODSC
NODSC1	SGEN3	-	Node number of subcooled/boiling boundary; NODSC + 1
NODSC2	SGEN3	-	NODSC1 + 1
NODSH	SGEN3	-	Number of cells within superheated zone in steam generator or evaporator
NODSHO	SGEN3	-	Initial value of NODSH
NODSHT	SGENS3	-	Number of cells within superheater
NODSH0	SGEN3	-	Total number of cells in steam generator or evaporator; NODSC + NODTP + NODSH
NODSH1	SGEN3	-	NODSHT + 1; or total number of nodes in superheater
NODT	SGEN3	-	NODSH0 + 1; or total number of nodes in steam generator or evaporator
NODTP	SGEN3	-	Number of cells within boiling zone
NODTPO	SGEN3	-	Initial value of NODTP
NODTP0	SGEN3	-	NODSC + NODTP
NODTP1	SGEN3	-	Node number of boiling/superheat

			boundary; NODSC + NODTP + 1
NODTP2	SGEN3	-	NODTP1 + 1
ON	SGEN2	-	1.0
PD	SGEN2	Pa/PSI	Conversion factor for pressures since functions are in PSI
PDOT	SGEN2	Pa/s	Time derivative of steam generator average pressure
PI	SGEN2	-	π
PSW	SGEN2	-	ρ_g/ρ_f
PWAVEP	SGEN2	PSI	PWAVES/PD
PWAVES	SGEN2	Pa	Steam generator pressure
PWAVSP	SGENS2	Pa	Pressure in superheater
PWVSPP	SGENS2	PSI	PWAVSP/PD
P25	SGEN2	-	0.25
P5	SGEN2	-	0.5
QMT(100)	SGEN2	w/m^3	Volumetric heat source for each cell in the tube wall
QMTS(100)	SGENS2	w/m^3	Volumetric heat source for each cell in the tube wall
QST(100)	SGEN2	w/m^3	Volumetric heat source for each cell in the sodium side
QSTS(100)	SGENS2	w/m^3	Volumetric heat source for each cell on the sodium side
QWB(100)	SGEN1	w/m^3	Volumetric heat source for each cell on the water side at the beginning of step
QWBS(100)	SGENS1	w/m^3	Volumetric heat source for each cell on the water side at the beginning of step
QWE(100)	SGEN1	w/m^2-K	Total heat transfer coefficient from tube wall center to bulk water

			including possible fouling for each cell center
QWES(100)	SGENS1	w/m^2-K	Total heat transfer coefficient from tube wall center to bulk water including possible fouling for each cell center
QWT(100)	SGEN2	w/m^3	Volumetric heat source for each cell on the water side at the end of step
QWTS(100)	SGENS2	w/m^3	Volumetric heat source for each cell on the water side at the end of step
RMDEWO	SGEN2	m^2-K/w	Tube wall heat resistance on the water side
RMDEWS	SGENS2	m^2-K/w	Tube wall heat resistance on the water side
RMDNAA	SGEN2	m^2-K/w	Tube wall heat resistance on the sodium side
RMDNAS	SGENS2	m^2-K/w	Tube wall heat resistance on the sodium side
ROB(100)	SGEN1	kg/m^3	Water density at each node at beginning of step
ROBS(100)	SGENS1	kg/m^3	Water density at each node at beginning of step
ROE(100)	SGEN1	kg/m^3	Water density at each node at end of step
ROES(100)	SGENS1	kg/m^3	Water density at each node at end of step
ROFG	SGEN2	kg/m^3	ρ_g-ρ_f
ROFSAT	SGEN2	kg/m^3	ρ_f
ROGSAT	SGEN2	kg/m^3	ρ_g
ROHFG	SGEN2	J/m^3	$\rho_g h_g$ - $\rho_f h_f$
ROZ1	SGEN2	kg/m^3	Average water density in subcooled zone

TBPODS	SGENS2	-	Tube pitch-to-diameter ratio
TIMCUR	SGEN2	s	Time at end of current steam generator time step
TIMEIN	SGEN2	s	Time at beginning of current primary loop time step
TIMENP	SGEN2	s	Time at end of current primary loop time step
TLIM	SGEN2	-	Largest fractional change in selected parameters for new time step selection
TMB(100)	SGEN1	K	Temperature at each cell center of tube wall at beginning of step
TMBS(100)	SGENS1	K	Temperature at each cell center of tube wall at beginning of step
TME(100)	SGEN1	K	Temperature at each cell center of tube wall at end of step
TMES(100)	SGENS1	K	Temperature at each cell center of tube wall at end of step
TO	SGEN2	-	2.0
TSB(100)	SGEN1	K	Temperature of sodium at each node at beginning of step
TSBS(100)	SGENS1	K	Temperature of sodium at each node at beginning of step
TSC(100)	SGEN2	K	Temperature of sodium at each node at beginning of step
TSCS(100)	SGENS2	K	Temperature of sodium at each cell center at beginning of step
TSE(100)	SGENS2	K	Temperature of sodium at each node at end of step
TSES(100)	SGENS1	K	Temperature of sodium at each node at end of step
TUBNO	SGEN2	-	Number of tubes in steam generator

TUBNOS	SGENS2	-	Number of tubes in superheater
TUBPOD	SGEN2	-	Tube pitch-to-diameter ratio
TWB(100)	SGEN1	K	Temperature of water at each node at beginning of step
TWBS(100)	SGENS1	K	Temperature of water at each node at beginning of step
TWC(100)	SGENS1	K	Temperature of water at each cell center at beginning of step
TWCS(100)	SGENSG	K	Temperature of water at each cell center at beginning of step
TWE(100)	SGEN1	K	Temperature of water at each node at end of step
TWES(100)	SGENS1	K	Temperature of water at each node at end of step
TWSAT	SGEN2	K	Water saturation temperature
UWZ1	SGEN2	kg/m-s	Average viscosity in the subcooled zone
XKTUBE	SGEN2	w/m-K	Conductivity of tube wall
XWB(100)	SGEN1	-	Quality at each node in boiling zone at beginning of step
XWE(100)	SGEN1	-	Quality of each node in billing zone at end of step
ZMAX	SGEN2	m	Zone length threshold above which the number of nodes is restored to the initial value when the previous number of nodes is one
ZMIN	SGEN2	m	Zone length threshold below which the number of nodes in reduced to one
ZO	SGEN2	-	0.0
ZONLB(3)	SGEN2	m	Lengths of each zone at beginning of step
ZONLE(3)	SGEN2	m	Lengths of each zone at end of step

ZSG	SGEN2	m	Length of steam generator or of evaporator
ZSUP	SGEN2	m	Length of superheater

Selected Variables not in COMMON

Name	Routine	Units	Explanation
AWZ2	SGUNIT INIT	-	Average void fraction in nucleate boiling zone
AWZ3	SGUNIT INIT	-	Average void fraction in film boiling zone
DELP1	SGUNIT INIT	Pa	Pressure drop across subcooled zone
DELP2	SGUNIT INIT	Pa	Pressure drop across nucleate boiling zone
DELP3	SGUNIT INIT	Pa	Pressure drop across film boiling zone
DELP4	SGUNIT INIT	Pa	Pressure drop across superheated zone
DHF	SGUNIT	J/kg-Pa	Derivative of h_f with respect to pressure
DHG	SGUNIT	J/kg-Pa	Derivative of h_g with respect to pressure
DRODH	SGUNIT	kg^2/m^3-J	Derivative of ρ(h,P) with respect to enthalpy in superheated zone
DRODP	SGUNIT	kg/m^3-Pa	Derivative of ρ(h,P) with respect to pressure in superheated zone
DROF	SGUNIT	kg/m^3-Pa	Derivative of ρ_f with respect to pressure
DROG	SGUNIT	kg/m^3-Pa	Derivative of ρ_g with respect to pressure
DTSG(100)	TSBOP	s	Array to store time steps over LMPDOT steam generator time steps in order to calculate .

GDOT	SGUNIT	$kg/m^2\text{-}s^2$	in pressure drop calculation
GWO	INIT	$kg/m^2\text{-}s$	Steady state mass flow
GWZ	SGUNIT INIT	$k/m^2\text{-}s$	End of time step regional average mass flow for pressure drop calculation
GWZ0	SGUNIT	$kg/m^2\text{-}s$	Beginning of time step regional average mass flow for pressure drop calculation
HTAV	INIT	$w/m^2\text{-}K$	Average heat transfer coefficient at tube wall surface on water side in one-node approximation or region
HTAVT	INIT	$w/m^2\text{-}K$	Total water side average heat transfer coefficient in one-node approximation of region
HWAV	INIT	J/kg	Average water enthalpy in one-node approximation of region
HWIN	INIT	J/kg	Steady state inlet water enthalpy
HWOUT	INIT	J/kg	Steady state outlet water enthalpy
IGO	INIT	-	Indicator which is set when the DNB node is found in the boiling zone so that a switch is made from the nucleate to the film boiling regime
INITER	INIT	-	Counter on the number of iterations in the search on the calibration factor in the film boiling calculation for each iteration on the nucleate boiling regime
IOPT1	INIT	-	Indicator which shows whether length (=2) or calibration factor (=1) is to be searched on for subcooled zone
IOPT2	INIT	-	Indicator which shows whether length (=2) or calibration factor (=1) is to be searched on for superheated zone
IOPT3	INIT	-	Indicator which shows how many heat transfer regimes there are in the steady state calculation
IPASS	SGUNIT	-	Indicator which stops iterative search on Z_{TP} in boiling zone when the zone reaches the top of the steam generator or when Z_{TP} changes more than a maximum amount allowed

ITER	SGUNIT INIT	-	Iteration counter either on boiling zone length searches in SGUNIT or searches in all three zones in INIT
LMPDOT	TSBOP	-	Number of time steps and pressures stored in DTSG and PTSG arrays for calculation
PTSG(100)	TSBOP	Pa	Array to store pressures over LMPDOT steam generator time steps in order to calculate
ROAV	INIT	kg/m^3	Average water density in one-node approximation of region
ROEDNB	SGUNIT INIT	kg/m^3	Water density at the DNB point used in pressure drop calculation
ROZ2	SGUNIT INIT	kg/m^3	Average density in nucleate boiling zone for pressure drop calculation
ROZ3	SGUNIT INIT	kg/m^3	Average density in film boiling zone for pressure drop calculation
ROZ4	SGUNIT INIT	kg/m^3	Average density in superheated zone for pressure drop calculation
R32	SGUNIT INIT	-	Thom friction factor in nucleate boiling zone
R33	SGUNIT INIT	-	Thom friction factor in film boiling zone
TIMDIF	TSBOP	s	Time difference between beginning of primary loop time step and the end of current steam generator time step
TMAV	INIT	K	Average tube wall temperature in one-node approximation to region
TNAINB	TSBOP	K	Inlet sodium temperature at the beginning of primary loop time step
TNAINE	INIT	K	Inlet sodium temperature at the end of primary loop time step
TSAV	INIT	K	Average sodium temperature in one-node approximation to region

TSHF	INIT	K	Sodium temperature at the point of h_f on the water side at steady state
TSHG	INIT	K	Sodium temperature at the point of h_g on the water side at steady state
TSIN	INIT	K	Steady state sodium inlet temperature
TSOUT	INIT	K	Steady state sodium outlet temperature
TWAV	SGUNIT INIT	K	Average water temperature in one-node approximation to region
UZ2	SGUNIT INIT	kg/m-s	Average viscosity in nucleate boiling zone for pressure drop calculation
UZ3	SGUNIT INIT	kg/m-s	Average viscosity in film boiling zone for pressure drop calculation
UZ4	TSBOP	kg/m-s	Average viscosity in superheated zone for pressure drop calculation
WNAINB	TSBOP	kg/s	Sodium flow rate at beginning of primary loop time step
WNAINE	SGUNIT	kg/s	Sodium flow rate at end of primary loop time step
ZITER	SGUNIT INIT	m	Current value of Z_{TP} during search on region length in boiling zone calculation
ZONLE2	SGUNIT INIT	m	Length of nucleate boiling zone used in pressure drop calculation
ZONLE3		m	Length of film boiling zone used in pressure drop calculation

APPENDIX 7.5:
MATERIAL PROPERTIES DATA

This Appendix documents material properties correlations employed throughout the balance-of-plant network model, the steam generator model, and the component models for thermal and physical properties data. These data are used in heat transfer and fluid dynamics calculations.

On the sodium side of the steam generator, the correlations used for liquid sodium density, liquid sodium specific heat, and liquid sodium viscosity are documented in Section 12.12.

On the water side of the steam generator and throughout the balance-of-plant models, the dynamic viscosity of steam and water is caluclated from [7-13]:

$$\mu = \mu_o \exp\left[\frac{\rho}{\rho^*}\sum_{i=0}^{5}\sum_{j=0}^{4} b_{ij}\left(\frac{T^*}{T}-1\right)^i\left(\frac{\rho}{\rho^*}-1\right)^j\right]$$

with

$$\mu_o = 10^{-6}\left(\frac{T}{T^*}\right)^{1/2}\left[\sum_{k=0}^{3} a_k\left(\frac{T^*}{T}\right)^k\right]^{-1}$$

where μ is the viscosity in Pa-s, ρ is the density in kg/m, T is the temperature in Kelvins, and the constants ρ^* and T^* are

$\rho^* = 317.763 \quad kg/m^3$,

$T^* = 647.27 \quad K$,

The coefficients in the expression for μ_o are:

$a_0 = \quad 0.018\ 1583$

$a_1 = \quad 0.017\ 7624$

$a_2 = \quad 0.010\ 5287$

$a_3 = -0.003\ 6744$

and the values for b_{ij} are given in Table A7.5-1.

Table A7.5-1. Numerical Values of the Coefficients b_{ij}

i=	0	1	2	3	4	5
j=0	0.5601 938	0.162 888	-0.130 356	0.907 919	-0.551 119	0.146 543
1	0.235 622	0.789 393	0.673 665	1.207 552	0.067 0665	-0.084 3370
2	-0.274 637	-0.743 539	-0.959 456	-0.687 343	-0.497 089	0.195 286
3	0.145 831	0.263 129	0.346 247	0.213 486	0.100 754	-0.032 932
4	-0.027 0448	-0.025 3093	-0.026 776	-0.082 2904	0.060 2253	-0.020 2595

Correlations for the enthalpy of saturated liquid water and saturated steam are taken from the RETRAN-02 code documentation [7-14]. The specific enthalpy of liquid water is given by

$$h_g = \begin{cases} \sum_{i=0}^{8} CF1_i \left[\ell n(P)\right]^i & \text{for } 0.1 \text{ psia} \le P \le 950 \text{ psia} \\ \sum_{i=0}^{8} CF2_i \left[\ell n(P)\right]^i & \text{for } 950 \text{ psia} < P \le 2550 \text{ psia} \\ \sum_{i=0}^{8} CF3_i \left[\left(P_{CRIT} - P\right)^{0.41}\right]^i & \text{for } 2550 < P \le P_{CRIT}, \end{cases}$$

and the specific enthalpy of saturated steam is given by

$$h_g = \begin{cases} \sum_{i=0}^{11} CG1_i \left[\ell n(P)\right]^i & \text{for } 0.1 \text{ psia} \le P \le 1500 \text{ psia} \\ \sum_{i=0}^{8} CG2_i \left[\ell n(P)\right]^i & \text{for } 950 \text{ psia} < P \le 2650 \text{ psia} \\ \sum_{i=0}^{6} CG3_i \left[\left(P_{CRIT} - P\right)^{0.41}\right]^i & \text{for } 2650 < P \le P_{CRIT} \end{cases}$$

where h_f and h_g are the specific enthalpy in units of BTU/1bm, P is the pressure in psia, P_{CRIT} is the critical pressure (3208.2 psia), and the constant coefficients are given in Table A7.5-2. Expressions for the temperatures of subcooled water superheated steam as functions of pressure and enthalpy are taken from RETRAN-02 [7-14]:

$$T_\ell = \sum_{i=0}^{i=1} \sum_{j=0}^{j=3} CT1_{i,j} \, P^{i_h j}$$

and

$$T_v = \sum_{i=0}^{i=4} \sum_{j=0}^{j=4} CT3_{i,j} P^{i_h j}$$

where T_ℓ and T_v are the subcooled water and superheated steam temperatures in degrees Fahrenheit, P is the pressure in psia, h is the enthalpy in BTU/1bm, and the constant coefficients $CT1$ and $CT3$ are given in Table A7.5-3. The specific heats at constant pressure for subcooled water and superheated steam are calculated as the inverses of the partial derivations of the expressions for T_ℓ and T_v with respect to enthalpy. The saturation temperature is obtained from the expression for T_ℓ evaluated at the ambient pressure and the saturated liquid water specific enthalpy at that pressure.

Correlations for the specific enthalpies of subcooled liquid water and superheated steam as functions of pressure and enthalpy are taken from RETRAN-02 [7-14]:

$$v_\ell = \exp\left[\sum_{i=0}^{2} \sum_{j=0}^{4} CN1_{i,j} P^{i_h j}\right]$$

and

$$v_v = \sum_{i=-1}^{2} \sum_{j=0}^{2} CN2_{i,j} P^{i_h j}$$

where v_ℓ and v_v are the subcooled water and superheated steam specific volumes in ft^3 / lbm, P is the pressure in psia, h is the enthalpy in BTU/1bm, and the constant coefficients $CN1$ and $CN2$ are listed in Table A7.5-4. The satruated liquid water density is computed from the value for v_ℓ at the ambient pressure and the saturated steam specific enthalpy at that pressure. Similarly the saturated steam density is obtained from v_v at the ambient pressure and the satruated steam specific enthalpy at that pressure.

Table A7.5-2. Constant Coefficients in Expressions for Saturated Liquid Water and Saturated Steam Enthalpies as Functions of Pressure

i	$CF1_i$	$CF2_i$	$CF3_i$
0	$.6970887859 \times 10^{2}$	$.8408618802 \times 10^{6}$	$.9060030436 \times 10^{3}$
1	$.3337529994 \times 10^{2}$	$.3637413208 \times 10^{6}$	$-.1426813520 \times 10^{0}$
2	$.2318240735 \times 10^{1}$	$-.4634506669 \times 10^{6}$	$.1522233257 \times 10^{1}$
3	$.1840599513 \times 10^{0}$	$.1130306339 \times 10^{6}$	$-.6973992961 \times 10^{0}$
4	$-.5245502284 \times 10^{-2}$	$-.4350217298 \times 10^{3}$	$.1743091663 \times 10^{0}$
5	$.2878007027 \times 10^{-2}$	$-.3898988188 \times 10^{4}$	$-.2319717696 \times 10^{-1}$
6	$.1753652324 \times 10^{-2}$	$.6697399434 \times 10^{3}$	$.1694019149 \times 10^{-2}$
7	$-.4334859629 \times 10^{-3}$	$-.4730726377 \times 10^{2}$	$-.6454771710 \times 10^{-4}$
8	$.3325699282 \times 10^{-4}$	$.1265125057 \times 10^{1}$	$.1003003098 \times 10^{-5}$
i	$CG1_i$	$CG2_i$	$CG3_i$
0	$.1105836875 \times 10^{4}$	$-.2234264997 \times 10^{7}$	$.9059978254 \times 10^{3}$
1	$.1436943768 \times 10^{2}$	$.1231247634 \times 10^{7}$	$.5561957539 \times 10^{1}$
2	$.8018288621 \times 10^{0}$	$-.1978847871 \times 10^{6}$	$.3434189609 \times 10^{1}$
3	$.1617232913 \times 10^{-1}$	$.1859988044 \times 10^{2}$	$-.6406390628 \times 10^{0}$
4	$-.1501147505 \times 10^{-2}$	$-.2765701318 \times 10^{1}$	$.5918579484 \times 10^{-1}$
5	$.0000000000 \times 10^{0}$	$.1036033878 \times 10^{4}$	$-.2725378570 \times 10^{-2}$
6	$.0000000000 \times 10^{0}$	$-.2143423131 \times 10^{3}$	$.5006336938 \times 10^{-4}$
7	$.0000000000 \times 10^{0}$	$.1690507762 \times 10^{2}$	
8	$.0000000000 \times 10^{0}$	$-.4864322134 \times 10^{0}$	
9	$-.1237675562 \times 10^{-4}$		
10	$.3004773304 \times 10^{-5}$		
11	$-.2062390734 \times 10^{-6}$		

Table A7.5-3. Constant Coefficients in Expressions for Temperature as a Function of Pressure and Specific Enthalpy

			$CT1_{i,j}$		
i=	0	1	2	3	
j=0	$.3276275552 \times 10^{2}$	$.9763617000 \times 10^{0}$	$.1857226027 \times 10^{-3}$	$-.4682674330 \times 10^{-6}$	
j=1	$.3360880214 \times 10^{-2}$	$-.5595281760 \times 10^{-4}$	$.1618595991 \times 10^{-6}$	$-.1180204381 \times 10^{-9}$	
			$CT3_{i,j}$		
i=	0	1	2	3	4
j=0	$-.1179100862 \times 10^{5}$	$.2829274345 \times 10^{2}$	$-.2678181564 \times 10^{-1}$	$.1218742752 \times 10^{-4}$	$-.2092033147 \times 10^{-8}$
j=1	$.1256160907 \times 10^{3}$	$-.3333448495 \times 10^{0}$	$.3326901268 \times 10^{-3}$	$-.1477890326 \times 10^{-6}$	$.2463258371 \times 10^{-10}$
j=2	$-.1083713369 \times 10^{0}$	$.2928177730 \times 10^{-3}$	$-.2972436458 \times 10^{-6}$	$.1342639113 \times 10^{-9}$	$-.2275585718 \times 10^{-13}$
j=3	$.3278071846 \times 10^{-4}$	$-.8970959364 \times 10^{-7}$	$.9246248312 \times 10^{-10}$	$-.4249155515 \times 10^{-13}$	$.7338316751 \times 10^{-17}$
j=4	$-.3425564927 \times 10^{-8}$	$.9527692453 \times 10^{-11}$	$-.1001409043 \times 10^{-13}$	$.4703914404 \times 10^{-17}$	$-.8315044742 \times 10^{-21}$

Table A7.5-4. Constant Coefficients in Expressions for Specific Volume as a Function of Pressure and Specific Enthalpy

			$CN2_{i,j}$		
i=	0	1	2	3	4
j=0	$-.4117961750 \times 10^{1}$	$-.3811294543 \times 10^{-3}$	$.4308265942 \times 10^{-5}$	$-.9160120130 \times 10^{-8}$	$.8017924673 \times 10^{-11}$
j=1	$-.4816067020 \times 10^{-5}$	$.7744786733 \times 10^{-7}$	$-.6988467605 \times 10^{-9}$	$.1916720525 \times 10^{-11}$	$-.1760288590 \times 10^{-14}$
j=2	$-.1820625039 \times 10^{-8}$	$.1440785930 \times 10^{-10}$	$-.2082170753 \times 10^{-13}$	$-.3603625114 \times 10^{-16}$	$.7407124321 \times 10^{-19}$
			$CN2_{i,j}$		
i=	0	1	2		
j=-1	$-.1403086182 \times 10^{4}$	$.1802594763 \times 10^{1}$	$-.2097279215 \times 10^{-3}$		
j=0	$.3817195017 \times 10^{0}$	$-.5394444747 \times 10^{-3}$	$.1855203702 \times 10^{-6}$		
j=1	$-.6449501159 \times 10^{-4}$	$.8437637660 \times 10^{-7}$	$-.2713755001 \times 10^{-10}$		
j=2	$.7823817858 \times 10^{-8}$	$-.1053834646 \times 10^{-10}$	$.3629590764 \times 10^{-14}$		